SOUTHAMPTON OCEANOGRAPHY CENTRE

CRUISE REPORT No. 38

RRS *JAMES CLARK ROSS* CRUISE 67
19 NOV - 17 DEC 2001

Drake Passage repeat hydrography: WOCE Southern Repeat Section 1b – Burdwood Bank to Elephant Island

Principal Scientist
S Bacon

2002

James Rennell Division for Ocean Circulation and Climate
Southampton Oceanography Centre
University of Southampton
Waterfront Campus
European Way
Southampton
Hants SO14 3ZH
UK

Tel: +44 (0)23 8059 6441
Fax: +44 (0)23 8059 6204
Email: S.Bacon@soc.soton.ac.uk

DOCUMENT DATA SHEET

AUTHOR
BACON, S et al

PUBLICATION DATE
2002

TITLE
RRS *James Clark Ross* Cruise 67, 19 Nov-17 Dec 2002. Drake Passage repeat hydrography: WOCE Southern Repeat Section 1b – Burdwood Bank to Elephant Island.

REFERENCE
Southampton Oceanography Centre Cruise Report, No. 38, 118pp.

ABSTRACT

This report describes the seventh repeat hydrography section across Drake Passage, first established during the World Ocean Circulation Experiment. Thirty CTD/LADCP stations were carried out across the 753 km section from Burdwood Bank to Elephant Island, plus one test station, one station in Drake Passage to provide sound speed information for concurrent geophysical activities, and one station at the Rothera Time Series (RaTS) site, just off Biscoe Wharf at Rothera. Maximum station spacing on the section was 33 km, with stations closer together on the continental shelves. Water samples were drawn for salinity analysis, for subsequent CTD conductivity calibration. The LADCP was a new 2-instrument setup comprising upward– and downward–looking RD Instruments Workhorse ADCPs. The CTD was a SeaBird 911*plus* with dual temperature and conductivity sensors. Various underway measurements included navigation, vessel-mounted ADCP, sea surface temperature and salinity, water depth and meteorological parameters.

KEYWORDS
ANTARCTIC CIRCUMPOLAR CURRENT, ANTARCTIC OCEAN, ACOUSTIC DOPPLER CURRENT PROFILER, CTD OBSERVATIONS, DRAKE PASSAGE, *JAMES CLARK ROSS*, CRUISE 67 2001, LOWERED ADCP, SOUTHERN OCEAN, VESSEL MOUNTED ADCP, WOCE, WORLD OCEAN CIRCULATION EXPERIMENT, ADCP, LADCP

ISSUING ORGANISATION
Southampton Oceanography Centre
Empress Dock
European Way
Southampton SO14 3ZH UK

Copies of this report are available from: **National Oceanographic Library, SOC** *PRICE*: £25.00
Tel: +44(0)23 80596116 Fax: +44(0)23 80596115 Email: nol@soc.soton.ac.uk

CONTENTS

SCIENTIFIC PERSONNEL

Name:	**From:**	**Role:**
Bacon, Sheldon	SOC	PSO, CTD, Salinity
Afanasyev, Vsevolod	BAS	Electronics engineer
Collins, Julie	UEA	Simrad, salinity
Hawker, Liz	SOC	VM-ADCP, navigation
Kent, Liz	SOC	CTD
King, Brian	SOC	LADCP
Meredith, Mike	BAS	CTD
Robst, Jeremy	BAS	Computing support
Sen Gupta, Alex	SOC	LADCP, Oceanlogger

Key:

BAS:	British Antarctic Survey
SOC:	Southampton Oceanography Centre
UEA:	University of East Anglia

SHIP'S PERSONNEL

Name:	**Rank:**
Elliott, Christopher	Master
Paterson, Robert	Chief Officer
Gooberman, David	Second Officer
Baker, Scott	Third Officer
Waddicor, Charles	Radio Officer
Cutting, David	Chief Engineer
Kerswell, William	Second Engineer
Armour, Gerard	Third Engineer
Eadie, Steven	Fourth Engineer
Wright, Simon	Deck Engineer
Thomas, Norman	Electrician
Olley, Kenneth	Catering Officer
Elliott, Thomas	Engineering Cadet
Adams, Paul	Navigation Cadet
Stewart, George	Bosun
Williams, David	Bosun's Mate
McGowan, John	Seaman 1
Baker, James	Seaman 1
Blaby, Marc	Seaman 1
Jenkins, Derek	Seaman 1
Rees, David	Seaman 1
Smith, Sydney	Motorman
Robinshaw, Mark	Motorman
Davies, Clive	Chef
Baldwin-White, Lawrence	2nd Cook
Pratley, Clifford	Senior Steward
Lee, Derek	Steward
Weston, Kenneth	Steward
Newall, James	Steward

LIST OF TABLES

LIST OF FIGURES

ACKNOWLEDGEMENTS

It is a pleasure to acknowledge the efficiency and hospitality of the Master, Officers and Crew of the *James Clark Ross*; also thanks to the Master for organising, and John the Rothera boatman and Dave 'Spock' Rees (amongst others) for carrying out, the excursion in the Humber; thanks again to Dave for a copy of his beautiful picture of the ship (see Plate 1); thanks to Simon Wright for the nice job on the JCR Diary web pages, and for the winch driving, along with Dave Williams and Derek Jenkins. Finally thanks to Neptune for the implausibly calm days for the section in the midst of a spell of grotty weather.

OVERVIEW

This report describes the seventh occupation of the Drake Passage section, established during the World Ocean Circulation Experiment as repeat section SR1b, first occupied by Southampton Oceanography Centre in collaboration with the British Antarctic Survey in 1993, and re-occupied in most years since then. As stated in Cunningham (2001), the cruise report for the sixth occupation of the section (cruise JR55), the main objectives are:

i. To determine the interannual variability of the position, structure and transport of the Antarctic Circumpolar Current (ACC) in Drake Passage;
ii. To examine the fronts associated with the ACC, and to determine their positions and strengths;
iii. By comparing geostrophic velocities with those measured directly (by the lowered ADCP), to determine the size of ageostrophic motions, and to attempt to estimate the barotropic components;
iv. To examine the temperature and salinity structure of the water flowing through Drake Passage, and to identify thereby the significant water masses;
v. To calculate the total flux of water through Drake Passage by combining all available measurements.

This year, there were two additional technical objectives: (a) the evaluation of the performance of the SeaBird 911*plus* CTD system, new to us after many years of using different equipment, and (b) the setting-up, operating and evaluating a new two-way L-ADCP system based on upward- and downward-looking RD Instruments Workhorse ADCPs.

The first three of our party (JC, EH, ASG) left the UK on 8 Nov, 11 days prior to the ship sailing, because a more suitable flight was not available. They travelled via Madrid and Santiago to Mount Pleasant on the Falkland Islands. The next three (SB, ECK, BAK) arrived at Heathrow on 15 Nov to find their flight to Madrid cancelled, which necessitated an overnight stop in a Heathrow hotal because the Santiago connection was, thereby, missed. This in turn necessitated a change of carrier (one which would enable us to make the connection with the flight from Santiago to the Falklands), so we flew via Paris to Santiago, but arrived, regrettably, minus two items of luggage. We arrived in the Falklands, rather weary and exasperated, on the 17th. Mobilisation proceeded until the 19th, when we were joined by MM, flying out with the RAF.

We sailed from Stanley at 1755L (Z-3) and proceeded directly to the test station (no. 1) in over 2000 m water depth, in the west end of the Malvinas Chasm, between the Falklands and Burdwood Bank, early on the 20th Nov The weather was blustery, overcast, NW6/7. The section proper began on the south side of Burdwood Bank in 235 m water depth on the afternoon of the 20th; one the same day, we

also completed stations 3–6. The 21st saw stations 7–11; station 10, notably, suffered a failure of the CTD termination while on the way down at 3000 m; we decided that time, being extremely tight, did not permit a repeat, so we proceeded to the next station. In this time, the wind had dropped to NW4/5. Stations 12–16 were completed on the 22nd, with the wind now dropped right away and the weather turning fine. Stations 17–21 were completed on the 23rd, in continuing fine weather and light airs. Towards the end of station 20, around 1400L, two Humbers were launched, to enable SB (in one boat) and the BBC (in the other) to take some footage of the ship at work. Stations 22–27 were completed on the 24th, and 28–31 on the 25th, ending off Elephant Is. in 405 m water depth at 0330L. The spell of fine, calm weather continued to the end of the section.

The following day saw the arrival of gales. JR69 geophysics was rather curtailed. Much of the remainder of the voyage was spent in poor weather. We looked at, but did not enter, Deception Is. on the 28th, and arrived at Lockroy on the 29th in a blizzard. We passed through Neumayer Channel and made a round trip through Lemaire Channel, which was blocked by ice at the end, before arriving at Palmer Station on the 30th. On the 1st December, we headed off for Rothera where we arrived on the 4th, having difficulties with ice on the way. There were two fine, calm and clear days here. Base relief was completed on the 7th but poor weather prevented departure on the 8th, so we finally left on the 9th, returning to Palmer on the 11th having been held up again by ice. There then followed a return to Lockroy, where we parked bows into the fast ice, and departed later the same day, heading out via Neumayer Channel and Gerlache Strait. Geophysics was resumed for the remainder of the voyage. We arrived back in Stanley on the 17th.

1 CTD DATA ACQUISITION, PROCESSING AND QUALITY

Liz Kent, Sheldon Bacon and Mike Meredith.

1.1 Introduction

This section will describe the Conductivity-Temperature-Depth (CTD) system used on Cruise JR67, the method of data acquisition, processing and the results of some assessments of data quality. 34 stations were sampled, a test station, 30 stations across the Drake Passage section, a station to measure sound velocity for the swath bathymetry survey performed on JR69 (the following cruise) and a two final stations at the Rothera Time Series Station (the first of which failed near the surface). The CTD worked well giving good data apart from a termination failure on the downcast of Station 010 and a connector failing near the surface of the downcast of the first Rothera Time Series Station (033). Both these events led to complete data loss for the remainder of the cast.

1.2 Configuration

The BAS CTD system was used, a SeaBird 911plus system which was fitted to the Southampton Oceanography Centre CTD 24-bottle frame with a 12 bottle pylon. The system consisted of dual temperature and conductivity sensors, a pressure transducer, the LADCP (see Section 2) and an altimeter. Only 11 Niskin bottles were fitted to the frame, the bottle position 5 being taken by the LADCP system. Figure 1.1 shows a schematic of the system. Details of the sensor types, serial numbers and calibration dates are given in Table 1.1, calibration coefficients are given in section 1.11. BAS has a full set of spares for the CTD system apart from the altimeter and swivel.

1.3 Deployment

Before the CTD was deployed the LADCP workhorses had to be woken up and disconnected from the charger. The CTD was then deployed from the midships gantry and hauled on the winch. Two of the ships crew used hand lines to control the CTD as it left the deck and entered the water. The CTD was lowered to about 10 metres depth and left to soak for a couple of minutes. The pumps are water activated and so do not operate until the CTD is in the water. The soaking ensures the pumps are running when the cast starts and that the CTD system has had some time to adjust to the water temperature from the atmospheric temperature. Strong air-sea temperature differences were not encountered so a long soaking was not thought necessary. After soaking the CTD was brought to the surface, the wireout zeroed, and the CTD lowered to about 10 metres above the seabed. Judgement of the height above the seabed was complicated by the 'false bottoms' seen in the altimeter record. Figure 1.2 shows the altimeter output for Station 016, Figure 1.2a for the full cast and Figure 1.2b for the bottom 350 metres. The true reading can be seen to be much cleaner than the false signals that precede it, but the fact that the multiple echoes are close together makes the approach to the seabed nerve-wracking, especially if the seabed is sloping and the ship drifting. It is thought that the

altimeter has too high a ping rate (V. Afanasyev, pers. comm.) but it is not possible to change the rate with particular model of altimeter used. It is possible to set the altimeter to only ping when interrogated by the CTD system, but the SeaBird system cannot be set to interrogate the altimeter. A new altimeter would be a good investment.

Water samples were taken on the upcast with the winch stopping at 11 depths to fire the 11 bottles for which there was room on the frame. The CTD was stopped for about 10 seconds before the bottle was closed. The CTD was brought onto deck, again with the help of the ship's crew and secured to the deck with bolts. Salts were sampled from the 11 bottles, on most casts a duplicate sample was taken from the deepest bottle (bottle 1). The LADCP data was downloaded and the unit put onto charge. The CTD was then set up for the next station.

1.4 Data Acquisition

The raw binary data are logged to the pc, a Viglen Genie 4Dx266, attached to the deck unit. The deck unit was usually switched on when the CTD was in the water and the control for the pylon 'homed'. Data was logged using the SeaBird *seasave* software from the *seasoft* version 4.226 set of utilities. *seasoft* runs under DOS and has been configured to be accessed using a menu by typing *ctdmenu*. Calibration data are entered using the utility *seacon.* Logging to the pc was normally started when the CTD was soaking at 10 metres. This meant that few deck pressures were obtained as it was thought that switching on the pumped CTD system before the package was in the water was not good for the sensors. However as the pumps are salt water activated after 60 seconds using a conductivity switch it is not clear that any damage would occur. Deck pressures may have been useful in calibrating the CTD pressure. It should be noted that in this system deck temperatures will not be equivalent to the air temperature but will record the temperature of any water remaining in the cell. If the word display on the Deck Unit is set to 'E' then the least significant digit on the display indicates whether the pumps are off (0) or on (1). The pc screen display was set to show the temperature, salinity and altimeter reading as a function of pressure and also to display spot values of the pressure, depth, temperature and altimeter reading. Data loss is indicated by a beeping of the Deck Unit but usually little data was lost. Bottles were closed either using the SeaBird software or by pressing the fire button on the Deck Unit. Either way the firing of the bottle was confirmed on the pc display. Logging was stopped when the CTD reached the surface. The raw data was logged as a binary file 67ctdNNN.dat where NNN is the station number.

The time written to the data file is seconds after the start of logging. The logging start time has to be obtained from the file header and derives from the pc clock. The time should therefore be synchronised with the ships master clock before each station, but this was not often done on this cruise. The pc clock was 34 seconds fast before Station 15 and was synchronised with the ships clock on Station 15. The time was reset periodically on the remainder of the section. For merging with the

navigation data a time error of this size is not significant. When merging the CTD data with LADCP data, for example, care is needed to ensure that the differences in the time base were accounted for. The time base of the CTD files has been altered to best match with the LADCP output, details are given in Section 1.9.1.

The data acquisition system is not ideal as the pc is the only source of the raw data. In the event of a pc disk failure, any data which had not been promptly transferred to the UNIX system would be lost. The pc used to log the data was very old and slow, had a small hard disk and a very low data transfer rate. The keyboard was also very tired. It is understood that this pc will be replaced following the reporting of its inadequacies on this cruise.

1.5 Stations Sampled

Thirty-four stations were sampled during the cruises JR67 and JR69. Details are given in Table 1.2. Figure 1.3 shows the positions of the bottles fired, note the gap representing Station 010 where no bottles were fired as the termination failed on the downcast.

1.6 Data Processing

1.6.1 Data Processing the SeaBird Software on PC

After logging had been stopped the data are extracted from the SeaBird binary file 67ctdNNN.dat, calibrated and output to ASCII format in a file 67ctdNNN.cnv using the SeaBird utility *datcnv*. The channels output are given in Table 1.3:
The altimeter data was not extracted initially and so the extraction was rerun later to retrieve this information. datcnv also creates a file 67ctdNNN.bl which contains the bottle firing datacycle numbers extracted from the raw data file.

1.6.2 Conductivity Cell Thermal Mass Correction

The effect of the thermal mass of the conductivity cells was removed from the data using the standard SeaBird software *celltm*. The ASCII input file 67ctdNNN.cnv was converted to 67cnvNNN.cnv. The algorithm used was:

$$dt = t_i - t_{i-7}$$

$$ctm_i = -b * ctm_{i-7} + a * dcdt * dt$$

$$c_{cor,i} = c_{meas,i} + ctm_i$$

$$a = \frac{2\alpha}{7\Delta * \beta + 2}$$

$$b = 1 - \frac{2a}{\alpha}$$

$$dcdt = 0.8 * (1 + 0.006 * (t_i - 20))$$

where α, the thermal anomaly amplitude is set at 0.03 and β, the thermal anomaly time constant, is set at 1/7 (the SeaBird recommended values for SBE9/11 plus pumped system). Δ is the sample interval (1/24 second), dt is the temperature (t) difference taken at a lag of 7 sample intervals. $c_{cor,i}$ is the corrected conductivity at the current data cycle (i), $c_{meas,i}$ the raw value as logged and ctm_i is the correction required at the current datacycle, dcdt is a correction factor which is a slowly varying function of temperature deviation from 20 deg C.

An effort was made to understand the effect of the thermal mass correction using Station 016 as an example. Figure 1.5 shows the size of the correction (ctm), corrected data – uncorrected data as a function of pressure for this cast. As expected maximum values are found where there are strong temperature gradients in the surface layers. The peak values are about 0.01, negative for decreasing temperature and positive for increasing temperature. These values were reproduced using a short FORTRAN program which revealed features of the calculation that were not obvious from the documentation.

- The units of the correction are in S/m (no units were given in the documentation), we therefore needed to multiply the value of the correction calculated by 10 to agree with the differences in the data which were recorded in mS/cm.

- The lag is applied over 7 datacycles (7/24 second) rather than using adjacent datacycles. It seems therefore that the value 1/β of 7 therefore defines the datacycle interval as well as providing the time constant for the correction

- The correction needs at least a minute to reach its correct value. Before this time it clearly shows the effect of the 7 datacycle differencing as spikes every 7 cycles as each of the seven cycles has to reach its correct value independently.

An estimate of the size of the correction was made assuming steady-state conditions. In steady state $ctm_i = ctm_{i-7}$ and the equations above reduce to:

$$ctm = \left(\frac{a}{a+b}\right) dcdt(t_i - t_{i-7})$$

the first term is 0.72 and dcdt at a temperature of 0ºC is 0.088. Values for other temperatures are given in Table 1.4. The value of ctm is therefore 0.72*0.088 x temperature difference over 7 cycles. The value of β also defines the inertia of the system. The time taken to react to a step change in temperature is defined by the value of b, the e-folding decay time is 7 seconds. The maximum gradients observed in Station 016 were of order 0.1ºC over 7 datacycles (Figure 1.4), leading to a maximum correction of 0.01ºC, agreeing with Figure 1.5.

1.6.3 Preliminary Data Processing on the UNIX system.

After *celltm* had been run the data were transferred to the UNIX machine *jruf* using ftp. Until the raw .dat file has been transferred there is no backup of the logged data. Once on the UNIX system the data is processed using pstar data format using c-shell scripts.

67seactd0: reads in the ASCII file to pstar format using *pascin*. The start time is extracted from the ASCII file and will be the pc clock time. The header time was set to the 1st January 2001 and time resulting time in the pstar file was seconds after the start of the year. The water depth is extracted from the simrad file and latitude and longitude from the navigation file and inserted into the pstar header. The output file is 67ctdNNN.raw.

67seactd1: extracts data from 67ctdNNN.raw corresponding to the bottle firing times taken from the ASCII file 67ctdNNN.bl. Data extracted for 3 seconds before the bottle close start datacycle and 5 seconds after the bottle close end datacycle. The bottle closing time is about 1.5 seconds meaning that just under 10 seconds of data are extracted. These 10 seconds of data are averaged using *pbins* to give a file containing a single datacycle for each bottle firing. These are appended using *papend* to give a pstar file of CTD data corresponding to each bottle firing 67ctdNNN.btl. As 12 datacycles were required absent data was appended to the end of the file if fewer than 12 bottles were fired.

The file 67ctd016.raw from Station 016, which was a deep cast with strong near-surface vertical gradients, was used to examine the data quality of the SeaBird CTD system which is described in the following section.

1.7 Data Quality

Figure 1.6 shows the salinity and potential temperature plotted against pressure for Station 016. These values are calculated from the temperature and conductivity as shown in Figure 1.4. No quality control has been applied to this data.

1.7.1 Noise in each channel

Figure 1.7 shows the difference of the individual 24Hz values from a filtered 1 second mean (actually 25 cycles) for the salinity measured from the primary temperature and conductivity. Also plotted is the primary salinity itself. Most of the noise in the data occurs in the surface 300 metres but for most of the cast the noise is small and fairly constant. Figure 1.8 shows histograms of the noise in the data defined as the difference from the one second mean. The salinity from the primary sensor combination is least noisy (black line). Similar noise levels are seen in the salinity from the secondary sensor combination (red line) and the combination of the secondary temperature with the primary conductivity (blue line). The additional noise in the secondary conductivity sensor is therefore roughly equivalent to the environmental noise between the first and second sensor locations. The worst data is obtained by combining the noisier secondary conductivity with the non-collocated primary temperature (green line). The potential temperature noise is very similar for all the primary and secondary sensor pairings and only the noise in the primary sensor pairing is shown in Figure 1.8 (light blue line). Table 1.5 gives the mean values for each sensor combination.

1.7.2 Relative Sensor Drift

Using data from below 500 metres the relative drifts between the primary and secondary sensors were calculated. The temperature sensors showed a negligible drift throughout the section but the salinity sensor readings diverged. Figure 1.9 shows the mean difference between the primary and secondary conductivity sensors as a function of station number. The mean offset in salinity (red line) is –0.002 psu with the secondary sensor reading higher than the primary. There is also a drift of the same order in the salinity difference. Comparison with the seawater samples suggest that the secondary sensor is responsible for the bias and the primary sensor for the drift (see Section 1.8) Section 1.7.1 shows that the secondary conductivity sensor initially contains slightly more noise than the primary but Section 1.7.3 shows that this is mainly due to the non-application of the conductivity advance to the secondary channel by the Deck Unit.

1.7.3 Conductivity Advance

The temperature and conductivity sensors are separated in space within the pumped system and the seawater first passes the temperature sensor and then the conductivity sensor. Details are given in SeaBird Electronics Application Note 38, "Fundamentals of the TC duct and pump-controlled flow used on SeaBird CTDs", December 1992. The default time separation of the temperature and conductivity measurements is 0.073 seconds (1.75/24 seconds). The Deck Unit is set up to advance the primary conductivity by this amount but the secondary conductivity is not shifted in time. The Deck Unit was opened to examine the switch settings to check that the conductivity advance was set to its default value. Figure 1.10a shows the inside of the Deck Unit and 10b a close-up of the S4 switch settings which determine the conductivity advance. The default positions for an advance of 1.75

cycles is ON,OFF,OFF,OFF,ON,ON for positions 1 to 6 of the 8 switch positions. Confusingly the switches are actually ON when the dip switches are closest to the side of the switch labelled OFF. An email to seabird (seabird@seabird.com) confirmed that the factory default settings were shown by switch S4 and the conductivity advance applied to the primary sensor only was 1.75 cycles. The manual recommends that the true time difference between the measurements is determined by reducing the spiking in salinity that results from the mistiming of the signals in regions of strong gradient.

Station 016 was again used as an example. The measure used to assess the optimum correction was the minimisation of the noise in the salinity signal where noise is again defined as the difference from a 25 sample (slightly over a second) average. The conductivity data were shifted in time using datacycle number as a merging variable. It was found to be necessary to use datacycle rather than time for the merging variable as for the 24Hz data the time in seconds was not stored to sufficient accuracy in the pstar file. (Note: The final processing was changed to use the start time of the cast in the pstar header rather than the start of the year. This removed the precision problems in the time variable.) Firstly therefore datacycle number was added to the file (*pcopya* to duplicate a variable, *pheadr* to rename it, *pedita* to set the new variable to absent, *peditb* to change the first value to 0 and the last to the number of datacycles minus one, then *pintrp* to generate the intermediate values). *pcopya* was then used to copy the merging variable and conductivity data to a new file, and *pcalib* to shift the merging variable by the required time difference in cycles (where 1 cycle = 1/24 second). The data from this second file were then merged back onto the original file in which the merging variable remained unchanged with *pmerg2*. Salinity was then calculated from the original temperature and the shifted conductivity (using *peos83*) and the noise estimated by taking the difference (with *parith*) of the salinity from its 25 value running mean value calculated with *pfiltr*. The resulting noise values were averaged into 5 metre bins with *pbins* then the ratio of the averaged noise values calculated with *parith*. A single mean value of the ratio was calculated by averaging the ratio into a single bin with *pbins*. Figure 1.11 shows the ratio of the noise in the time shifted secondary salinity to the noise in the primary salinity as a function of the time shift. The figure shows two curves which illustrate a shortcoming of this method. The upper black crosses shows the noise ratio for integer shifts and shows the expected minimum at a conductivity advance of about 1 cycle. The lower red crosses show the same ratio for shifts of half cycles (.... -1.5, -0.5, 0.5 ....). These values are lower than the integer values as the remerging of the data has effectively applied a two point filter to the data and reduced the noise level. These two curves span the maximum and minimum values for the noise with other shifts falling between them in a predictable manner. It was therefore not possible to 'home in' on the optimal shift by making small changes to the shift as the ratio moves between the two curves every datacycle causing peaks in the data. It still seemed like a

good way to determine the optimal shift in the data so integer shifts were used and the minimum in the curve estimated by fitting a quadratic to the bottom five points using *plreg2*.

The optimal shifts were found to be -1.25 cycles for the primary conductivity and -1.00 cycles for the secondary conductivity. The primary conductivity therefore needs to be retarded by 0.5 cycles from its default advance of 1.75 cycles. Figure 1.12 shows a short section of data from Station 18 in a region of strong salinity gradients. Figure 1.12a shows the original data and Figure 1.12b shows the data with the optimal time shifting applied. The correctly time shifted data is much less noisy than the original data confirming the time shifts calculated are reasonable. It should be noted however that the shift of +0.5 applied to the primary sensor will have effectively reduced the noise slightly due to the effect seen in Figure 1.11. The secondary conductivity has been shifted by –1.0 cycles and so the noise reduction seen in the red traces is therefore the true value due to the improved alignment of the data. The processing was applied to each station in turn and the optimal shifts did not vary with time. For station 016 no systematic or significant change in shift with pressure or haul rate could be detected. The optimal shifts of +0.5 for the primary sensor and –1.0 for the secondary sensor are therefore recommended for the CTD configuration used on this cruise.

1.7.4 Ship Motion Effects

The portion of data from 30 db to 130 db on Station 016 chosen to show the effects of the conductivity advance also shows some interesting features in both temperature and conductivity for both the primary and secondary sensor pairs. Figure 1.13 shows the potential temperature and salinity for both sensor pairs for the time period corresponding to the 100 db portion of the cast shown in Figure 1.12. The data are plotted following the conductivity time shift described in the previous section. There are peaks in the data in the region of strong gradient which are seen in all sensors. Properties in the peak tend towards values seen slightly higher in the water column. Figure 1.14 shows the same potential temperature data as plotted in Figure 1.13 but for the primary sensor only. Superimposed is the vertical velocity of the CTD in arbitrary units calculated from the gradient of 1-second averaged pressure. The temperature data is plotted in green for periods when the CTD is moving faster through the water and in red for when the descent rate is lower or the CTD is moving upwards in the water column due to the ship rolling. The peaks are clearly associated with low or negative descent rates and this could be used as the basis for an automated quality control procedure in regions of strong gradient.

Figure 1.14 shows that there does not need to be an upwards velocity of the CTD to introduce a peak in the data, only that the vertical velocity decreases. The pumped system used on the SeaBird CTD means that water should pass over the sensor at a constant rate whatever the rate of descent of the CTD package. Discussions with Sheldon Bacon and Brian King resulted in the suggestion that what was being seen was the effect of the turbulent wake of the CTD when the CTD descent rate decreased.

On the downcast the sensors precede the bulk of the package and a turbulent wake will form behind. When the package slows or rises this wake may overtake the sensors resulting in the sensors sampling water that has come from higher in the water column. After our analysis of the effects of ship motion on the BAS SeaBird CTD data it was brought to our attention that similar effects had been noted on the RVS CTD system used on the RRS Discovery MarProd Cruise (R. Pollard, pers. comm.).

1.7.5 Pressure Hysteresis

Station 016 was examined looking for possible pressure hysteresis. Figure 1.15 shows 1Hz averaged upcast and downcast salinity and their difference for pressures below 1500db. The natural variability of the waters in Drake Passage hides any hysteresis effects which are expected to be small for the type of pressure sensor used in the SeaBird CTD.

1.8 CTD Calibration

This section describes the process for calibrating the CTD conductivity sensors against the sample salinity measurements.

1.8.1 Processing path

i. an ascii file `sam67.names` was created, with 2 columns: variable name, and associated units. All variables required in subsequent processing were included.

ii. a cshell script *pblankexec* was run to create a blank pstar sample file, called `sam67.blank`, containing 12 data cycles corresponding to the 12 positions on the BAS rosette.

iii. for each cast, a cshell script *samblank.exec* was run, to create an empty copy of `sam67.blank` called `sam67nnn`, where `nnn` = cast number. Date, time, position and depth information is written into the header.

iv. for each cast, a cshell script *samfir* was run, to paste variables from CTD file `67ctdnnn.btl` into `sam67nnn` (pressure, plus temperature, conductivity and derived salinity for each sensor pair).

v. for each cast, a cshell script *sal.exec* was run, to retrieve an ascii file `sal67nnn.txt` containing sample salinity data from the Mac iBook using the cshell script *getexcel.exec*, which converts the ascii file into a pstar file `sal67nnn`.

vi. for each cast, a cshell script *passal* was run, to paste sample salinity data from file `sal67nnn` into `sam67nnn`.

vii. for each cast, a cshell script *botcond* was run, to calculate sample conductivity from bottle salinity, CTD pressure and (primary) temperature. Bottle minus CTD conductivity was calculated for each sample and for both CTD conductivity sensors. These operations all pertain to file `sam67nnn`.

1.8.2 Comparison of bottle and CTD conductivities

The aim is to determine any dependence of CTD conductivity with depth, temperature or time (station). We considered first the mean station-by-station conductivity offset (the average of bottle minus CTD conductivity). It was clear that both the primary and secondary conductivity sensors were accurate throughout to the water column to *ca*. ±0.002 mS/cm. Any temperature or pressure dependence was small. Our first obstacle to detailed evaluation of these observations is illustrated in figure 1.16, which shows the conductivity offset for each station, together with the salinometer standardisation history expressed as the (equivalent) salinity correction (with arbitrary zero) applied to each station as derived from the measurement of the SSW. It appears, rather unusually, that the salinometer was 'jumpy' over the course of the section, adopting (broadly) one of two settings, with a 'high' and a 'low' value, separated by ~0.003 in salinity. It appears further that these jumps are visible in the calculated conductivity offsets: see particularly the jumps from stations 13 to 14 and from 19 to 20. The impression of contamination of the sample salinity is further enhanced by the correlation between offsets and standardisation history: see figure 1.17. We are not certain if the jumpiness is short-period noise such that individual samples are in error with the same range as the standardisation; the mean difference in salinity between replicate salinity samples is 0.0003, with standard deviation 0.0012 for 25 pairs, with 1 outlier; the standard deviation of the equivalent salinity corrections is 0.0018 for 15 values. At the same time, the standard deviation of the offset for each sensor is ~0.001 (figure 1.16), which is extraordinarily good compared with past experience given that these comparisons are with raw CTD conductivities. A couple of stations have higher offset standard deviations – most noticeably, 16 and 29 – but given the high quality of the raw CTD data, we decided to look at θ / S continuity across the section to see whether it supported the suggestion of odd salinometer behaviour.

Figure 1.18 shows contoured sections of potential temperature, salinity (derived from primary conductivity and temperature) and density (σ_3), below 2500 dbar, to avoid higher upper-ocean variability. Even so, there is considerable variability at depth, both in terms of large horizontal and vertical property gradients and smaller-scale variability. Figure 1.19 (CTD θ / S data below 2500 dbar) illustrates the latter: excursions from the central θ / S line of order 0.005 in salinity can be seen at most densities. These excursions are most likely to be real, since they are of greater magnitude than the offset scatter, and also are monotonic in density: were they random, then density inversions would be expected at least occasionally. In order to investigate the lateral variability of salinity as a function

of potential temperature, it was necessary to select overlapping groups of stations covered by potential temperature bands (which become colder from north to south) which avoid the smaller-scale station-to-station variability while remaining in the deeper water. The chosen temperature bands, their thicknesses and mean salinities are given by station in Table 1.6. It can be seen that, for both sensor pairs, the mean salinity over the ranges of stations are constant to within a range of about 0.001 in salinity. There is no evidence for station 16 being an outlier.

Referring again to figure 1.16, we notice further that the two sensor offsets grow further apart. They are initially separated by <0.001, and finally by >0.002. A linear fit of offset to station number for both sensors produces for the primary sensor a slope of 8.35E–5 and intercept of –1.75E–3, and for the second sensor a slope of 4.02E–6 and intercept of –1.94E–3. For the primary sensor, the slope is statistically significant (based on analysis of variance), for the secondary sensor, it is not.

The conclusions so far are, therefore:

(a) The primary conductivity is nearly accurate without application of any salinity sample derived correction, but that the sensor exhibits a trend over the section equivalent, on a linear basis, to an offset at station 1 of –0.0018 mS/cm, and at station 31 of +0.0008 mS/cm;

(b) The secondary conductivity likewise is nearly accurate, with a mean offset of –0.0018, and there is no identifiable trend across the section;

(c) The salinometer is, on the whole, *not* more accurate than the CTD. For example, the apparent offset outlier at station 16 (fig. C1) is not evident in the CTD θ / S analysis, and nor are the jumps or steps in offset (stations 13/14, 19/20 etc., fig. C1).

Next we remove the trend in the primary conductivity by station with constants as above, and examine both sensors for pressure and temperature dependence. Rather extraordinarily there proves to be none. We fit the usual model (to the sample data from all stations), $\delta C = A + BP + CT$, where δC is sample minus CTD conductivity, P pressure, T temperature, and A and B constants. For the primary sensor, the standard deviation of δC (after removal of trend) is 0.0013; the residual standard deviation after fitting the model is 0.0012. The improvement is not significant. The standard deviation of δC for the secondary sensor is 0.0012; the model residual is the same. Therefore our final calibrations are below:

$$C1_{cal} = C1_{raw} - 1.75E\text{-}3 + 8.35E\text{-}5 \times N$$

$$C2_{cal} = C2_{raw} - 1.88E\text{-}3$$

where C1 and C2 are primary and secondary conductivities, subscripts *raw* and *cal* indicate raw and calibrated data, and N is station number. Figure 1.20 shows residual sample minus conductivity difference after calibration for both sensors, plotted as a function of pressure. Note that samples from all depths were included in the process. No shallow samples were removed. Statistics for (e.g.) data below 500 dbar are not significantly different from those cited above for all data. This is probably a beneficial consequence of the SeaBird pumped system.

1.9 Final Processing and Quality Control

1.9.1 Reading in Data

67seactd0: was rewritten to use time from the start of the station in the pstar header. A time offset can optionally be added to make the CTD time agree with the ships clock or the LADCP clock. This exec reads in the ASCII file to pstar format using *pascin*. The start time is extracted from the ASCII file and will be the pc clock time. Offsets of the CTD pc time and the LADCP pc time were added to the CTD time as shown in Table 1.6. The header time was set to this adjusted time and the time in the pstar file was therefore seconds after the start of the station. The water depth is extracted from the simrad file and latitude and longitude from the navigation file and inserted into the pstar header.
Output file is 67ctdNNN.raw.

1.9.2 Time shift conductivity data, calculate salinity and potential temperature

Following the results of the conductivity advance analysis the primary conductivity was retarded by 0.0208333333 seconds (+0.5/25 cycles) and the secondary conductivity advanced by 0.0416666667 seconds (-1.0/24 cycles). This was done by using *pcopya* to copy time and the conductivity variable into another file, *pcalib* to adjust the time base and *pmerg2* to combine the files again. This was done for each conductivity variable separately. The salinity and potential temperature were recalculated from the adjusted conductivities using *peos83*.
Output file: 67ctdNNN.tsh.

1.9.3 Edit on Salinity Standard Deviation

An attempt was made to automatically remove conductivity data before the CTD was in the water. The first 20 minutes and last 5 minutes of the cast were binned with *pbins* into 10 second bins. The start of good conductivity data was defined as the first bin in which the standard deviation of conductivity was less than 0.05 $mScm^{-1}$ and similarly for the end of good conductivity data. These times were identified using *datpik* and conductivity and salinity data outside these times removed using *peditc*.
Output file: 67ctdNNN.ed1

1.9.4 Edit on Noise

Further automatic editing was performed using the definition of noise from Section 1.7.1. The differences of salinity and potential temperature from their 1 second filtered values were calculated for both the primary and secondary sensors. *pcopya* was used to duplicate these four variables, *pfiltr* to apply a 25 point running mean and *parith* to take the difference of the instantaneous and filtered quantities. *peditc* was then used to remove conductivity and salinity values where the absolute difference from the filtered salinity value was greater than 0.01 psu and to remove temperature and potential temperature were the absolute difference from the filtered temperature value was greater than 0.05ºC.

Output file: 67ctdNNN.ed2

1.9.5 Manual editing

The final stage of the editing procedure was to manually edit the data using *plxyed*. The normal version of *plxyed* does not have a large enough buffer to effectively edit the 24Hz data so a version with a larger buffer was compiled. There were few spikes left in the data and cleaning up of the start and end were the most common edits performed.

Output file: 67ctdNNN.ed3

1.9.6 Calibration

Pressure

After the section had been finished it was discovered that out of date pressure calibration values had been used. The correction to the original pressure calibration is applied using a slope and an offset. The effect of the incorrect values was removed from the pressure and the new calibration applied in the following way.

$slope_{old}$ = 0.99999

$offset_{old}$ = -0.494200

$slope_{new}$ = 0.99992

$offset_{new}$ = -0.8815

$$P_{new} = \frac{slope_{new}}{slope_{old}} P_{old} + \left(offset_{new} - \frac{slope_{new}}{slope_{old}} offset_{old} \right)$$

i.e.

$$P_{new} = 0.99993 P_{old} - 0.387273$$

This calibration was applied to the pressure using pcalib.

Output file: 67ctdNNN.cal

Conductivity

Following the results of the comparison with the salinity samples described in Section 1.8 the following calibrations were applied to the conductivity:

$C1_{new} = C1_{old} - 0.00175 + 0.0000835$*station number

$C2_{new} = C2_{old} - 0.00188$

pcalib was used to apply the offsets to the conductivity data.

Output file: 67ctdNNN.cal

peos83 was then used to recalculate salinities and potential temperatures.

Output file: 67ctdNNN.24Hz

1.9.7 Generation of Final Files

The edited file 67ctdNNN.24Hz is the master file for the station. From this file several other files are generated.

67ctdNNN.dwn: the downcast extracted from the master file

67ctdNNN.1Hz: the master file averaged to 1Hz using *pavrge*.

67ctdNNN.1db: the downcast sorted on pressure with *psort* and averaged on pressure to 1db with *pavrge*.

These files were used to generate a 5db section across Drake Passage using *pgridp*. Figure 1.21a shows the salinity across the section and Figure 1.21b the difference in the two salinity measurements after calibration (primary minus secondary). Systematic variations can be seen between the calibrated salinities between the primary and secondary sensors. The primary sensor gives higher readings than the secondary at depth near the end of the section and the secondary sensor is higher near the surface in the middle of the section. Away from the surface differences are less than the 0.001 target accuracy for these types of measurements. As the primary sensor exhibited drift throughout the section it seems reasonable to attribute the remaining variations in salinity to this sensor and to use the secondary sensors in final data products. Figure 1.22 shows the potential temperature for the section, differences between the two sensors were negligible.

1.10 Summary

The SeaBird CTD performed very well and produced extremely stable temperatures and conductivities with little editing required. The primary conductivity sensor drifted slightly through the cruise and so salinities derived from the secondary sensor are to be preferred. Although the mean offset from the bottle sample salinity values was larger for the secondary sensor, the offset remained constant with

time. Therefore both temperature and salinity should be taken from the secondary sensors after adjustment to the bottle salinity values.

The conductivity advance was changed from the manufacturers recommended values by post processing the data. The primary conductivity channel was advanced by 1.75 cycles by the deck unit, this was reduced to 1.25 cycles by post processing. The secondary conductivity is not advanced by the deck unit and required an advance of 1.00 cycles to reduce noise in the derived salinities.

The effect of the variable descent rate of the CTD package is clearly visible in this high quality data in regions of strong gradients. Whilst this is not thought to be a serious problem when deriving oceanic sections this will need to be considered further if use is to be made of the 24Hz data for studies of small-scale oceanic structure.

Deck pressure was not routinely measured on this cruise and this should be considered for future cruises.

The time in the CTD files is obtained from the pc clock and an effort should be made to synchronise this with the ships master clock. It would be preferable if a feed from the master clock could be made to the CTD datastream.

The altimeter used on this cruise gave up to three false bottom readings in close succession near to the real seabed. The purchase of a more suitable sensor should be considered.

The pc used to log the data was very old and slow with a small hard disk. It is understood that this pc will be replaced soon. Consideration should be given to logging a backup datastream either by splitting the signal before it reaches the Deck Unit and logging a copy of the data directly to the SCSS or by using the tape output on the back of the Deck Unit.

1.11 Calibration Equations and Coefficients

Temperature, ITS-90 Scale

$$T\left[^{o}C\right] = \frac{1}{g + h\ln\left(f_0/f\right) + i\ln^2\left(f_0/f\right) + j\ln^3\left(f_0/f\right)} - 273.15$$

where f is the frequency output of the temperature channel

Coefficient	Primary (03P2709)	Secondary (03P2705)
	12-Sep-00	02-Jul-01
g	4.35035131e-03	4.38984778e-03
h	6.47012417e-04	6.52769056e-04
i	2.40770641e-05	2.51801691e-05
j	2.36437825e-06	2.48675852e-06
f_0	1000.0	1000.0

Conductivity

$$C\left[\text{Siemens}\,m^{-1}\right] = \frac{\left(g + hf^2 + if^3 + jf^4\right)}{10 * \left(1 + \delta t + \varepsilon p\right)}$$

where f is the frequency output of the temperature channel, t is the temperature in ºC and p is the pressure in db.

Coefficient	Primary (04225)	Secondary (04222)
	13-Sep-00	13-Sep-00
g	-1.02684784e+01	-1.02139754e+01
h	1.41619041e+00	1.52205944e+00
i	-3.49761775e-03	-7.95763911e-03
j	3.29567425e-04	6.83027120e-04
δ (nominal)	3.25e-06	3.25e-06
ε (nominal)	-9.57e-08	-9.57e-08

Pressure

Sensor model: Digiquartz 410K-105

Sensor serial number: 67241

Installed in: CTD 09P15759-0480

Calibrated: 30-Jun-00

$$P = C * \left(1 - \frac{T_0^2}{T^2}\right)\left(1 - D\left(1 - \frac{T_0^2}{T^2}\right)\right)$$

where P is the pressure in psia, T is the pressure period in μs and C is given by:

$$C = C_1 + C_2U + C_3U^2$$

and D is given by:

$$D = D_1 + D_2U$$

U is the temperature in ºC and T_0 is given by:

$$T_0 = T_1 + T_2U + T_3U^2 + T_4U^3 + T_5U^4$$

Digiquartz Coefficients

C1 = -4.461418e+04 [psia]

C2 = 3.038286e-02 [psia $ºC^{-1}$]

C3 = 1.224130e-02 [psia $ºC^{-2}$]

D1 = 3.645500e-02

D2 = 0.000000e+00

T1 = 2.999608e+01 [μs]

T2 = -3.512191e-04 [μs $ºC^{-1}$]

T3 = 3.729240e-06 [μs $ºC^{-2}$]

T4 = 4.918760e-09 [μs $ºC^{-3}$]

Calibration correction: Slope = 0.99992, Offset = -0.8815

[Calibration used: Slope = 0.99999, Offset = -0.494299, this calibration removed and correct one applied as part of post processing].

1.12 SBE35

SeaBird SBE35 Deep Ocean Standards Thermometer

1.12.1 Instrument setup and operation

On one station during JR67, the BAS SBE35 high-precision thermometer was fitted to the CTD frame. This was station 34, the occupation of the time series station close to Biscoe Wharf, Rothera, conducted to 365 m on 9th December 2001. For this station, the SBE35 was fixed vertically (sensor end up) along an outer upright of the CTD frame, and thus was outside the ring of Niskin bottles and approximately 1 m above the level of the SBE911*plus*.

The SBE35 is a self-recording instrument that logs a temperature measurement to erasable/programmable read-only memory (EPROM) each time a Niskin bottle is closed; in this respect it is used as a replacement for digital reversing thermometers. Communication with the SBE35 for programming and data downloading is via an SBE90248 Optobox situated in the winch control room of the UIC. This connects to the SBE35 via a cable that is run down to the water bottle annex via the cable entry to the main lab, and connects to the CTD PC via an RS232 connector that links to the COM1 port of the computer.

Before programming, the SBE35.CON (configuration file) needs checking to ensure the calibration coefficients are current and accurately entered. On JR67, the values used were:-

a0: 5.731929187e-3
a1: -1.634408781e-3
a2: 2.346628834e-4
a3: -1.294062389e-5
a4: 2.724825969e-7
slope: 0.999999
offset: 0.000000

where:-

$$\text{Temp (ITS-90)} = 1 / \{a0 + a1[ln(n)] + a2[ln^2(n)] + a3[ln^3(n)] + a4[ln^4(n)] \} - 273.15$$

and n = sensor output.

Values for a0-a4, slope and offset were determined by a linearization calibration on 6th May 1997 and a fixed-point calibration on 29th June 2001.

Once connected, the SBE35 is programmed using the *TERM35* program. Commands used are DS (Display Status; shows date/time of internal memory, datacycles logged, number of measurements to be averaged per reading etc), DD (Data Dump; writes stored datacycles to the file specified), and IL (Initialise Logging; clears EPROM and primes instrument for data acquisition). For JR67, the SBE35 was set to average 24 cycles per measurement. In a thermally quiet environment, the temperature noise standard deviation is 0.000029*sqrt(8/ncycles), equal to 0.000017 degC in our case.

When programmed, the SBE35 is connected to the subsea cabling ready for CTD deployment. After recovery of the package at the end of the cast, the SBE35 is reconnected to the CTD via the Optobox, and data is downloaded using the DD command under *TERM35*. (The SBE35 can actually log 157 measurements, so in general downloading data after every cast is not necessary). The sensor output is then converted to temperature (ITS-90) using the *CNV35* program, and transferred to Unix for sequestration into the Pstar environment and subsequent post-processing.

After use on station 34, a connector pin was broken on the SBE35, rendering the instrument unusable for the remainder of the cruise. The pin was badly corroded; given its condition, it is not entirely surprising that it broke. A badly corroded pin was noted on JR58, where it had been causing problems with data downloading. If it is the same pin and had not been examined and mended during the summer, then it is both unfortunate and remiss. If a second pin had become corroded, then there is clearly a repeating problem that requires attention.

1.12.2 SBE35 data

The SBE35 data were compared to the data from both the primary and secondary temperature sensors of the SBE911. For analysis, extraction of sections of SBE911 temperature data was performed according to two procedures:-

(1) the standard procedure, whereby a time segment between 3 seconds before bottle firing and 5 seconds after bottle firing is extracted, and

(2) a modified procedure more appropriate for the SBE35 comparison, whereby data between the time of bottle firing and 24 seconds afterwards are extracted.

Figure 1.23 shows the difference between the SBE35 and primary SBE911 temperature (black), the difference between SBE35 and secondary SBE911 temperature (red), and the difference between primary and secondary SBE911 temperatures (green). SBE911 temperatures were extracted according to method 2 (above), with all temperatures plotted as a function of bottle number. Bottle 1 was deepest (365 m) and bottles 11 and 12 shallowest (10 m).

Some key features apparent in Figure 1.23 are:

(1) the difference between SBE35 and SBE911 temperatures are predominantly negative from bottles 1 to 9, and predominantly positive above.
(2) bottles 6 and 10 show extremely large differences between SBE35 and SBE911 temperatures (SBE35 colder for bottle 6 and warmer for bottle 10).
(3) the differences between the primary and secondary SBE911 temperatures are very much smaller than the differences between SBE35 and SBE911 temperatures.
(4) the difference between primary and secondary SBE911 temperature is almost always positive.

Data extracted using method 1 (not shown) exhibit the same general pattern, but with a much greater noise level, including significantly larger differences between the primary and secondary SBE911 temperatures. This can be seen in Table 1.8.

The most likely explanation for the large offsets between SBE35 and SBE911 temperatures for bottles 6 and 10 is the comparatively large oceanic vertical gradients in temperature at these depths, combined with the different positioning on the frame of the instruments. (The vertical stratification in Marguerite Bay is such that the temperature minimum is centred close to 50 m depth; this is the remnant of the previous winter's mixed layer. This creates strongest vertical temperature gradients at around 30 and 100-150 m depth, corresponding with the depths of bottles 6 and 10). The sense of the difference (negative for bottle 6, positive for 10) agrees with the sense of the oceanic vertical temperature gradient at these depths. However, the magnitude of the temperature gradient is probably not sufficient to explain the full differences between the SBE35 and SBE911 temperatures, thus it is likely that wake effects are also being observed. These are apparent in the downcast CTD profiles (see separate section); we note here their presence in the upcast data also, for periods when the package was not being hauled. The positioning of the instruments, with the SBE911 inside the ring of Niskins and the SBE35 outside, will probably lead to different magnitudes of wake effects, but this is not readily addressable with the data available. The sense of the oceanic vertical temperature gradient also explains the differences in SBE35 and SBE911 temperatures being predominantly negative between bottles 1 and 9, and positive above.

1.12.3 Summary

1) The main purpose of the SBE35 is to monitor possible changes in calibration of the SBE911 within or between cruises. As such, it is important that the SBE911 data extracted for comparison cover the same time interval as the SBE35 averaging period, rather than the standard 3 seconds before firing to 5 seconds afterwards. This is an easy task, but one that seems not to have been conducted routinely in the past.

2) Having the SBE35 fixed on the edge of the frame and at a different height to the SBE911 reduces its usefulness in monitoring the SBE911's performance. It should ideally be sited on the same level as the SBE911, and as close to it as is practicable.

3) Shallow stations with moderately large temperature gradients are not ideal for attempting to use the SBE35 to monitor the SBE911's performance. Deep stations with smaller gradients in the deep waters are much more suitable, and the above remarks should be reconsidered in the light of data to be collected from such stations in the future.

2. LADCP

Brian King, Alex Sen Gupta and Mike Meredith

2.1 Background

This was the first SOC cruise to make use of the new RDI Workhorse WH300 ADCPs purchased with JIF equipment funds. Three instruments had been purchased, s/nos 1855, 1857, 1881. The instruments were initially configured at SOC, immediately prior to packing for JR67. Although the instruments had been tested individually on the bench, they had not been tested using the 'star' cable which enables synchronisation for dual use.

The star cable acts as an in-line cable between the controlling PC and the WHs. It also connects two WHs for synchronised pings, and connects each WH to a single external battery pack. Although the WHs are able to use either RS422 or RS232 comms, the star cable only supports RS232 comms. Much of the allocated mobilisation time at SOC was spent attempting to establish comms through the newly-delivered star cable, without success. The situation arose because Jeff Benson, the real local expert, was at sea. Eventually it was realised that the WHs had been delivered with the Monitor factory settings (RS422) instead of Sentinel (RS232). Under Jon Wynar's supervision, the pressure cases were opened and a jumper on a circuit board reset to RS232 comms.

Once comms had been established through the star cable, the question of battery charging was addressed by BAK and Terry Edwards. The battery charger that was to be used was a Wynall intelligent charger, previously used with the BB150 battery packs. It turns out that this charger only supplies voltage if it can 'see' the voltage of batteries to be charged. Unknown to BK and TE, the star cable includes two diodes, to prevent open contacts on the RDI data leads showing live voltage when a battery pack is connected to the star cable. Therefore the Wynall charger could not be used to charge the battery pack using the terminal pickup on the RDI data leads. This was very puzzling and resulted in more lost time while the puzzle was solved and a method for charging the batteries was worked out. The solution worked out was to introduce a branched ('Y') cable between the battery pack and the star cable, so that a charging lead could be plugged into the battery in parallel with the star cable. The Y-cable and a long charging lead, with a connector which could if necessary plug directly onto the battery case, were ordered and hand-carried to the cruise.

As a result, all mobilisation time was used before the WHs could be properly tested with the planned seagoing configuration files: the equipment needed to be packed for sea. The SOC tests had not even included tests of the synchronisation function.

This lack of a proper test in synchronised LADCP mode proved to be costly to the LADCP trials on JR67. In advance of the cruise, BK had been supplied with some suitable command files by

colleagues in the USA (described further in the section on data processing). These CMD files included Master/Slave synchronisation commands and LADCP commands. We note in passing that neither of these functions are mentioned, much less described, in the RDI manual supplied with the instruments. Details of the commands may be found in the WH Expert Commands help file on CD. When the command files were tried on the ship, it was found that the L commands were not recognised. This is because the LADCP option, in which the WH performs bottom tracking, had not been installed before delivery, and the shortcoming not noticed at SOC. Consultation with RDI revealed that the option could be installed as a field upgrade, and three .EXE upgrade files (roughly 300k bytes each) were emailed to the ship. The upgrade files need to be built for the particular instrument concerned.

It was decided that the first priority was to ensure all three new WHs were tried underwater, at least in water track mode. Since firmware upgrades can sometimes go wrong and disable an instrument, it was decided not to attempt an upgrade until after the first swapping out of an instrument midway through the section (after stn 13). Once the first instrument had been swapped out after a reasonable number of deep stations, the upgrade was attempted. Although the .EXE file executed, the upgrade failed with an error, although the normal functioning of the instrument was not affected. RDI then requested the output from the PS0 command (shown in Box 1), and on the basis of that sent a new upgrade .EXE for one instrument. This attempt was successful on 1881, and the LADCP commands became recognised. However, with only five days CTD work in all, the main CTD section had by now been completed, so the LADCP option could not be tested. PS0 output was sent to RDI for the remaining two instruments. RDI then sent a succession of incorrect files over the following days, some of which produced failure errors, and one for 1855 which failed with a report that it was built for the wrong CPU. By late in the cruise (13 Dec, day 347) there was still no upgrade for 1855. Since the need for upgrade to include LADCP option was not discovered until we reached the ship, and as a result of RDI's failure to be able to prepare working upgrade files, almost no testing of the LADCP option was possible. By the time of aborted stn 33 in Marguerite Bay on the way in to Rothera, only uplooking 1881 had been upgraded. Some 'bottom tracking' of the surface was achieved. By the time of station 34 in Marguerite Bay on the way out from Rothera, 1857 had also been upgraded. So the LADCP bottom track of only one instrument was tested, on a single station. We have therefore not managed an extensive trial of this option.

We note in passing that in addition to bottom tracking from WT pings in LADCP mode, there is a genuine BT ping mode upgrade also available. We suggest that if this is a no-cost option it should be obtained and installed. Dedicated BT pings offer the potential for bottom tracking at greater range than analysis of WT pings, and this facility might be desirable. At the very least, we expect to want to

undertake some comparisons between BT data from BT pings and from analysis of WT pings. The list of available and installed options can be obtained with the command 'OL'.

2.2 JR67 operations.

Figure 1.1 shows the disposition of instruments on the frame. One side of the star cable connects to each WH and the battery pack. The other side has two tails for data transfer. These are trailed to the edge of the frame, where they can be conveniently accessed. The battery pack bulkhead connector is attached to a branching 'Y' cable. One branch of the Y connects to the star cable and the other trails to the edge of the frame, where the charging lead can be connected. Connectors are compatible so that either the star cable or the charging lead could connect directly to the battery pack if the Y cable was damaged.

Two workhorses were used at any one time; a downward facing 'master' unit and an upward facing 'slave' unit, (RDI recommend the Master should be downlooking). The master / slave configuration is necessary in order to synchronise the workhorses. During deployment the workhorses are powered using an external battery pack, described below. While the package is on deck, the battery is connected to a Wynall 240V charger unit and the workhorses are connected to a windows 98 based PC via com 1 (master) and com 2 (slave) serial ports. A more detailed configuration description can be found in the Workhorse ADCP Technical Manual P/N 957-6000-00 – January 1998 (change 2), from RDI Instruments.

Unit 1857 was used as downlooking Master throughout. The first 13 stations had unit 1855 as the uplooking Slave. After station 13 unit 1881 was swapped into the upward facing position, in order to test all the workhorses. All workhorses functioned without problems throughout the JR67 section.

We note in passing that a WH would sometimes not wake up easily after disconnection from a power supply. This was usually remedied simply by disconnecting and reconnecting the power supply. Such disconnections were avoided by the cable layout used on this cruise, where the charger could be connected in parallel with the instruments.

2.3 Battery pack.

Two new battery packs were supplied. Pack number TSN-1855A was used throughout. This contains 24 times 2V 8Ah lead-acid gel E cells. Pack number TSN-1857A was not used. The battery packs had been made up shortly before leaving UK, and it was found that four of the 48 E cells were damaged (dented) when delivered to SOC. Replacement cells could not be obtained in time for shipment to Grimsby. Pack TSN-1857A was assembled as a backup with the damaged cells, with the intention of replacing the damaged cells with replacements hand-carried to the ship. Unfortunately,

the replacement cells were contained in checked baggage lost en route to the ship, so TSN-1857A could not be modified. It was thought best to avoid using it unless absolutely needed.

The battery pack worked well throughout and there seemed to be ample time between stations to fully recharge. In this regard, experience was better than with the previous BB150 system. Since the battery packs for the BB150 system were of nominally 50% greater capacity, and were still liable to have insufficient charge time when working closely-spaced deep stations on this section, we conclude that the power requirements of the two WH300s is rather less than the single BB150. It may also be that the brand new batteries (different model to the older packs) had better charging characteristics, or that they maintain voltage better but then die more abruptly. The lowest voltage seen on recovery after any station was 47.4 volts.

It was found that if left connected to the battery pack but with power off, the charger would completely drain the battery pack over a period of 24 to 48 hours. Therefore if there is a prolonged period without stations, it is necessary either to leave the charger powered on (not necessarily desirable) or to isolate the charger from the battery pack. At present this can only be done by disconnecting the lead at either the frame end or the charger end. The latter is especially undesirable, because it leaves a live 48V bare wire open.

Beware also that at the unterminated end of the charging lead in use on JR67, the black wire is +48V when connected to the battery pack. This wire was wrapped in red tape during JR67 to signify positive. The convention on the battery pack bulkhead connector is small pin = power+; large pin (pin1) = power negative. The bulkhead connector is Impulse VSK-2(#6#8)-BCL.

We therefore recommend that attention be given to a better arrangement for connecting the charging lead to the charger. This should include:

(a) The charger lead should terminate in some sort of secure terminal block, so there is no possibility of live leads floating when connected to a battery pack.

(b) There should be an easily-accessible fast-acting fuse at the charger end of the charging lead, to protect the battery pack in case of short circuits

(c) There should be a switch near the charger to isolate the charger from the battery pack without the need for disconnecting any leads.

Since the WH300s do not seem to have their own utility for reporting battery voltage (unlike the BB150), it is necessary to measure the battery voltage with a multimeter, which must be kept to hand near the LADCP operation. **A multimeter should therefore be packed up** with the battery packs as a ‘kit’ item.

The battery case is fitted with a vent plug. This is actually not very convenient to use. The vent plug is secured in place by a nylon retaining plate which forks in from the side. This in turn is secured by an allen-keyed bolt into the endcap. In order to slide the nylon retainer sideways to release the vent, the allen bolt must be completely unthreaded from the endcap, and then relocated after use**. Could the whole vent arrangement be replaced** by a bleed valve which seals onto the face of the endcap with an O-ring? Also, since it has two bore seals, any interior pressure is not vented until the vent plug is completely removed. Since this is carried out on deck, at low level, beneath Niskin Bottles, there is a small chance of getting seawater splashed into the pressure case through the open vent. The vent was used every 10 stations or so, and no significant buildup of pressure was noted. A very gentle hiss generally accompanied the removal of the vent plug.

2.4 WH300 technical spec

Since this is the first cruise to utilise the WH300s, we include a summary of their technical spec, in the form of output from the PS0 (numeral zero) command:

Box. 1 Sample readout from PS0 command for workhorse 1855

```
>ps0
  Instrument S/N:  1855
       Frequency:  307200 HZ
   Configuration:  4 BEAM, JANUS
     Match Layer:  10
      Beam Angle:  20 DEGREES
    Beam Pattern:  CONVEX
     Orientation:  UP
       Sensor(s):  HEADING  TILT 1  TILT 2  TEMPERATURE
Temp Sens Offset:  -0.30 degrees C

    CPU Firmware:  16.12 [0]
   Boot Code Ver:  Required:  1.13   Actual:  1.13
    DEMOD #1 Ver:  ad48, Type:  1f
    DEMOD #2 Ver:  ad48, Type:  1f
    PWRTIMG  Ver:  85d3, Type:   6

Board Serial Number Data:
   31  00 00 02 48 A4 68  09 DSP727-2001-04F
   16  00 00 02 48 7A DC  09 REC727-1000-04A
   13  00 00 02 48 77 CA  09 CPU727-2000-00H
   C0  00 00 02 48 A3 E5  09 PIO727-3000-04C
```

2.5 Workhorse configuration and deployment

The workhorses needed to be configured with the appropriate parameter settings, which are distinct for the master and slave units. The configuration files were uploaded to the workhorses using the BBSC utility (see Instructions for use of LADCP) just prior to each deployment.

Master configuration: WTM.CMD (NB. Italicised remarks not included in file)
See Workhorse ADCP Technical Manual P/N 957-6000-00 – January 1998 (change 2) or on-line help files, for further information on specific commands.

	Control System Commands
CR1	*Resets parameter set to factory defaults*
CF11101	*Sets various workhorse data flow control parameters*
	Environmental Commands
EA00000	*Corrects for any misalignment between Beam 3 and heading reference*
EB00000	*Corrects for electric / magnetic bias between the ADCP heading value and the heading reference*
ED00000	*Sets the depth of the ADCP transducer*
ES35	*Sets a water salinity value for use in speed of sound calculations*
EX11111	*Sets the coordinate transformation processing flags*
EZ0111111	*Selects the source of environmental sensor data*
	Timing Commands
TE00:00:01.00	*Sets a minimum interval of 1 second between data ensembles*
TP00:01.00	*Sets a minimum time of 1 second between pings*
	Water-Profiling Commands
WD111100000	*Selects the data types collected by the ADCP:*
WF0500	*Moves the location of first depth cell away from the transducer head by 500cm to allow the transmit circuits time to recover before the receive cycle begins, thus blanking bad data close to the transducer head.*
WN016	*Sets 16 depth cells*
WP00001	*Sets the number of pings to average per ensemble. 1 ping per ensemble*
WS1000	*Sets the volume of water in each depth cell – 1000cm*
WV250	*Sets the radial ambiguity velocity to 250cm/s.*
WJ1	*Use normal receiver gain*
WB1	*Set narrow bandwidth for increased profiling range*
	Ping Synchronization Commands
SM1	*Sets the RDS3 master mode, enabling SA and SW commands*
SA001	*Sets the rough timing of the synchronization pulse. Send (wait for) pulse before a water ping.*
SW05000	*Sets the amount of time to wait after sending the pulse. 5000 x 0.1ms*
	Control System Commands
CK	*Stores present parameters to non-volatile memory.*
CS	*Starts the data collection cycle.*

Slave configuration: WTS.CMD (Same as above unless stated)

```
CR1
CF11101

EA00000
EB00000
ED00000
ES35
EX11111
EZ0111111

TE00:00:01.00
TP00:01.00
WD111100000
WF0500
WN016
WP00001
WS1000
WV250
WJ1
WB1

SM2
SA001
ST0

CK
CS
```

Sets the RDS3 master mode, enabling SA and SW commands

Sets the amount of time a slave will wait to hear a synch pulse before proceeding on it's own, ST = 0 tells the slave to wait indefinitely.

The upgraded Lowered ADCP configurations (LM.CMD & LS.CMD) were achieved by replacing the water-profiling commands (those starting with W) for the following Lowered ADCP commands, in both the master and slave configuration files. The L commands were simply not recognised before upgrade:

LD111100000	*Selects the data types collected by the ADCP:*
LF0500	*Moves the location of first depth cell away from the transducer head by 500cm to allow the transmit circuits time to recover before the receive cycle begins, thus blanking bad data close to the transducer head.*
LN016	*Sets 16 depth cells*
LP00001	*Sets the number of pings to average per ensemble. 1 ping per ensemble*
LS1000	*Sets the volume of water in each depth cell – 1000cm*
LV250	*Sets the radial ambiguity velocity to 250cm/s.*
LJ1	*Use normal receiver gain*
LW1	*Set narrow bandwidth for increased profiling range*
LZ30,220	*Amplitude, correlation threshold*

2.6 JR67 Instructions for use of LADCP

(To be used in conjunction with LADCP Deployment / Recovery Log Sheet)

2.6.1 Introduction

Connections: The two workhorses are connected to the controlling PC via two serial cables, with an additional cable connected from the battery unit to a charging unit (see Figure 2.1 for installation configuration). The downward looking LADCP was chosen as the master unit and was connected through the com1 port. The upward looking LADCP was the slave unit and was connected through the com2 port. If at any stage a cable is disconnected from either COM port and then reconnected the PC will require rebooting. The cables may be disconnected and reconnected at the workhorse end without the need for rebooting the PC.

Software: The BBTALK DOS-based utility acts as the primary interface between the user and the LADCP workhorses. Workhorse parameters can be read and set using a series of prompt line commands (see Workhorse manual or on-line help file). In addition, two other utilities are used for the batch processing of commands. BBSC is used to load configuration files to the workhorses and whcom.ht is used to transfer data from the workhorse to the PC. Two versions of whcom.ht were set up: whcom1.ht and whcom2.ht to handle data transfer from the master and the slave respectively. The only difference between the two setups is the com1 / com2 specification. All software needs to be configured for a baud rate of 38400 bps and a YMODEM connection.

2.6.2 Pre-Deployment

Both coms leads and the battery lead should be connected at this stage.

1. Run the BBTALK utility. Create a log file in which all subsequent BBTALK output will be stored:
Press F3, and enter filename of the form J67###.txt (where ### is the cast number).

2. Wake up the master unit. Press F5, and toggle to com1. Press <ESCAPE> to return to main screen. Press <END> to wake up master, a 'Workhorse Broadband ADCP…' message will appear. If the connection fails, disconnect and reconnect the data cable at the workhorse end and retry.
Check the workhorse clock against the scientific clock. Type TS? <ENTER> for a time in the form YYMMDDhhmmss. If the times differ by more than a second, reset the workhorse clock: type TSYYMMDDhhmmss <ENTER>.

3. Check the available memory available on the workhorse; the maximum available memory is 46Mb. Type RS? <ENTER>.

If insufficient memory is available, the memory can be cleared. Type RE ErAsE <ENTER>. There is no selective erase, all data will be removed from the workhorse when this command is issued. Data should only be removed after all data has been transferred and checked. This was usually performed between widely spaced stations when sufficient time was available. NB. maximum file size for a deep station was ~ 4Mb.

4. Run diagnostic checks. Type PT200 <ENTER>. NB. The Receive Bandwidth test (PT6) usually fails if the transducers are not in water. Other tests should pass.

Repeat steps 2 – 4. for the slave workhorse on com2. Exit from BBTALK: <Alt-X>.

2.6.3 Deployment

5. Switch off the battery charge unit and check battery voltage. NB. maximum voltage ~52V.

6. Run the BBSC utility. From the communication menu, select com2 (for the slave) and <OK>. From the deploy menu select load and enter the name of the slave configuration file (e.g. WTS.CMD). Press the <DEPLOY> button. If the workhorse memory is not empty the user is prompted to continue, press <OK>. This may safely be done without any loss of data – data is appended not overwritten. An error message {Problems sending command "CS" TIMEOUT} is always encountered at this stage, but does not seem to indicate a problem. Press <OK> and note the time of deployment. Press file and enter the filename for the BBSC log: J67###S.log <OK>. Press <ESCAPE> twice to return to main menu.

7. From the communication menu, select com1 (for the master) and <OK>. From the deploy menu select load and enter the name of the master configuration file (e.g. WTM.CMD). Press the <DEPLOY> button. After proceeding through the various alert boxes, note the time of deployment. NB. Neither slave nor master will begin logging data until the master is deployed. Save the BBSC log: J67###M.log <OK>. Press <ESCAPE> twice to return to main menu and exit <Alt-X>. At this stage the two workhorses should start pinging. This may by heard when close to the units.

Detach charger and coms cables and fit blanks to all cable ends. If the battery venting-plug has previously been removed, ensure this is replaced. Inform winch operator to proceed with deployment.

2.6.4 Recovery

Remove blanks and attach the coms and charger cables.

8. Run BBTALK. Select com1 for the master unit and press <END> to terminate logging. Note the time. Both master and slave will stop logging. Select com2 for the slave and press <END> to re-establish communication. Exit from BBTALK.

9. Check battery voltage and switch on charger.

2.6.5 Data Transfer

10. Run whcom1.ht. Check the number of deployments stored on the unit. Type RA? <ENTER>.

11. To open the data channel type RY# (where # is the result to the RA? command). From the transfer menu, select receive file - the data transfer will commence. Note the default filename.
Whcom2.ht may be run concurrently in order to transfer slave data. NB. File paths may be entered for the data files; this should be done to put master and slave into separate directories. The default name for files seems to be controlled by the command RN.
Once the data is transferred the workhorse can be powered down, type CZ <ENTER>. A workhorse will automatically power down if left unused for an extended period.

12. Rename the default filenames to J67M###.000 for the master and J67S###.000 (where ### is the cast number).

13. Run BBLIST and load the master data file. Note the file size.

14. Note the number of ensembles

Repeat 13 & 14 for the slave data file.

[Data files were up to 4Mb for a 4700m station, and took 20 minutes to download at 38400 baud. Faster comms rates may be possible but were not tested.]

2.6.6 Initial data investigation

Data must be processed as soon as possible after the station, since this is the only indication that the instruments have worked correctly. Even before data processing begins, files should be checked for sensible size: master and slave should match to within a few ensembles and be of appropriate size for depth/duration of station. The data processing path is described below.

2.6.7 LADCP Logsheet

CTD CAST		Date:		JDAY	
Lat:		Long:		Depth:	

J67. LADCP Deployment / Recovery Log Sheet

Pre-Deployment (Comms. and Charge leads should be in place)

In BBTALK:

1. Log file name (F3) .txt

	MASTER	SLAVE
2. Time check (TS?) and time correction if necessary	: :	: :
3. Memory unused (RS?) and erase if necessary (RE ErAsE)	Mb	Mb
4. Run tests (PT200)		

5. Battery Voltage V (max. 52V)

Deployment

In BBSC

6. SLAVE deployment time, from master clock : : and log file J67 S.log

7. MASTER deployment time, from master clock : : and log file J67 M.log

Recovery

In BBTALK

8. Time of stopping MASTER logging : : . Stop SLAVE

9. Battery Voltage V

Data Transfer

In whcom1.ht (for MASTER); whcom2 (for SLAVE)	MASTER	SLAVE
10. Number of deployments (RA?)		
11. Default filename	RDI .000	RDI .000
12. Renamed file	J67M .000	J67S .000

In BBLIST	MASTER	SLAVE
13. File size	Kb	Kb
14. Number of ensembles		

15. Comments

2.7 First-look Data processing

The initial steps of data processing on JR67, as an initial performance check, were as follows:

1. Transfer the raw data files J67M###.000 and J67S###.000 into data/ladcp2/raw/ directory, on JRUF. (Drag and drop on LADCP PC; takes a few seconds per file.)

2. In the data/ladcp2/pro/ directory run the script 'scanexec ###', (where ### is the cast number). This script may well be changed in the future as the path is refined. On JR67 it made use of the UH utility scanbb to extract times of first and last good data and to make an initial estimate of maximum package depth from integrating vertical velocity. It also extracted position at start and end of the cast from the RVS navigation file. A couple of ascii files were built with this information in a suitable format to commence the LDEO processing. These were required inputs for the LDEO processing.

3. In MATLAB, type: clear <ENTER> to initialise variables; type stn= '###' and run the spar.m script to set parameters based on the ascii files from (2), followed by ladrun.m which performs a first cut at processing. This generates a file data/ladcp2/pro/J67###.ps, which may be sent to the B/W printer. This process takes up to 10 minutes for the deepest station.

2.8 Further LADCP data processing.

The deployment of new WH300 LADCPs in the configuration generally referred to as LADCP2 required a new approach to data processing. Previous SOC experience was with software originating from Eric Firing's group at University of Hawaii. This software suite will be referred to as UH. UH software, at least as configured by SOC, can accept data from just one instrument at a time.

Another software suite, made available by Martin Visbeck's group at Lamont Doherty, is already adapted to accept data from pairs of instruments, since the LDEO group deploys WH300s in this configuration. This software will be referred to as LDEO.

In mobilizing for the cruise, we were greatly helped by sample LADCP2 datasets being made available by both Martin Visbeck at LDEO and Daniel Torres at WHOI (who also uses an implementation of LDEO).

2.9 Software summary

The two software suites are different in both mathematical approach and programming. The main problem in constructing LADCP profiles is to take account of the unknown horizontal velocity of the package from which measurements are being made. UH removes the unknown velocity from each

ping by calculating vertical shear (du/dz). These shear estimates are binned and averaged, and then accumulated in the vertical to produce top-to-bottom shear. This defines the velocity profile except for a barotropic component that can be calculated by reference to ship navigation. UH does not make use of bottom track data. The software uses a combination of perl scripts, matlab .m files and compiled programs originally written in c.

LDEO considers that each bin of each ping results from the combination of an unknown water velocity and an unknown package velocity. There are therefore two sets of unknown velocities defined with some vertical resolution (u_water(z) and u_package(t)), and a much larger set of bins/pings. This can be cast as a constrained least squares problem, where the requirement is to solve for the unknown water and package velocities. When in range of the bottom, LDEO software will calculate motion relative to the seabed by examining the Doppler shift in bins in which the return signal is strong. If either of RDI Bottom Track (BT) data or LDEO-calculated BT data are available, LDEO can employ this information in the least-squares problem. The software uses only matlab .m files.

2.9.1 Analysis of JR55 BB150 data

Two complete datasets were analysed during the cruise, to enable investigation of differences between the approaches and differences between instruments. The set of BB150 files from JR55 (2000/01 season) were brought from SOC. These data files included BT data from separate RDI BT pings. These had previously been analysed with UH, and were re-analysed during the cruise with LDEO. Summary plots were produced for each JR55 station that included the following:

(a) UH analysis of WT data; including ship's position;
(b) LDEO analysis of WT data; including ship's position;
(c) LDEO analysis of WT data; including ship's position and RDI BT data;
(d) Near-bottom profiles RDI BT pings, as extracted by LDEO;
(e) Near-bottom profiles RDI BT pings, as extracted by SOC;
(f) VMADCP single averaged profile of data collected on station: independent check.

The JR55 BB150 configuration consisted of 10 * 16 metre bins, with an ensemble period of 2 seconds. Each ensemble contained one WT and one BT ping. Basically, we would like (a) and (b) to agree with each other and to produce correct answers, when tested against (d), (e), (f). Ideally, (b) should produce the true currents without BT information, which will not always be available. We do not attempt to include here the detailed results of this study, since the study is incomplete and present conclusions are likely to go out of date. Generally, there was much reassuring similarity between the various measures of current. In particular, the small-scale vertical structure was often very similar in

the UH and LDEO solutions. However, the overall impression was that on stations with large shear (a) was superior to (b), being more likely to agree with (e) and (f). It appeared that (b) produced rather consistently less shear than (a), and that VMADCP in particular tended to support the results of (a). Result (c) tended to be better than (b), but this may just be a happy consequence of the mathematics. If the barotropic component of (a), (b) and (c) all match ship positioning, so that (b) and (c) have the same mean, and if the BT data drag the bottom of profile (c) towards truth, then the shallow end of (c) must also be steered towards truth. At present therefore, we suggest that the LDEO approach underestimates strong top-to-bottom shear, and we hypothesise that this may be a consequence of the initialization of LDEO and the norms used. This could be tested with fake data. It may be that we have not yet made best use of the various weighting parameters available in LDEO. We have used default values for most of them so far. We intend further discussion with M. Visbeck on these points. We are grateful for his valuable input thus far.

2.9.2 Analysis of JR67 data

We found that UH can process data from a single downlooking WH300 without modification. Out of curiosity we tried feeding UH the raw data from an uplooking WH300. There seems to be no reason in principle why the UH approach should not work for such an instrument, and we know from Eric Firing that he has processed dual-Sontek data. Although the UH processing ran without crashing, the answers did not seem to be sensible. We suspect therefore that the version of the software we used had some aspect that hard-wired an assumption about the instrument, rather than being fully general for up/down cases.

The data from WH300s on JR67 therefore enabled us to make the following analyses, to be included in station summary plots:

(a) UH analysis of downlooking instrument, with ship position;
(b) LDEO analysis of downlooking instrument only, with ship position;
(c) LDEO analysis of both instruments, with ship position;
(d) LDEO analysis of both instruments, with ship position and LDEO BT;
(e) Near-bottom profiles from LDEO analysis of WT pings;
(f) VMADCP data on station.

The preliminary conclusions of this study are very similar to those from examining JR55 data. Succinctly: LDEO seems to underestimate total shear in regions of strongest shear, although we may not be using it to best advantage yet. We also note that results from (a), UH analysis of one instrument only, are better than might have been expected. They are not obviously worse than had been previously achieved from BB150 data, although we do not yet have a statistical analysis to

support this impression. Subjectively, agreement between (a) and (e) or (f) still seems to be good. The range penetration of the WH300s was also better than expected. Sometimes 100 metres over the full depth of a cast.

The main conclusions are clear:

1) All three new SOC WH300s were employed. They seem to produce sensible data, though only the instrument used as downlooking has had its data examined in detail as single-instrument data. The two instruments which shared the uplooking slot have only been analysed in combination with downlooking data.

2) The UH software provides an acceptable route for processing data from a single downlooking WH300.

3) We have a working implementation of LDEO for processing LADCP2 data.

4) Further investigation of the different software options is needed before final conclusions can be reached about the relative strengths of either suite.

2.10 Comments on present implementation of LDEO

We do not attempt to detail all the data processing paths and program names for LDEO here. BAK is actively working on the software and the interface with other SOC datasets, so such details will become immediately out of date. At present, the 'business' part of LDEO is a subroutine named laproc.m; this calls matlab scripts as functions as follows. The steps can be run separately.
loadrdi [load raw data]
loadctd or *getdpth* [calculate package depth from integral of w or from CTD merged on time]
prepinv [prepare for inverse]
getinv [run inverse]

If the user wishes, the weighting parameters for the inverse can be adjusted and the inverse repeated with a function *resolve*.

Extensive use is made of three structures, f, p, and ps which control filenames and i/o of data, and parameters used in the inverse calculations. For example, ps.botfac and ps.barofac control the use of bottom tracking and navigation to constrain the inverse.

In LDEO, the data are pre-averaged to make the inverse acceptably quick, and *getinv* or *resolve* take only a few seconds on the main shipboard computer (a reasonably high spec Sun workstation). However, the previous steps, notably *loadrdi* and *prepinv* are slow. Processing an entire cast takes up

to 10 minutes for a full-depth 4500 metre station. Re-processing 100 stations from scratch would therefore be a major undertaking if it needed to be done at sea.

A new high-spec Sun has been purchased by JRD for the WH's next outing on CD139. It will be interesting to see how quickly the LDEO software runs on that machine.

2.10.1 Other comments

Depth of package in LDEO can be determined from integration of vertical velocity (*getdpth*), or from merging with CTD data on time (*loadctd*). It is unclear whether or not other users of LDEO employ CTD data or whether they rely on *getdpth*, which seemed to be rather more sophisticated in preparing flags to data-quality control near-bottom data. In order to employ the CTD data collected on JR67, BAK made extensive modifications to *loadctd*. In particular, the *bestlag* function was employed to compare vertical velocities from WHs with dz/dt from CTD and determine the offset in time bases. Some other functionality was also copied across from *getdpth*.

If *getdpth* is used, the user should supply the maximum depth in metres achieved by the package. This is supplied as element p.zpar(2). The Matlab array p.zpar generally takes the form [5 dpth 5] where the first and third values of 5 indicate the depth at start and end of the cast. The up and down casts are linearly stretched by *getdpth* to ensure that the package depth (d.z) fits the elements of p.zpar. Most depth arrays in LDEO use z is positive upwards from the sea surface; p.zpar is specified with submerged depths positive.

We began the cruise with the intention of undertaking an intercomparison between some combination of (i) RDI BT pings, (ii) RDI internal analysis of BT data from WT pings (which we expected to find reported in raw files), and (iii) LDEO analysis of BT motion from WT pings. This has not been done due to the absence of (i) and (ii).

We do not find anywhere in LDEO where true speed of sound is calculated, so we presume speed of sound is assumed constant at the value used within the WH. Particularly if CTD data are employed, it should be reasonably easy to make this correction.

3. NAVIGATION

Elizabeth Hawker, Brian King, Mike Meredith

During JR67 data from five of the scientific navigational instruments on RRS James Clark Ross were routinely processed. Primary positional, attitude and heading information were obtained from the Trimble 4000 GPS receiver; Ashtech ADU-2 GPS receiver, and the Sperry Mk 37 Model D Gyrocompass, respectively. Additional positional information was obtained from the Ashtech GG24 GLONASS/GPS receiver for comparison with the Trimble 4000 GPS data and from the SEATEX SEAPATH 200 unit, which provides heading data for the EM120 Swath System. A Racal Satcom received GPS SV range correction data via INMARSAT B from a fixed antenna in the Falkland Islands. This was passed to the Trimble and other GPS receivers to allow them to operate in differential mode (DGPS). All the instruments are logged to the SCS system and transferred to the RVS level C system. A series of UNIX scripts were used to process the navigation data in 12 hour periods from 0000 to 1159 (*am*) and 1200 to 2359 (*pm*). Each script requires the day of year number (jday), and whether *am* or *pm* data is to be processed.

3.1 Trimble 4000

The primary source of positional information on JR67 was the Trimble 4000 receiver in differential mode. The UNIX script *gpsexec0* was used to process the data. The pstar programmes called were *datapup* to transfer the data from RVS to pstar binary files; *pcopya* to reset the raw data flag on the binary file; *pheadr* to set up the pstar dataname and header; and *datpik* to remove data with a dilution of precision (hdop) greater than five. Two output files were created for each 12 hr period, 67gps[jday].raw and 67gps[jday], before and after the *datpik* stage respectively. The processed data were then appended to a master file 67gps01.

3.2 Ashtech GLONASS (GG24)

The Ashtech GG24 accepts data from both American GPS and Russian GLONASS satellite clusters (extending the constellation of available satellites to 48). Data was processed using the UNIX script *ggexec0* creating an output file of the form 67glo[jday][a/p].raw, upon which some basic quality control was performed and stored in 67glo[jday][a/p].

A comparison was made between the positional information obtained from the Trimble 4000 GPS data and the Ashtech GG24 GLONASS/GPS data. Data was compared for periods when stationary in Stanley, and during the Drake Passage SR1 section. For the Drake Passage section, the mean differences in latitude and longitude were 6.2m and 3.5m (with standard deviations of 6.2m and 6.9m) respectively. While alongside in Stanley, the standard deviations in latitude and longitude were 3.8m and 1.6m respectively for the GLONASS data; and 1.0m and 0.7m respectively for the Trimble GPS

data. This suggests that there would have been no particular advantage in using the GLONASS data as our primary source of positional information.

3.3 Ashtech ADU-2

The Ashtech ADU-2 GPS is used to correct errors in the heading of the ship's gyrocompass prior to input of the data into the ADCP processing stream. This is necessary as the gyrocompass can oscillate for several minutes after a manoeuvre due to an inherent error. Four UNIX scripts were used to process the Ashtech data in order to be able to correct the gyrocompass error as required.

On one occasion, while alongside at Rothera, the Ashtech did not log data (JDAY 338 18:38 to JDAY 340 11:13). The reason for this was unknown.

Ashexec0 This exec used *datapup* to read in data from the RVS data stream; *pcopya* to reset the raw data flag and *pheadr* to set the header information. The output file created was 67ash[jday].raw.

Ashexec1 This exec used *pmerge* to merge in data from the master gyro file; and *parith* and *prange* to calculate the difference between the gyro and Ashtech headings was forced within the range +/- 180 degrees. A timeshift of –0.9s was applied to the Ashtech data in order to obtain the best agreement with the gyro data (see section on Navigation Timebases). An output file 67ash[jday].mrg was created.

Ashexec2 This exec was used to edit the merged data file using the PSTAR programmes:

datpik to reject all data outside the limits given by:

- heading outside 0° and 360°;
- pitch outside –5° to 5°;
- roll outside –7° to 7°;
- attf outside –0.5 to 0.5;
- mrms outside 0.00001 to 0.01;
- brms outside 0.00001 to 0.1;
- heading difference ("a – ghdg") outside –5° to 5°;

pmdian to remove outliers in an "a-ghdg" of greater than 1° from a 5 point mean;

pavrge to set the data file to a 2 minute time base;

phisto to calculate the pitch limits;

datpik to reject further bad data:

- pitch outside the limits calculated by phisto;
- mrms outside the range 0 to 0.004;

pavrge to reset the data file to a 2 minute time base;

pmerge to remerge in the heading data from the master gyro file;
pcopya to change the order of the variables.

The output files were 67ash[jday].edit and 67ash[jday].ave.

Ashedit.exec This exec was used to manually remove obvious outliers from "a-ghdg" and to interpolate gaps in the data. The output file created was 67ash[jday].av.dspk.

Ashtec_67plot was then used to plot out the final interpolated "a-ghdg" with the original and gyro data.

3.4 Ashtech ADU2 parameter settings.

At BAK's request, J. Robst interrogated the ADU2 with a laptop PC to determine the control parameter settings used in the receiver. This was done while alongside at Rothera. Unfortunately, this required power cycling the receiver to establish serial comms, and after power up, the receiver had lost memory of the antenna geometry. This was unexpected, since it appears from documentation that these parameters should be saved during power cycling. (We suspect, without extensive testing, that the command $PASHS,SAV,Y should be the last command used after configuration.) It was therefore necessary to re-enter the antenna geometry and other parameters. Surprisingly, there was no definitive listing of the antenna geometry to be used. A number of sets of antenna geometry were available on printouts, based on various sets of calibration data. We decided to install a geometry set listed in a file of documentation prepared by Richard Bridgeman in Sep 1999, and normally kept in the electronics workshop. The relevant pages were duplicated and added to the documentation (i/c manufacturers manuals) kept in a box file on the bridge. Note that this antenna geometry was identical to a listing dated Grimsby September 1996, even though we know that the receiver and antennas were replaced after a failure of the old 3DF system on Albatross (JR40, 1999; Heywood and Stevens, 2000). However, the antenna backplanes were not altered, so it is reasonable to suppose that the centres of the new antennas matched those of their predecessors to millimetre accuracy.

The parameters listed in R. Bridgeman's file are as follows (output from $PASHQ commands, retyped for this report):

```
$PASHQ,PAR
POS:0 FIX:0 UNH:0 PDP:40 HDP:04 VDP:04
ELM:10 RCI:000 MSV:4 SIT:??? SAV:Y PDS:ON
ONE SECOND UPDATE: Y ALT:+00.00
OUT MBN PBN AT2 SNV PSA DSO BIN RTCM
PRT A:
```

```
PRT B:
NMEA: GL…. HDT
PRT A:
PRT B:
NMEA: GSA…SA4
PRT A:
PRT B:
PER:000
```

Antenna definition

1 Port Aft
2 Port Fwd
3 Starboard Fwd
4 Starboard Aft

```
$PASHQ,3DF
V12:  +002.955    +004.751    +000.000
V13:  +011.499    +004.754    +000.000
V14:  +013.227    +000.000    +000.000
OFFSET ANGLE:     +000.00     +00.00          +000.000
MAX CYC: 0.200    SMOOTHING; N
MAX BRMS: 0.035   MAX ANGLE: 10
MAX MRMS: 0.005   SRCHRAT: 0.5
HKF: 999 000      1.0E-2      1.0E+0
PKF: 020 000      4.0E-2      1.0E+0
RKF: 020 000 4.0E-2    1.0E+0
STATIC: N
```

These parameter settings produce a very high proportion of good PRH determinations (85 to 90% of 1Hz pings accepted after quality control over a 12 hour period). The parameters were noted in order to compare with settings used on RRS Charles Darwin, where a much poorer data return was being achieved in Nov 2001.

Thus the above parameter settings were definitely in use after the Rothera call. There was no evidence of a change in performance of ashtech-gyro offset after the re-entry of parameters and geometry.

3.5 SeaTex

Further to investigation during the 2000/01 season (JR55), some further investigation was undertaken of the headings reported by the SEATEX SEAPATH 200 unit, which provides heading data for the EM120 Swath system.

The Seatex system takes heading input from the ship's gyro and its own GPS heading unit. There are two antennas for the Seatex GPS heading unit, mounted on the main mast. The absolute heading measurement is referenced to the antenna alignment, with any gaps in GPS heading bridged using input from the ship's gyro.

In 2000/2001 (cruise JR55), a number of shortcomings were noticed in the Seatex heading product, a sample of which was transferred to the unix system for analysis. The file inspected in unix contained some out of range values (> 360), and, more significantly, periods in which the heading quality was poor. This was assessed by comparison with the independent Ashtech ADU heading product. There was generally a fixed offset between Seatex headings and ADU2 headings, but there were periods in which the Seatex product tended towards ship's gyro. This was interpreted as periods in which the ADU2 was delivering good data, but the Seatex GPS heading system was not.

During the 2001 refit, the antennas for the Seatex GPS heading were resited. Jeremy Robst copied Seatex heading data for the period 325/1307 to 328/2359 onto the SCS system. The UNIX script *stxexec0* was used to read the data from the RVS files into PSTAR, and a second script *stxexec1* was used to merge the Seatex and gyro data. None of the data gaps and defects noticed in JR55 were obvious in the JR67 data. We therefore conclude that the resiting of antennas has had the desired effect. However, see note elsewhere on Navigation Time bases.

The present offset between SeaTex and ADU2 heading was determined from 12 hours data (328a). The two streams were interpolated onto a common time base and differenced. The median difference (ASH-STX) was 1.003 degrees from 41000 good differences, with standard deviation 0.37 degrees.

Recommendation: We still note however, that because of its superior antenna geometry and spacing, the ADU2 should be capable of providing a better pitch-roll-heading input than the Seatex GPS heading input. It would seem logical that the Seatex should be able to accept a number of GPS heading feeds, just as it must accept a number of GPS position feeds, and to be able to select the appropriate feed by availability. If this is an option, an interface between the Seatex and ADU2 should be arranged. If it is not an option, the manufacturer should be encouraged to introduce it.

3.6 Gyrocompass

Data obtained from the gyrocompass gives the most continuous information available on the ship's heading. It was used in the processing of data from meteorological instrumentation (derivation of true wind velocity) and the Acoustic Doppler Current Profiler (ADCP). It was also used in the bestnav data stream to derive positional information by dead reckoning in the absence of GPS data coverage. Data was processed using the UNIX script *gyroexec0.* This called the following pstar programmes: *datapup* to transfer data from the RVS to pstar binary files; *pcopya* to reset the raw data flag; *pheadr* to set up the pstar header and dataname; and *datpik* to force all heading data to lie between 0 and 360 degrees. One output file was created 67gry[jday].raw, and the data appended to a master file 67gyr01. The RVS SCS system can provide duplicate time stamps in the gyro data hence *gyroexec0* also calls a pstar program *pcopym* to exclude this data from the processed data stream.

3.7 Bestnav

Bestnav provides 30 second interval position data using the best available data source. GPS is used when available, else dead reckoning using data from the ship's gyrocompass and velocity data. The script *navexec0* was used to process the data in 12 hour periods, appending them to a master file abnv671. The following pstar programmes were called; *datapup* to retrieve data from the RVS files; *pcopya* and *pheadr* to set header information; *posspd* to calculate east and north velocities; *pdist* to calculate distance run; *pcopya* to remove the RVS distance variable; and *papend* to append the data to the master file. A second script *navexec1* was then run to average and filter the navigation data. This takes a straight copy of the unsmoothed navigation and smoothes and despikes it, putting the data in abnv671.av.

3.8 Navigation (heading) Timebases

The time stamping of three different heading products remains a mystery. We refer here to three data streams. Ship's gyro (GYR), Ashtech ADU2 (ASH) and Seatex (STX).

A period of two hours' data was examined in detail: 328/0400 to 328/0600, being representative of various ship states, including periods of steaming on a steady course. Even when steaming on a steady course, ship yaw causes a clear oscillation in the heading. The phase of this oscillation can be used to determine the offset between the timebases of the three heading products.

Each data stream was interpolated onto a timebase of 0.05 seconds. The phase difference was determined by use of a matlab function *bestlag* borrowed from the LDEO LADCP2 software. This program tries different lags in increments of a single time step (here 0.05 seconds) and determines the lag with best fit. The misfit at each candidate offset is the median of the absolute differences between the time series. The minimum misfit defines the lag.

The two hour period was subdivided into 30 minute segments, and the lag determined for each 30 minute segment.

ASH: It was found that in order to obtain best agreement between GYR and ASH, ash times require an offset of between –0.7 and –0.9 seconds. The offset is definitely non-zero. Indeed, if a few minutes of ASH and GYR data are overplotted on a suitable scale, the phase difference is apparent to the unaided eye. The ASH time adjustment to bring it into phase with GYR was estimated on JR55 to be –0.9, and this value was used on JR67.

STX: Similar analysis for STX data suggested a similar correction would be required to bring STX in phase with GYR. On JR55 the offset was estimated to be –1.7, but a value nearer -1.0 is appropriate for the segment of JR67 data analysed.

The origin of these timing shifts is unclear. Potentially, the three data streams are time-stamped on three different systems.

Recommendation: The time stamping of the three data streams should be investigated. The ADU2 sends a data message that includes the time at which the attitude determination is valid. Under the old Level A system this information was stored as part of the data, so that it was possible to check for offsets between the timestamp of the data (previously supplied by the Level A and now supplied by the SCS) and the time at which the data were valid. Unfortunately the SCS discards the data-valid time, and a zero is logged to the 'sec' variable in the 'rvs file'. In the absence of J. Robst post-Rothera, we are unable to investigate the times tamping of the other data streams. GYR must be time stamped either by its Level A interface (we believe GYR still uses one) or in SCS. We know nothing about STX timestamp. While it would be convenient if the problem could be traced to the GYR timing, it seems improbable that this is being timed consistently *early*. A more probable hypothesis is that ASH is being timed *late*. It is particularly desirable that a system be devised where the valid times for ASH and GYR agree. The two streams are merged to produce an accurate heading product for VMADCP work. Even in fine weather the ship is liable to yaw with a period of about 10 seconds. Phase differences in the data streams generate unnecessary noise in the difference series. At present this is successfully removed in post-processing, but it would be better to solve the problem at source. Likewise, the positioning of EM120 data will be optimised if the timing of the STX heading product has uncertainty of rather less than 1 second.

4. VM-ADCP

Elizabeth Hawker

4.1 Instrument configuration

The acoustic Doppler current profiler (ADCP) on the RRS *James Clark Ross* is an RD Instruments 153.6 kHz unit. It is mounted in a sea chest that is recessed within the hull of the ship to give protection from sea ice. The chest is filled with a mixture of 90% deionised water and 10% ethylene glycol, and is closed to the sea by a 33mm thick window of Low Density PolyEthylene (LDPE). The orientation of the transducer head is offset by approximately 45° to the fore-aft direction.

The VMADCP was configured to record data in 64 x 8m bins, in ensembles of 2 minute duration. The 'blank beyond transmit' was set to 4m such that the centre depth of the first bin was 14m, given the approximate transducer depth of 6m. The system uses 17.07 firmware and version 2.48 of RDI Data Acquisition run on a Viglen IBM-type 286 PC. The two minute ensembles of data are passed via a printer buffer directly to the Level C. Data can be recovered from the PC files in the instance of any problems with the ship's Level C system.

The system was operated in two modes, configured through the Direct Command menu of the DAS Software. Bottom track data was collected in shallower waters, generally over Burdwood Bank and the Antarctic Peninsula shelf. Water track data was collected where water depth was sufficient to preclude useful bottom tracking, typically in depths greater than 500m. The command FH00004 was used to set the instrument to make one bottom track ping for every four water track pings.

4.2 Problems

On one occasion (JDAY 329, 12:29-13:11) the ADCP was off while investigating noise from the Simrad-EM120 echosounder. Immediately following this the heading was jammed on 360° (JDAY 329 12:11 to JDAY 330 04:18). Although not the reason in this instance, on a small number of occasions over the past 8 years this has occurred due to pinging not being stopped before the VMADCP was powered off. The solution is to reboot the VMADCP data logging PC and restart the RVS data processes. On another occasion (JDAY 344 12:12) the VMADCP was off briefly (while ice-bound) for a demonstration of its configurations. Full analysis of the VMADCP data could not be made during one period while alongside at Rothera (JDAY 338 18:38 to JDAY 340 11:13) due to an interruption in the logging of data from the Ashtech ADU-2.

4.3 Data Processing

All data was processed in 12 hour periods; from 0000 to 1159 hrs and 1200 to 2359 hrs. UNIX scripts (given in parentheses) were used to call up programmes from the PSTAR software for data processing.

*4.3.1 Read data into PSTAR (*67adpexec0)

Data was read from the RVS Level C system into PSTAR creating two output files 67adp[jday][a/p] and 67bot[jday][a/p], containing water track and bottom track data respectively. When the ADCP was configured to record water track information the bottom track file contained engineering data.

*4.3.2 Temperature correction (*67adpexec0.1)

The VMADCP DAS software assumes that the fluid surrounding the transducers is ambient seawater. A speed of sound is derived using the temperature measured at the transducer head and an assumed salinity of 35. A correction must be made to this to take into consideration the difference between the speed of sound in seawater and mixture of 90% deionised water and 10% ethylene glycol.

The required modification was derived by Mike Meredith and Brian King.

Measurements of the variation in sound speed versus temperature were obtained from RDI and used to derive an equation for the speed of sound through the mixture as a function of temperature:

$$c = 1484 + 3.6095 \text{ x } T - 0.0352 \text{ x } T^2$$

where the individual velocity measurements were given to an accuracy of 0.01%, and the environmental conditions were known to within ± 35 kPa pressure and ± 0.5°C temperature.

This equation was used to derive a correction term to adjust the assumed speed of sound such that it was appropriate for the fluid mixture within the sea chest:

$$(1484 + 3.6095\ T - 0.0352\ T^2) / (1449.2 + 4.6\ T - 0.055\ T^2 + 0.00029\ T^3)$$

This correction term was applied to both the raw water and bottom tracked velocities.

Also found was a residual dependence of A on temperature, probably due to the speed of sound in the fluid in the sea chest not being perfectly known. Following their estimates using bottom track data on JR55 (SR1 No. 6) a residual correction of:

$$1 - 0.00152\ T$$

was also applied.

The output files created were 67adp[jday][a/p].t and 67bot[jday][a/p].t.

*4.3.3 Clock Correction (*67adpexec1)

The VMADCP data stream was time stamped by the 286 PC clock running the DAS software. The PC clock drifts from the ship's master clock at an approximate rate of one second per hour. This results in there being a timing error associated with the raw data. The time difference was measured several times each day, and a correction was applied to the data. This step created the files 67adp[jday][a/p].corr, 67bot[jday][a/p] and clock[jday][a/p].

*4.3.4 Gyrocompass error correction (*67adpexec2)

The VMADCP measures the water velocity relative to the ship. To calculate true east and north water velocities information on the ship's heading is required. The ship's gyrocompass provides near-continuous measurements of heading, however it can oscillate for several minutes after a manoeuvre. The gyro heading can be corrected using data from the Ashtech ADU-2. However as the Ashtech system does not provide continuous data, a correction can only be applied on an ensemble by ensemble basis. The two minute averaged Ashtech-minus-gyro heading correction ("a-ghdg") was manually despiked and interpolated. The required correction was then applied to the data creating the output files 67adp[jday][a/p].true and 67bot[jday][a/p].true.

4.3.5 Calibration (67adpexec3)

The VMADCP data requires two further corrections:

(i) A an inherent scaling factor associated with the VMADCP velocities;

(ii) ϕ a compensation for the misalignment of the Ashtech antenna array relative to the VMADCP transducers.

Bottom tracked velocities were initially calibrated using a nominal scaling of A=1 (scaling factor) and ϕ=0 (misalignment angle).

The two minute ensembles of VMADCP data were merged with a smoothed version of GPS navigation, and 20 minute average absolute speeds and headings were derived from the satellite fixes. The bottom track VMADCP data were also used to derive 20 minute average speeds and headings. Data outside the range 400-740 cm/s were excluded from the calibration.

A and ϕ were calculated using

$$A = U_{gps} / U_{VMADCP}$$

$$\phi = \phi_{gps} - \phi_{VMADCP}$$

where U_{gps} and U_{VMADCP}, and ϕ_{gps} and ϕ_{VMADCP} are the 20 minute averaged speeds and headings, derived from the GPS and bottom track VMADCP data respectively. The direction of ϕ was reversed to put it in the correct orientation and it was put in the range $-180° < \phi < 180°$. From these calculations, excluding outliers, we derived

$A = 1.0314$ and $\phi = -1.81°$

The data were reprocessed using the new values for A and ϕ to produce calibrated water velocities relative to the ship, creating the output files 67adp[jday][a/p].cal and 67adp[jday][a/p].cal.

A water track calibration was also made, by comparing water tracked VMADCP data from periods when the ship was steaming between stations and maintaining attitude on station. Bad data collected during periods of manoeuvring were excluded from the comparison. The values of A and ϕ determined from this method had greater scatter and variability than those determined from bottom track data, hence it was decided to use the latter for our final calibration.

*4.3.6 Derivation of absolute velocities (*67adpexec4)

Ship's velocities between ensembles were derived by merging in position information from the RVS navigation data. The absolute water velocities were then derived by removing the ship's velocities from the VMADCP data. These final velocities were output to the files 67adp[jday][a/p].abs and 67bot[jday][a/p].abs.

4.3.7 Results

Figures 4.1, 4.2 and 4.3 show (respectively) the variation of %good with depth across the Drake Passage section, the depths from which good bottom track data were obtained, and the mean currents at 100 m

5. SAMPLE SALINITY

Sheldon Bacon, Julie Collins, Alex Sen Gupta

On this cruise, the BAS Guildline 8400B Autosal salinometer, s/n 63360, was used for sample analysis. Its last service and electronic alignment were performed by Ocean Scientific International on 12 June 2001. It was set up at the start of the cruise in the ship's Bio Lab on the Upper Deck. There is no constant-temperature laboratory on the ship, but past experience has shown that the ship's ambient air conditioning is perfectly adequate for holding temperature constant to within a degree or so. The Bio Lab was chosen because it has no direct access to the outside, so normal movement of people around the ship would not expose the lab to occasional draughts of cold air. The lab temperature was monitored constantly (every hour during the section, less frequently thereafter) and it remained within the range 20-21 ˚C, as desired. The salinometer was run at 24 ˚C. We note here that the salinometer appears to have an intermittent fault on the 'Standby' setting, whereby all numbers flash on and off; alternatively, the Standby reading itself, although not the temperature component (+24), goes to zero (0000), and the display flashes. This is symptomatic of a bad connection from the Standby switch and it should be fixed as soon as possible.

Water samples for analysis of salinity were drawn from each Niskin into 200 ml glass sample bottles which were then sealed with clean, dry, disposable plastic stoppers and screw-on caps. The neck of the sample bottle is dried before insertion of the cap. A replicate sample was drawn on most stations from the deepest bottle. Full crates were taken to the Bio Lab to equilibrate. Most of the analysis was performed by ASG and JC, with some done by SB. During the section, samples were drawn from the non-toxic supply for TSG calibration once every four hours. A total of 372 CTD and 32 TSG samples were analysed. The 26 CTD replicate pairs had a mean salinity difference of 0.0001 with standard deviation 0.0014. Nineteen bottles of standard seawater (SSW), batch P140, were consumed.

The salinometer standardisation history is shown in Figure 5.1. A peculiarity is noted whereby the salinometer appears to adopt two distinct standardisation levels, separated by about 0.003 in salinity. It is not clear whether this had affected adversely the sample salinity accuracy. This is discussed further in section 1.8 (CTD conductivity calibration).

As a continuation of the SSW monitoring project described in Bacon, Snaith and Yelland (2001), measurements were made of the salinity of three batches of SSW: P137 and P139 (in ampoules), and P140. Five ampoules of each batch were analysed, standardised on a bottle of P140. The results are shown in Table 5.1, and are consistent with all batches being at label salinity (conductivity ratio) to better than 0.001.

6. UNDERWAY

Alex Sen Gupta, Liz Kent

The oceanlogger system has recently been upgraded from the oceanlogger mark I configuration that was in operation for approximately 10 years. This essentially involves a doubling up of some of the meteorological sensors, a new junction box and a display logger.

The oceanlogger system is connected to meteorological sensors measuring air pressure, air temperature, humidity, total incident radiation (TIR) and photosynthetically available radiation (PAR) as well as sea surface sensors that gather data from the ship's non-toxic pumped sea water supply including sea surface temperature (SST), conductivity and temperature, as part of the thermosalinograph sensor and fluorescence. The oceanlogger has an input from the ship's master clock and provides a real time display of the data. A list of oceanlogger sensors is given in table 6.1.

Meteorological data was collected without interruption for the duration of the cruise. The oceanographic data was available during much of the cruise including the duration of the CTD section. The oceanographic sensors were however turned off during periods when the ship was in sea ice (approx. 334 12:00 – 346 13:00) during transit along the Peninsula.

6.1 Data Preparation

Met data was initially prepared in 12 hour segments to allow a running check of data throughout the cruise. Three scripts (initially written for JR16) that read in and processed 12hr data segments were updated and implemented to do this:

67oclexec0: Reads the ocean-logger data streams into a PSTAR format and merges in relative wind speed and direction from the anemometer data stream;

67oclexec1: Splits data into ocean data and met data files; de-spikes conductivity data and calculates a raw salinity value.

twvelexec: Merges the met data file with gyrocompass and navigation data streams in order to calculate ship motion and true wind velocity.

The 12 hour data segments were manually appended and de-spiked with the aid of the *pedita* utility.

6.2 Salinity

The TSG salinity was calculated using the utility *peos83* from the measured conductivity (cond) and temperature (fstemp) at the housing located in the hanger. During the JR67 section, bottled water samples were taken approximately every 4 hours from the non-toxic sea water supply. These were treated in the same manner as the samples taken for the CTD calibration: a 200ml sample bottle was

rinsed three times, the sample taken, the neck of the bottle dried and an air tight seal inserted. Samples were left to acclimatise by the salinometer for at least 24hrs prior to analysis using an Autosal 63360 model 8400B. This allowed a comparison between bottled samples and TSG salinity derived from the oceanlogger data. The bottle salinities have an average offset of +0.022 PSU (one outlier removed). For calibration a best fit regression between TSG and bottle samples yields an offset:

$$\Delta S = -0.4429 + 0.001423 \times JDAY$$

Mean salinity values for the top 10m of the each of the CTD casts were calculated. These compared well with the calibrated TSG salinities with a mean ± sd offset of –0.00014 ± 0.0044, (3 outliers removed). Figure 6.1 shows salinity measurements from calibrated TSG, underway bottle samples and CTD surface values.

6.3 Sea Surface Temperature

Figure 6.2 shows good agreement between oceanlogger SST data and mean values for the top 10m of the CTD casts. The Deck Log SST from the ship's hull sensor, shows a large offset off approximately 0.75^{o}C. Figure 6.3 shows SST measurements from oceanlogger, CTD surface values and deck log.

6.4 Total Incident Radiation (TIR)

There is a night time (i.e. zero TIR) offset between tir1 and tir2 of ~0.1 W/m^2 (figure 6.4a). The offset increases with increasing total TIR to approximately 2 W/m^2 (figure 6.4a). In figure 6.4a we see zero error for TIR sensors, and in figure 6.4b, tir2-tir1 for a typical day. Both sensors show saturation at high levels of TIR: 641.0256 W/m^2 for tir1, and 609.7561 W/m^2 for tir2 (figure 6.5). The sensors use the calibration equations:

$$\text{tir1}\ [\mathrm{W/m^2}] = \frac{\text{outputvoltage}\ [\mathrm{mV}]}{78\mathrm{E}-3}$$

$$\text{tir2}\ [\mathrm{W/m^2}] = \frac{\text{outputvoltage}\ [\mathrm{mV}]}{82\mathrm{E}-3}$$

which implies a maximum instrument output of 50mV.

6.5 Photosynthetically Active Radiation (PAR)

There is a night time offset between par1 and par2 of ~3 μmol s^{-1}m^{-2} (figure 6.6a). The offset increases with increasing PAR to between 20 – 40 μmol s^{-1}m^{-2} (figure 6.6b).

6.6 Air Pressure

Air pressure sensors show good agreement with each other (mean ± sd press2 – press1 = –0.0055 ± 0.01 mbar), as does the deck log barometer (figure 6.7) with the exception of a few outliers.

6.7 Humidity

Although the oceanlogger display shows outputs for both h1 and h2, the h1 data stream is missing and is outputting atemp1 data in its place. No comparisons of the humidity sensor could therefore be made. Both humidity values were displayed on the Oceanlogger monitor so it seems likely that the wrong datastream has been coded into the SCSS.

6.8 Air Temperature

Figure 6.8 shows the two air temperature sensors and the deck log temperature record, from a remotely read thermometer in Stevenson screens on the wheel house top. A large discrepancy is evident in the deck log temperatures, with the greatest overestimates occurring during increased insolation (scaled PAR is shown for reference). Figure 6.9 shows the offset between oceanlogger temperature sensors (atemp2 – atemp1). This offset has a mean value of 0.1843 ^{o}C, with a number of large positive and negative deviations. A possible explanation for this is demonstrated by figure 6.10 which shows (atemp2-atemp1) as a function of relative wind speed, for a number of different relative wind direction bands (0^{o} represents a wind coming directly over the bows). The two temperature sensors are situated on either side of the forward mast. Between the two sensors is situated a junction box with radiation sensors on top, which will offer some shelter to the sensors depending on the wind direction and speed. For low wind speeds two regions of large temperature offsets can be seen centred around 60^{o} and 260^{o} with a further positive offset centred around 100^{o} for stronger winds. These anomalies would be explained if atemp1 is the starboard sensor, receiving shelter during a wind coming from the port side and atemp2 is the port sensor receiving shelter during a wind coming from the starboard side.

6.9 Anemometer - winds

The anemometer produces relative wind direction and strength, with 0^{o} measured from the bow of the ship. The sensor operation was continuous for the duration of the cruise except for a short period (335 06:00 – 12:00) which coincided with a period of snow fall. The calculated true winds are in oceanographic notation (i.e. bearing is in the direction of flow).

6.10 Flow meter

The flow meter displayed negative data throughout with values between –3.8 and –2.4 l/min.

6.11 Results

For the section / whole cruise: figure 6.11 shows SST and calibrated salinity; figure 6.12 shows SST, humidity and air temperature, where air temperature is calculated by taking the minimum sensor value after the offset: atemp2-0.1843/2 and atemp1+0.1843/2 has been applied (the most exposed sensor would be expected to give the truest value); and figure 6.13 shows true wind speed, colour coded to show true wind direction (oceanographic convention).

7. ECHO-SOUNDER

Julie Collins

The *RRS James Clark Ross* is equipped with two SIMRAD echo sounders, the EM120 and the EA500. During the section the EM120 was periodically switched off as it was interfering with the signal of the EA500. The EA500 has one transducer mounted on the hull just to Starboard. A visual display of the data was displayed on the SIMRAD VDU located on the bridge. An assumed sound velocity of 1500 m/s was used.

Raw data were logged by the SCS into the simulated level C data stream SIM500 and retrieved into a twice daily PSTAR file using the script jr67_sim. The script takes raw data from the SCS every 30 seconds and runs a 5 point filter. The filter removes values greater than 100 metres from the median and assigns an absent data value to zero depths. The zero depths occur when no good data is available. This processing effectively removes many of the spikes in the data. *pintrp* was then used to interpolate between the data gaps and then navigation data was merged in from the BESTNAV data stream using *pmerge*. Finally the script uses *pcarter* to correct the depths.

The twice daily files were then appended together using *papend* and then plotted using *plotxy* for visual inspection. Manual despiking was performed to remove any obviously spurious values using *plxyed*, followed by *pintrp* to linearly interpolate onto the missing data points. After the data looked reasonable, they were reduced to a 1km distance resolution on variable distrun using *pavrge*. This resolution corresponds to approximately a three minute time interval.

Two files exist of the outward journey, 67bathsim.cor and 67bathav.cor. 67bathsim.cor shows a peak at around 56.75 S, which is not present in the bathymetry from JR55. It is thought that this peak arises from the ship drifting whilst on station up and down the slope. It has been left in this file but taken out of 67bathav.cor. The latter version of the data is used for the bathymetry in figure 1.3.

Unfortunately only the outward journey of the transect was completed as another route was taken from the peninsula heading back to Stanley in order for the swath bathymetry to be completed which was abandoned due to bad weather on the outward journey.

8. COMPUTING

Jeremy Robst, Sheldon Bacon

The RRS *James Clark Ross* system for acquiring and processing real-time data is called the Scientific Computing System (SCS; Benigni *et al.*, 1999). SCS version 2.3 is run at present. It acquires sensor data from shipboard and oceanographic sensors which are timestamped and provided to the scientists in real time via text and graphic displays, while simultaneously logging the data to disk for later analysis. SCS runs on a Windows NT 4.0 Server and a Windows NT 4.0 Workstation.

Navigation data (Trimble 4000 GPS and Ashtech ADU-2 GPS) and echosounding data were logged to SCS. These were converted to equivalent RVS Level C files using the utility *scs2levC* and stored on the UNIX workstation JRUF (Sun4u sparc SUNW, Ultra 60 with a 52 Gbyte hard disk).

Gyro data, VM-ADCP and oceanlogger data were logged via Level A's or instrument dedicated PCs to JRUB (Sun4u sparc Ultra1) and then passed to JRUF using the usual RVS utility to convert to PSTAR format (*datapup*). CTD data were logged directly to the PC connected to the deck unit where preliminary processing by SeaBird software was carried out, then FTP'd to JRUF for further processing. This PC is old and slow and should be replaced. Changing network cards and hard disks did nothing to improve either PC processing time or the FTP transmission rate.

Two Xterminal emulators (tektronix; one in the UIC room, one in the data prep. room) were used for logging into JRUF for data analysis; a Mac iBook was used for Telnet to JRUF, and word processing etc.; four PCs in the data prep. room could run Exceed in order for them to be used as terminal emulators connected to JRUF.

Much of the processing used Pstar version 5 and Matlab version 6.1.

Daily (Monday-Saturday) and monthly (Sunday 1-4) backups were carried out for JRUB (to DAT tape), JRUF and SCS (to DLT tape), amongst others.

9. TECHNICAL SUPPORT

Simon Wright, Julie Collins

9.1 Winch

The Winch used for the CTD casts has a maximum wire length of 8000 metres, 10mm diameter and weighs 3648 kg. The wire consists of a copper conductor, a plastic coating and two steel sheaths wound in opposite directions. The breaking load of this wire is 8074 kgf with a recommended safe working load of 3220 kgf.

Winch data was recorded on a PC connected with the winch console and copied to the JCR level A data logging. The data is logged every 15 seconds while the winch is working. The cableout value was manually reset to zero on every CTD deployment when the instrument was at the surface. The usual processing of the winch data involves merging with the CTD files of corresponding times. However, the PC clock was unstable and its difference to the master clock on board was not recorded. Therefore the data has not been merged onto the CTD files.

The raw data is retrieved from the winch file using the script *win0*. The station number, start and end time of the cast are required to create files for each cast. The start and end of the casts are when the cableout value is zero which does not correspond to the start and end of the file. The data were then plotted using *plotxy* to check that there were no irregularities. Station 17 appears to have a time gap of 6 minutes on the downcast, which causes a step feature. Data from approximately 630 metres to 1060 metres is missing. The rest of the file appears normal and the total wireout corresponds to the depth achieved by the CTD.

9.2 Engineering

The cruise required the amalgamation of the BAS CTD, water bottles, pylon and associated equipment with the large SOC frame to allow spaces for the LADCP units. This should have been a straight-forward operation as it used standard components. However, the lower bottle clamping blocks required machining due to a change in design. On the BAS CTD the lower support ring, that the bottle blocks rest on, is a slot right across the surface of the ring; where on the SOC one this is a machined recess. This makes the distance between hole for the locating pin in the nylon block and the edge of the block critical. On the BAS bottles this distance is approximately 6mm, but this was too great to allow the bottles to sit down on the pins of the SOC frame. Approximately 0.9 mm was machined off each block to a height of 20 mm, allowing the bottles to be fitted. Further blocks were machine to secure the CTD unit, but this was due to the provided been lost in transit.

During the stations off Rothera Research Station a cast was done to calibrate the base Chelsea Instruments “Aquapak”. This was secured to the frame by removing one bottle and suspending in by a strop alongside the Seabird instrument and tied to the frame to prevent collisions occurring and seemed to work well.

The cable only suffered one termination failure during the cruise and the details of this are covered elsewhere in this report. Apart form this, the ship’s winch side of things operated correctly and did not cause any delays to the cruise programme. Any comments/recommendations the users wish to make would be most welcome and will be given full consideration for future modifications.

REFERENCES

Bacon, S., H. M. Snaith & M. J. Yelland, 2000: An evaluation of some recent batches of IAPSO standard seawater. *J. Atmos. Oceanic Tech.*, **17** (6) 854-861.

Benigni, D., D. Shields, T. Stepka and J. Brockett, 1999: Scientific Computer System (SCS) Version 2.3 for Windows NT 4.0. U. S. National Oceanic and Atmospheric Administration, Marine and Aircraft Operations, Software Engineering Division, Silver Spring, Maryland, various pagination.

Cunningham, S. A., 2001: RRS *James Clark Ross* Cruise JR55, 21 Nov – 14 Dec 2000. Drake Passage Repeat Hydrography: WOCE Southern Repeat Section 1b – Burdwood Bank to Elephant Island. Southampton Oceanography Centre, Cruise Report, No. 35, 75 pp.

Heywood, K. J. and D. P. Stevens, 2000: RRS *James Clark Ross* Cruise JR40, 15 Mar – 22 Apr 1999. Albatross: Antarctic Large-scale Box Analysis and the Role of the Scotia Sea. University of East Anglia, Cruise Report, No. 6, 61 pp.

Smith, W. H. F. and D. T. Sandwell, 1997: Global sea floor topography from satellite altimetry and ship depth soundings. *Science* **277** (5334) 1956-1962.

TABLES

Table 1.1: CTD Sensors Used on JR 67.

Instrument	Type	Serial Number	Calibration Date
Underwater Unit	SBE 9 plus	09P15759-0480	-
Deck Unit	SBE 11 plus	11P15759-0458	-
Primary Temperature	SBE 3 plus	03P2709	12-Sep-00
Primary Conductivity	SBE 4C	042255	13-Sep-00
Secondary Temperature	SBE 3 plus	03P2705	02-Jul-01
Secondary Conductivity	SBE 4C	042222	13-Sep-00
Pressure Transducer	Series 410K-105 Digiquartz pressure transducer.	067241	30-Jun-00
Altimeter	Tritech	2130.26993	-
Frame	SOC 24 bottle with fin		-
Pylon	SBE 32	90194U 3220391-0128	-
Niskin Bottles			-
Primary Pump	SBE 5 T	051813	
Secondary Pump	SBE 5 T	051807	
Swivel	Focal Instruments, Model 196	196111	10-Sep-01
seasoft software	Version 4.226		

Table 1.2: JR67 CTD Stations. The three lines for each station represent the start, maximum depth and end of the station. Water depth (metres) is the Simrad value corrected for speed of sound from the Carter Tables. Wireout (metres, figure in italics) is the maximum value from the winch file, maximum pressure (db) comes from the CTD data file. Calculated depth (metres) is calculated from the maximum pressure. Depth difference (metres, figure in italics) is water depth – (calculated depth + altimeter) where altimeter is the minimum depth off the bottom from the altimeter in metres.

Station	Day Time	Latitude	Longitude	Water Depth	*Wireout* Max. Pressure	Calc. Depth	*Depth difference* Altimeter	Notes
001	324 07:36:22	53 22.177 S	57 59.778 W	2091	*2040*		*+3*	Test Station
	324 08:16:27	53 25.208 S	57 59.242 W	2099	2075.5	2046	50.4	
	324 08:54:11	53 25.291 S	57 59.329 W	2109				
002	324 16:14:30	54 39.240 S	58 33.534 W	231	*222*		*-2*	Burdwood
	324 16:22:07	54 39.264 S	58 33.558 W	231	225.2	223	10.4	Bank
	324 16:33:28	54 39.270 S	58 33.576 W	231				
003	324 18:51:50	54 55.218 S	58 21.594 W	569	*606*		*-22*	
	324 19:04:20	54 55.296 S	58 21.648 W	597	616.9	610	9.3	
	324 19:32:14	54 55.446 S	58 24.768 W	614				
004	324 20:24:03	54 56.484 S	58 21.858 W	986	*1205*		*-76*	
	324 20:46:12	54 56.628 S	58 21.870 W	1142	1224.7	1210	7.8	
	324 21:25:06	54 56.652 S	58 21.960 W	1158				
005	324 22:09:53	54 57.522 S	58 22.068 W	1504	*1565*		*-30*	
	324 22:37:56	54 57.654 S	58 22.074 W	1553	1592.9	1572	10.9	
	324 23:21:00	54 57.750 S	58 22.026 W	1560				
006	325 00:42:23	55 04.182 S	58 17.382 W	2065	*2050*		*-2*	
	325 01:17:26	55 04.182 S	58 17.388 W	2066	2088.0	2059	9.3	
	325 02:12:40	55 04.446 S	58 17.238 W	2109				
007	325 03:17:11	55 07.248 S	58 15.372 W	2513	*2495*		*+1*	
	325 03:59:40	55 07.278 S	58 15.456 W	2518	2545.3	2507	9.7	
	325 05:02:45	55 07.422 S	58 15.336 W	2530				
008	325 06:09:35	55 10.212 S	58 13.902 W	2957	*2965*		*-30*	
	325 07:01:12	55 10.200 S	58 14.004 W	2955	3028.4	2979	5.5	
	325 08:08:07	55 10.458 S	58 13.980 W	3021				
009	325 09:17:10	55 12.846 S	58 13.686 W	3597	*3740*		*-89*	
	325 10:22:34	55 12.864 S	58 13.704 W	3682	3829.1	3760	10.7	
	325 11:43:30	55 13.128 S	58 13.536 W	3820				
010	325 14:24:35	55 31.482 S	57 59.094 W	4219	*3015*			Termination
	325 15:15:05	55 31.434 S	57 59.214 W	4229	3018.7	2970	-	failed
	-	-	-	-				
011	325 19:16:58	55 49.326 S	57 51.948 W	4649	*4650*		*+1*	
	325 20:37:40	55 49.590 S	57 51.576 W	4685	4768.7	4673	10.9	
	325 22:24:31	55 50.220 S	57 50.730 W	4726				
012	326 00:38:39	56 07.794 S	57 40.116 W	3671	*3579*		*-54*	
	326 01:39:27	56 07.842 S	57 39.018 W	3582	3694.9	3629	7.4	
	326 03:02:14	56 07.764 S	57 37.434 W	3453				
013	326 06:13:04	56 27.702 S	57 30.594 W	3575	*3550*		*-2*	
	326 07:12:08	56 27.744 S	57 29.556 W	3575	3627.2	3563	13.9	
	326 08:30:01	56 27.894 S	57 28.056 W	3601				
014	326 10:37:45	56 47.052 S	57 17.916 W	2606	*2900*		*-37*	
	326 11:35:00	56 46.818 S	57 16.284 W	2864	2920.1	2873	28.2	
	326 12:44:03	56 46.704 S	57 14.394 W	2914				
015	326 14:51:27	57 05.430 S	57 07.254 W	4410	*4400*		*+8*	
	326 16:09:10	57 05.124 S	57 06.366 W	4422	4489.3	4401	12.9	
	326 17:44:41	57 04.578 S	57 04.866 W	4433				

016	326 20:09:11	57 25.512 S	56 55.764 W	3974	*3940*		*+6*	
	326 21:17:40	57 25.662 S	56 55.932 W	3978	4036.9	3962	10.2	
	326 22:48:15	57 25.962 S	56 55.860 W	3979				
017	327 00:55:34	57 43.758 S	56 40.830 W	3440	*3395*		*+7*	
	327 01:54:05	57 44.064 S	56 40.620 W	3432	3473.7	3413	11.8	
	327 03:13:48	57 44.430 S	56 40.470 W	3472				
018	327 05:28:36	58 02.688 S	56 32.430 W	4017	*3985*		*-1*	
	327 06:36:32	58 2.6700 S	56 32.262 W	4016	4083.2	4007	9.6	
	327 07:59:50	58 02.562 S	56 32.046 W	4017				
019	327 10:07:30	58 21.798 S	56 21.144 W	3822	*3790*		*-1*	
	327 11:11:12	58 22.044 S	56 21.078 W	3820	3880.6	3809	11.5	
	327 12:38:45	58 22.530 S	56 20.832 W	3810				
020	327 14:46:28	58 41.148 S	56 09.366 W	3780	*3757*		*+4*	
	327 15:53:03	58 41.256 S	56 09.288 W	3782	3838.6	3769	8.9	
	327 17:17:43	58 41.604 S	56 09.024 W	3787				
021	327 20:06:36	58 59.412 S	55 57.870 W	3793	*3740*		*+2*	
	327 21:12:24	58 59.802 S	55 57.708 W	3772	3830.1	3760	10.1	
	327 22:43:59	58 59.994 S	55 57.414 W	3762				
022	328 00:52:42	59 18.714 S	55 42.876 W	3728	*3695*		*+3*	
	328 01:55:11	59 18.996 S	55 42.690 W	3727	3785.2	3716	7.6	
	328 03:17:00	59 19.398 S	55 42.420 W	3728				
023	328 05:32:12	59 38.940 S	55 31.020 W	3683	*3665*		*+5*	
	328 06:33:43	59 39.396 S	55 30.294 W	3687	3742.3	3674	8.4	
	328 07:50:35	59 39.948 S	55 29.388 W	3683				
024	328 09:57:47	60 00.006 S	55 18.924 W	3503	*3470*		*+4*	
	328 10:56:30	60 00.216 S	55 19.098 W	3503	3553.3	3490	8.6	
	328 12:22:04	60 00.678 S	55 18.840 W	3504				
025	328 14:36:12	60 20.166 S	55 04.644 W	3441	*3415*		*+4*	
	328 15:35:00	60 20.226 S	55 04.626 W	3441	3489.3	3428	9.2	
	328 17:00:52	60 20.784 S	55 04.110 W	3451				
026	328 19:12:37	60 40.092 S	54 48.888 W	3113	*3080*		*+10*	
	328 20:08:06	60 40.524 S	54 48.774 W	3115	3147.9	3095	10.2	
	328 21:26:44	60 40.584 S	54 48.780 W	3113				
027	328 22:36:47	60 47.658 S	54 43.188 W	2490	*2490*		-	
	328 23:22:17	60 47.586 S	54 43.404 W	2501	2542.4	2503		
	329 00:19:52	60 48.078 S	54 43.452 W	2449				
028	329 01:01:02	60 49.704 S	54 43.440 W	1808	*1580*		-	
	329 01:27:37	60 50.070 S	54 43.506 W	1610	1610.8	1589		
	329 02:08:53	60 50.148 S	54 43.446 W	1565				
029	329 02:40:48	60 50.620 S	54 43.020 W	1222	*1025*		*-44*	
	329 03:02:23	60 50.946 S	54 42.732 W	995	1045.2	1032	6.9	
	329 03:28:53	60 51.102 S	54 42.600 W	941				
030	329 04:40:16	60 58.650 S	54 37.254 W	597	*570*		*+5*	
	329 04:51:47	60 58.842 S	54 37.140 W	589	581.4	575	8.9	
	329 05:10:50	60 59.106 S	54 37.014 W	586				
031	329 06:01:13	61 02.880 S	54 36.264 W	404	*380*		*0*	Elephant
	329 06:08:38	61 03.018 S	54 36.336 W	393	386.6	382	10.7	Island
	329 06:23:22	61 02.958 S	54 36.654 W	410				
032	330 04:12:45	58 59.700 S	60 13.080 W	3954	*3880*		*-77*	For JR69
	330 05:17:40	58 59.704 S	60 13.020 W	3836	3971	3897	15.9	Geophysics
	330 06:26:47	58 59.709 S	60 13.023 W	3866				
033	338 20:30:37	67 35.312 S	68 08.648 W	311	*111*		-	Rothera,
	338 20:33:09	67 35.312 S	68 08.649 W	309	114	-	-	cast failed
	-	-	-	-				
034	343 10:28:14	67 34.734 S	68 08.088 W	372	*365*		*-6*	Rothera
	343 10:35:24	67 34.734 S	68 08.086 W	372	370	366	12.4	time series
	343 10:57:13	67 34.734 S	68 08.086 W	373				

Table 1.3: Variables extracted from raw SeaBird CTD file with *datcnv*.

0	Scan number
1	Time [s]
2	Pressure [db]
3	Primary Temperature [°C, ITS-90]
4	Primary Conductivity [$mScm^{-1}$]
5	Secondary Temperature [°C, ITS-90]
6	Secondary Conductivity [$mScm^{-1}$]
7	Pressure Temperature [°C]
8	Number of bottles fired
	Altimeter [m]

Table 1.4: Values of dcdt as a function of temperature for CELLTM calculation.

Temperature (ºC)	dcdt
-5	0.085
0	0.088
5	0.091
10	0.094
15	0.097
20	0.100
25	0.103
30	0.106
35	0.109

Table 1.5: Noise in derived quantities from combinations of primary and secondary sensors. Noise is defined as the standard deviation of the differences of instantaneous values from 1 second smoothed values.

Temperature Sensor	Conductivity Sensor	Salinity Noise [psu]	Potential Temperature Noise [°C]
Primary	Primary	0.0010	0.00273
Secondary	Secondary	0.0012	0.00273
Primary	Secondary	0.0036	0.00273
Secondary	Primary	0.0034	0.00274

Table 1.6: Mean salinity in potential temperature (θ, ˚C) bands for both primary (S1) and secondary (S2) sensors, with depth range (Pmax, maximum pressure, and Pmin, minimum pressure, in dbar), by station.

θ range: 0.9 ≤ θ ≤ 1.0				
Station	*S1*	*S2*	*Pmin*	*Pmax*
09	34.7184	34.7199	3298	3435
11	34.7183	34.7198	3661	3797
12	34.7187	34.7202	3332	3430
13	34.7184	34.7199	3026	3141
14	34.7172	34.7187	2658	2711

θ range: 0.75 ≤ θ ≤ 0.80				
Station	*S1*	*S2*	*Pmin*	*Pmax*
09	34.7134	34.7149	3598	3668
11	34.7137	34.7152	3994	4180
13	34.7134	34.7148	3231	3314
14	34.7128	34.7143	2754	2846
15	34.7128	34.7144	2561	2623

θ range: 0.2 ≤ θ ≤ 0.3				
Station	*S1*	*S2*	*Pmin*	*Pmax*
15	34.6907	34.6922	3544	3819
16	34.6907	34.6924	3251	3359
17	34.6905	34.6922	3164	3298
19	34.6906	34.6926	2830	2963
20	34.6919	34.6939	2753	2860
21	34.6914	34.6931	2771	2934
22	34.6903	34.6922	2673	2866

Table 1.6 continued.

θ range: –0.2 ≤ θ ≤ –1.0				
Station	*S1*	*S2*	*Pmin*	*Pmax*
18	34.6658	34.6677	3757	4004
19	34.6662	34.6680	3511	3870
20	34.6662	34.6680	3449	3839
21	34.6664	34.6681	3451	3758
22	34.6659	34.6677	3363	3673
23	34.6656	34.6675	3193	3498
25	34.6651	34.6672	2885	3346
26	34.6658	34.6680	2562	2962
27	34.6653	34.6676	2500	2542

θ range: 0.75 ≤ θ ≤ 0.85				
Station	*S1*	*S2*	*Pmin*	*Pmax*
24	34.6642	34.6662	2982	3251
25	34.6651	34.6672	2885	3346

Table 1.7: CTD header times and offsets. Original time in header file, offset added to header time to force agreement with the LADCP pc clock and final time as inserted into the CTD pstar header.

Station	SeaBird Start Time	Time Offset from LADCP (seconds)	Final Header Time
001	Nov 20 1901 07:22:54	-3	2001/11/20 07:22:51
002	Nov 20 1901 16:00:47	-11	2001/11/20 16:00:36
003	Nov 20 1901 18:48:11	-12	2001/11/20 18:47:59
004	Nov 20 1901 20:19:19	-13	2001/11/20 20:19:06
005	Nov 20 1901 22:05:03	-14	2001/11/20 22:04:49
006	Nov 21 1901 00:38:50	-16	2001/11/21 00:38:34
007	Nov 21 1901 03:13:38	-17	2001/11/21 03:13:21
008	Nov 21 1901 06:04:40	-18	2001/11/21 06:04:22
009	Nov 21 1901 09:14:11	-21	2001/11/21 09:13:50
010	Nov 21 1901 14:19:44	-24	2001/11/21 14:19:20
011	Nov 21 1901 19:11:03	-27	2001/11/21 19:10:36
012	Nov 22 1901 00:33:22	-30	2001/11/22 00:32:52
013	Nov 22 1901 06:06:53	-33	2001/11/22 06:06:20
014	Nov 22 1901 10:31:54	0	2001/11/22 10:31:54
015	Nov 22 1901 14:46:58	-2	2001/11/22 14:46:56
016	Nov 22 1901 20:02:39	-6	2001/11/22 20:02:33
017	Nov 23 1901 00:50:01	-8	2001/11/23 00:49:53
018	Nov 23 1901 05:22:45	-12	2001/11/23 05:22:33
019	Nov 23 1901 10:03:43	-2	2001/11/23 10:03:41
020	Nov 23 1901 14:42:46	-4	2001/11/23 14:42:42
021	Nov 23 1901 20:04:55	-8	2001/11/23 20:04:47
022	Nov 24 1901 00:46:45	-11	2001/11/24 00:46:34
023	Nov 24 1901 05:25:26	-14	2001/11/24 05:25:12
024	Nov 24 1901 09:54:19	-2	2001/11/24 09:54:17
025	Nov 24 1901 14:32:35	-5	2001/11/24 14:32:30
026	Nov 24 1901 19:04:07	-7	2001/11/24 19:04:00
027	Nov 25 1901 22:30:22	-9	2001/11/24 22:30:13
028	Nov 25 1901 00:55:02	-10	2001/11/25 00:54:52
029	Nov 25 1901 02:35:22	-12	2001/11/25 02:35:10
030	Nov 25 1901 04:34:37	-13	2001/11/25 04:34:24
031	Nov 25 1901 05:56:11	-15	2001/11/25 05:55:56
032	Nov 26 1901 04:07:37	0	2001/11/26 04:07:37
033	Dec 04 1901 20:29:28	0	2001/12/04 20:29:28
034	Dec 09 1901 10:21:43	0	2001/12/09 10:21:43

Table 1.8: Summary statistics for comparison between SeaBird CTD and SBE35 standard thermometer. The upper number in each cell is the mean difference in temperature and the lower number is the standard deviation.

	Method 1 (3 seconds before firing to 5 seconds afterwards)	Method 2 (0 to 24 seconds after bottle firing)
SBE35 – SBE911 primary	-0.0133 0.0319	-0.0029 0.0212
SBE35 – SBE911 secondary	-0.0060 0.0297	0.0000 0.0217
SBE911, primary - secondary	0.0073 0.0107	0.0030 0.0040

Table 5.1: Results of salinity analysis of Standard Seawater. Five of each batch were analysed, standardised on a bottle of P140. Label salinity was calculated from label conductivity ratio (K15). sd is standard deviation.

Batch	Label salinity	Mean salinity	Salinity sd
P137	34.9965	34.9961	0.0001
P139	34.9972	34.9979	0.0002
P140	34.9980	34.9975	0.0003

Table 6.1: Meteorological Instrumentation.

Instrument	Make / Serial No.	Location	Data Stream	Last Calibrated
Digital Barometer	Vaisala PTB210 Classe B V145002	Logger rack	BAR1	10-04-00
DigitalBarometer	Vaisala PTB210 Classe B V145003	Logger rack	BAR1	10-04-00
Air humidity and temperature	Rotronic MP103A-CG030-W4W, Sn. 15619015	For'd mast	HT2	29-03-00
Air humidity and temperature	Rotronic MP103A-CG030-W4W, Sn. 15619025	For'd mast	HT1	29-03-00
Thermosalinograph	SBE45 4524698-0016	Prep lab	SST Cond fstemp	04-12-00
Fluorometer		Prep lab		
TIR sensor (pyranometer)	Kipp & Zonen SP LITE 990684	For'd mast	TIR2	18-11-99
TIR sensor (pyranometer)	Kipp & Zonen SP LITE 990685	For'd mast	TIR1	18-11-99
PAR sensor	Kipp & Zonen Quantum PAR LITE 990069	For'd mast	PAR2	08-10-99
PAR sensor	Kipp & Zonen Quantum PAR LITE 990070	For'd mast	PAR1	08-10-99
Flow meter	45/59462	Prep room		03-5-01
Uncontaminated seawater temp		Transducer space		
Ultrasonic Anemometer	Solent Meteorological (standard anemometer) software v4.xx	For'd mast		1994 (during installation)

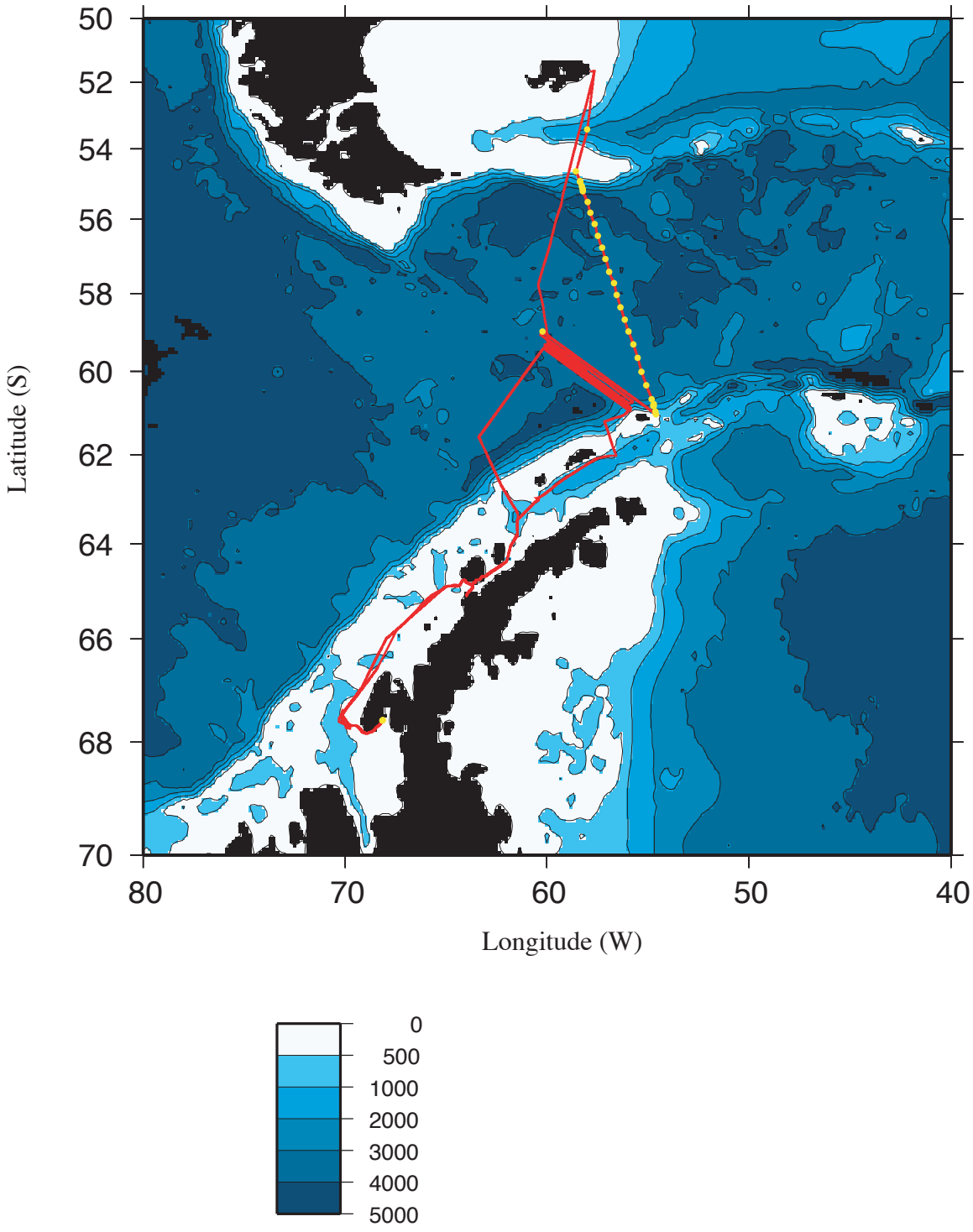

Figure 0.1: Cruise track for RRS James Clark Ross cruise 67 (red line) showing CTD station positions (yellow dots). The bathymetry is from the Smith and Sandwell (1997) dataset. The key shows depths in metres.

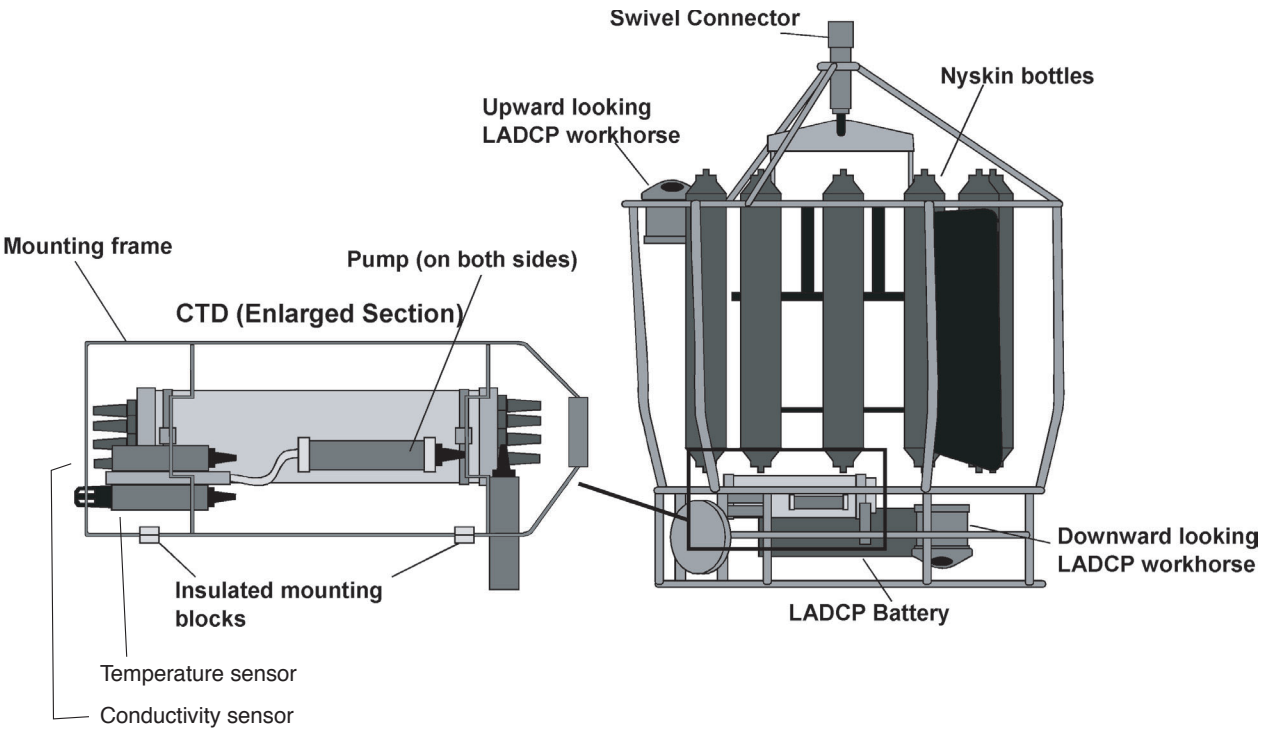

Figure 1.1: Schematic of frame, showing upward and downward looking Workhorse ADCPs and the ADCP battery position; the enlarged section shows the CTD and indicates the position of one set of pump and sensors, with temperature sensor below and conductivity sensor above. A similar second sensor set is located on the opposite side of the CTD. The sea cable is connected to the electronics via a conducting swivel. The supporting tripod is non-load-bearing, it merely serves to keep the swivel upright and away from the Niskin bottles when on deck.

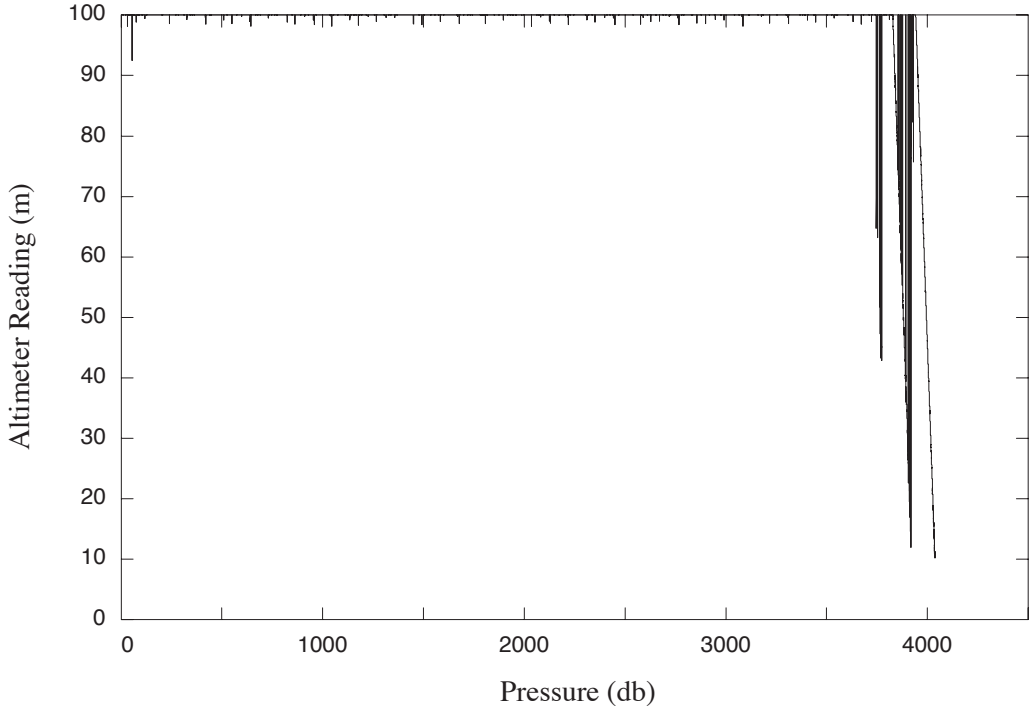

Figure 1.2a: Altimeter output for station 16.

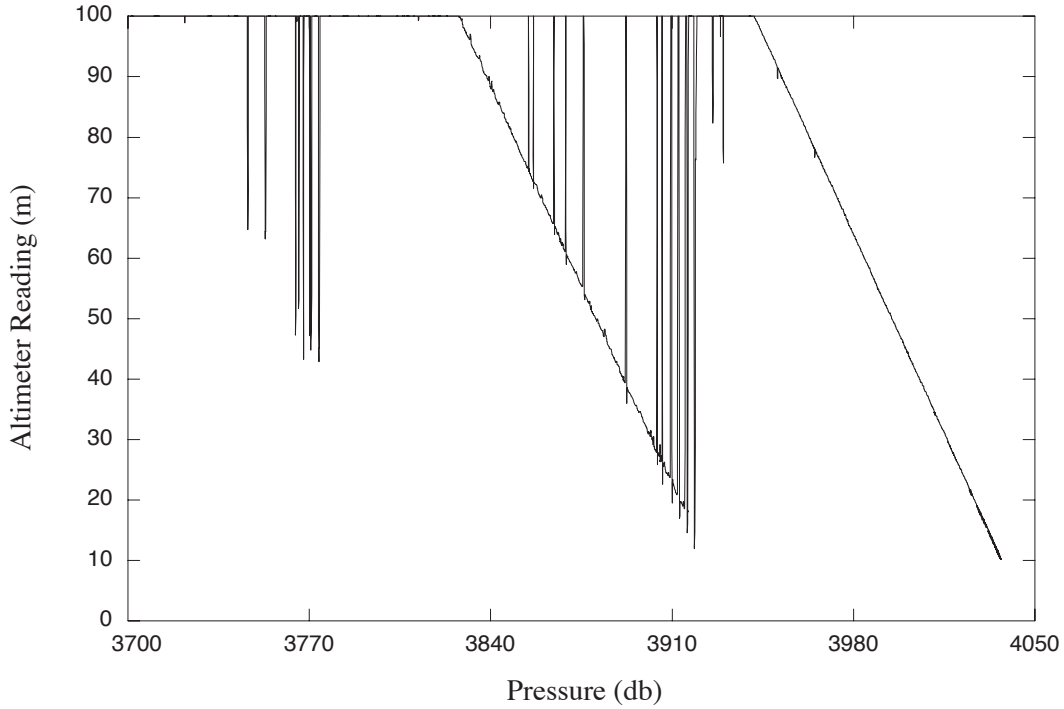

Figure 1.2b: Altimeter output for the bottom 350 db of station 16. The true signal of the seabed is much cleaner than the false signal that precedes it. Some noise is also seen above the false signal.

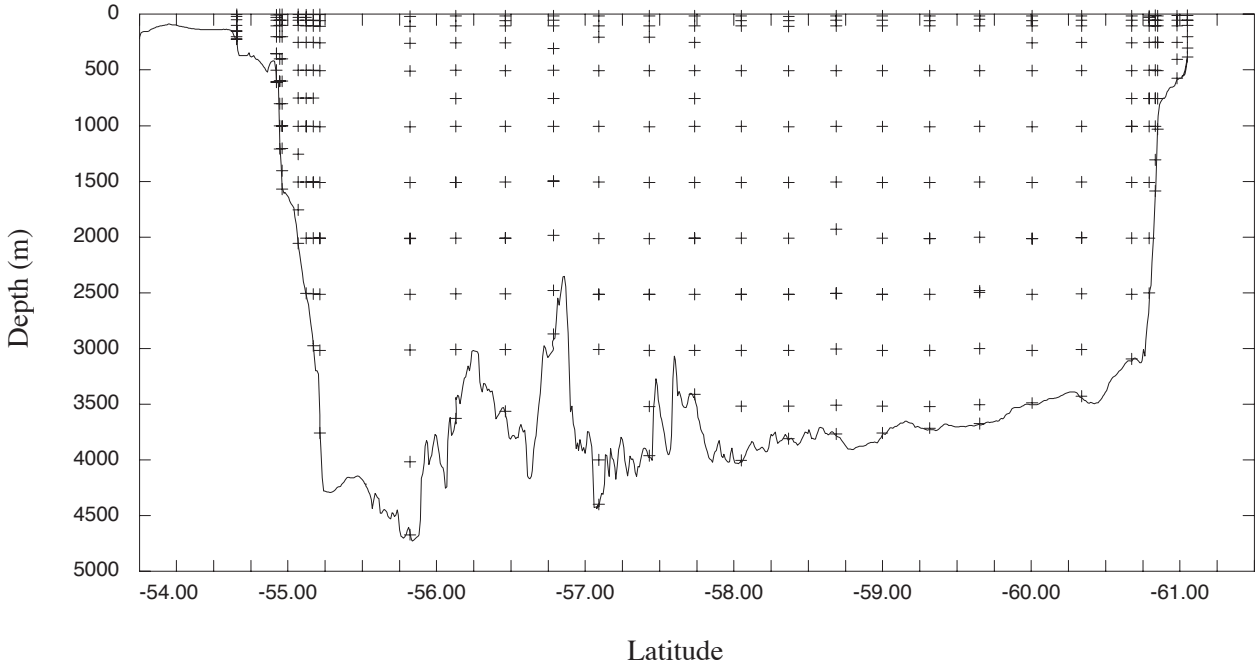

Figure 1.3: The bathymetry of the section across Drake Passage from the Simrad echosounder. Crosses (+) show the latitudes and depths of the bottle samples taken to calibrate the CTD conductivity sensors. Note the gap near the north end of the section where the CTD termination failed leading to no bottles being fired on station 10.

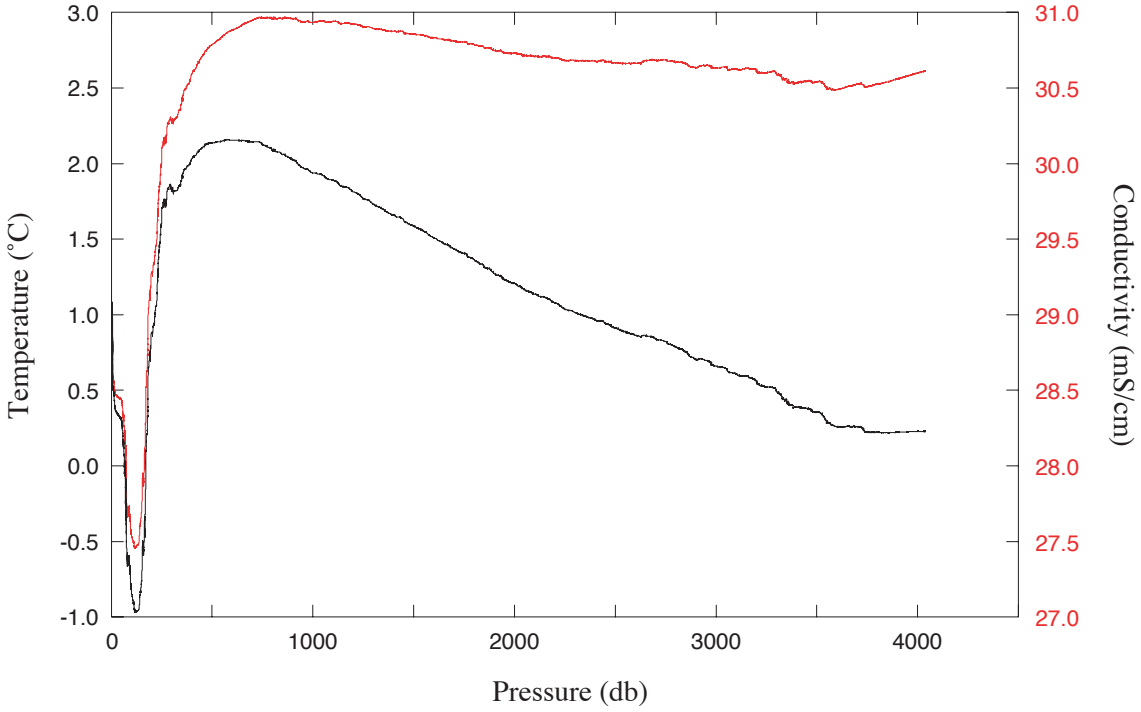

Figure 1.4: Temperature (˚C, black line) and conductivity (mS/cm, red line) from the primary sensor pair for station 16. Downcast only is plotted and the data have not been edited.

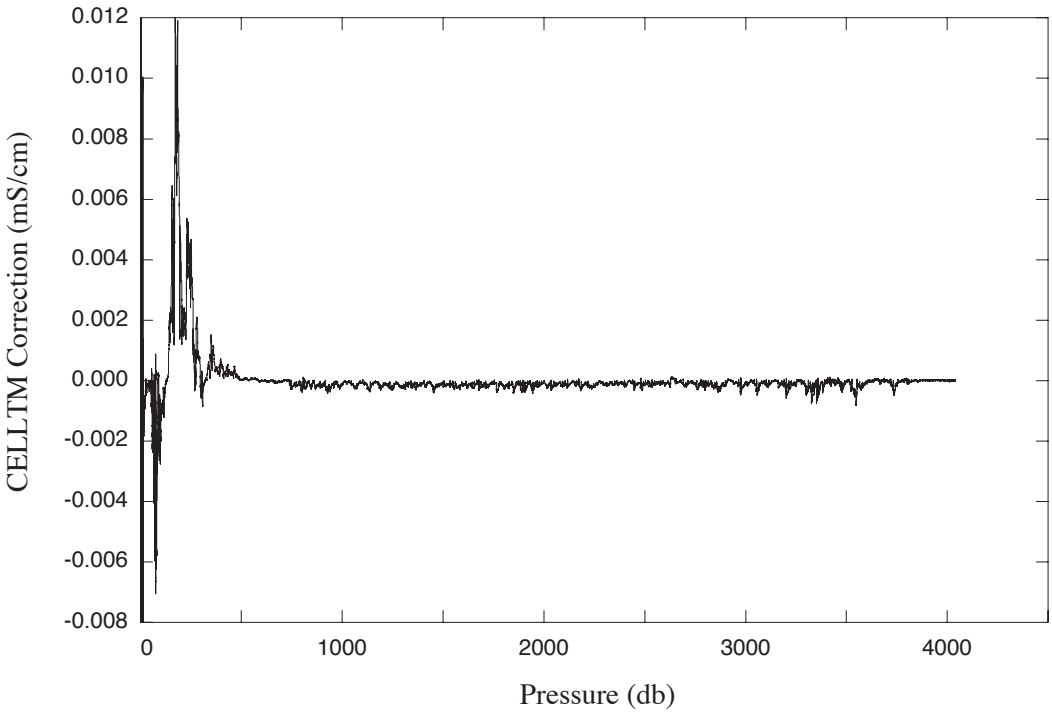

Figure 1.5: The value of the conductivity cell thermal mass correction (mS/cm) applied to station 016.

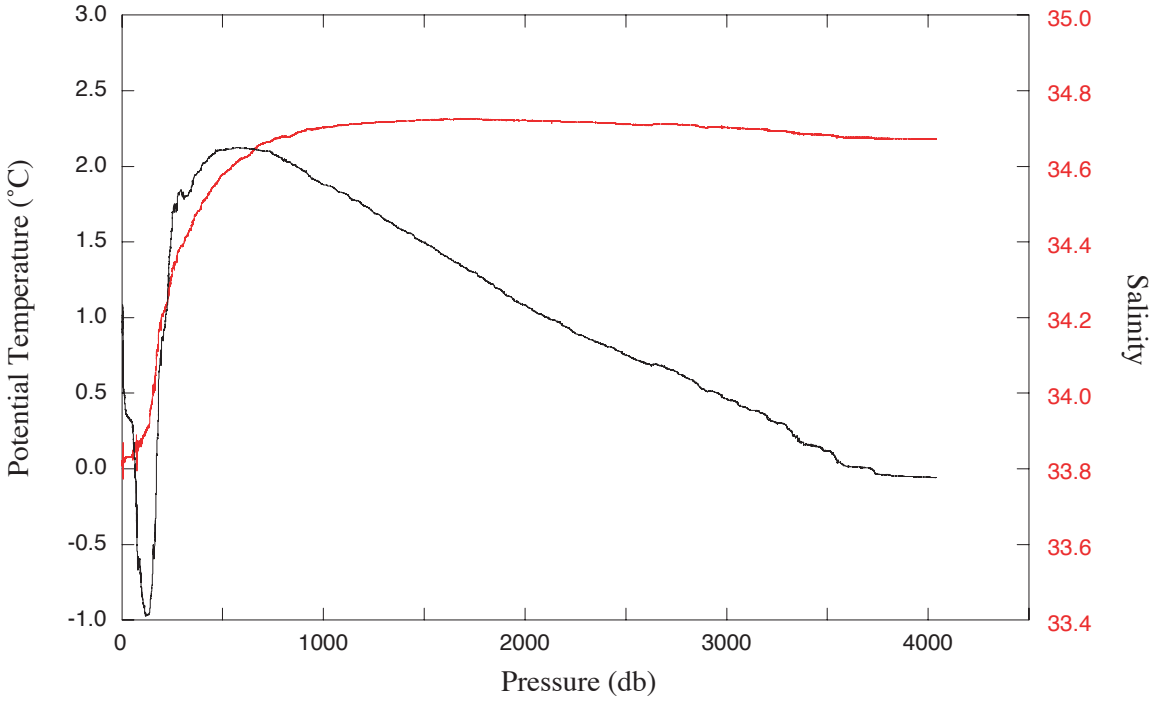

Figure 1.6: Potential Temperature (ºC, black line) and Salinity (psu, red line) from the primary sensor pair for the downcast of Station 016.

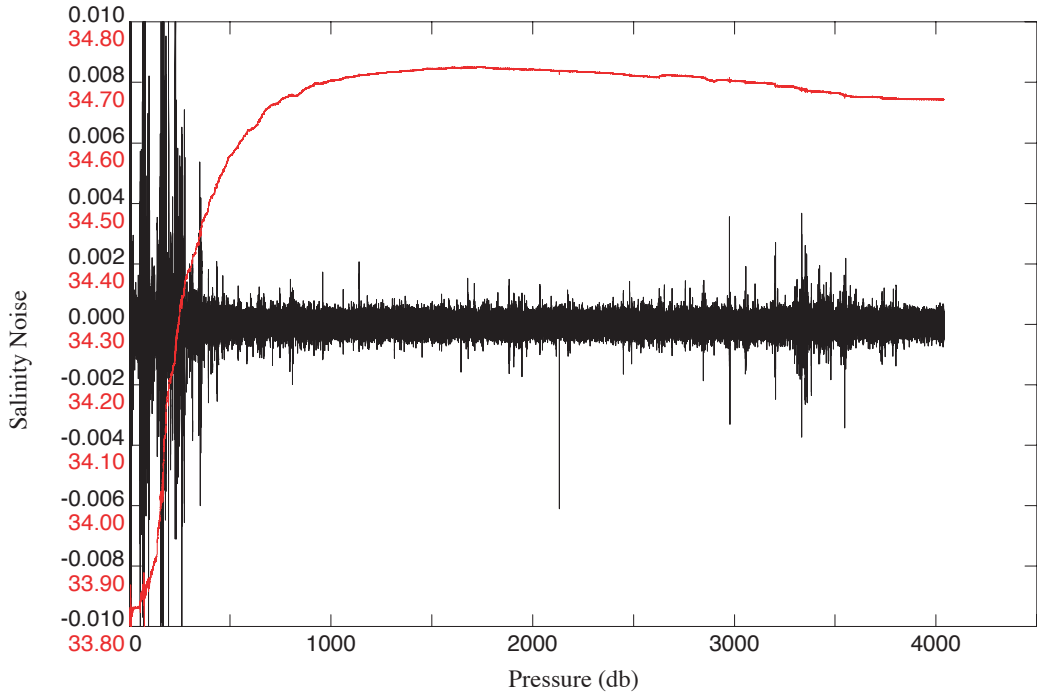

Figure 1.7: Instantaneous salinity difference (psu, black line) from a 25/24 second filtered salinity from the primary sensor for station 016. Also plotted in red is the same salinity from figure 1.6.

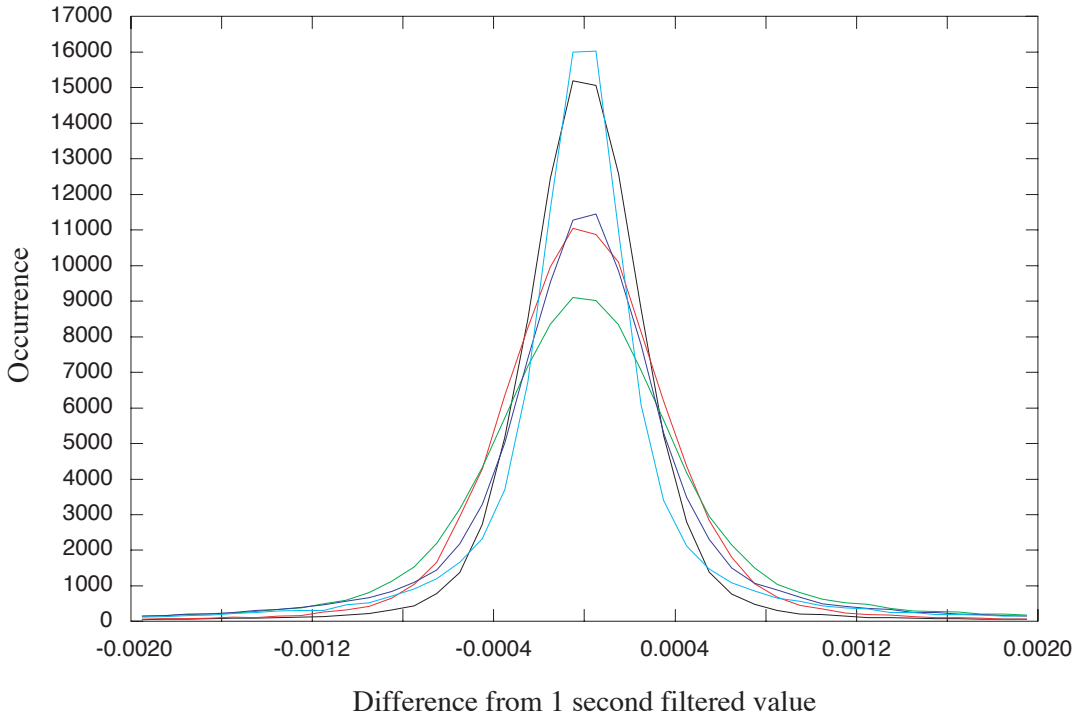

Figure 1.8: Histograms of the occurrences on Station 016 of the instantaneous differences in salinity (psu) and potential temperature (ºC) as shown in Figure 1.7. The black line is the distribution of the salinity calculated from the primary sensor pair, the red line from the secondary sensor pair. The green line is salinity calculated from the primary temperature and secondary conductivity sensor and the dark blue line the salinity from the secondary temperature sensor and the primary conductivity sensor. The light blue line shows the distribution of noise in potential temperature calculated for the primary sensor pair. The other distributions for temperature are very similar.

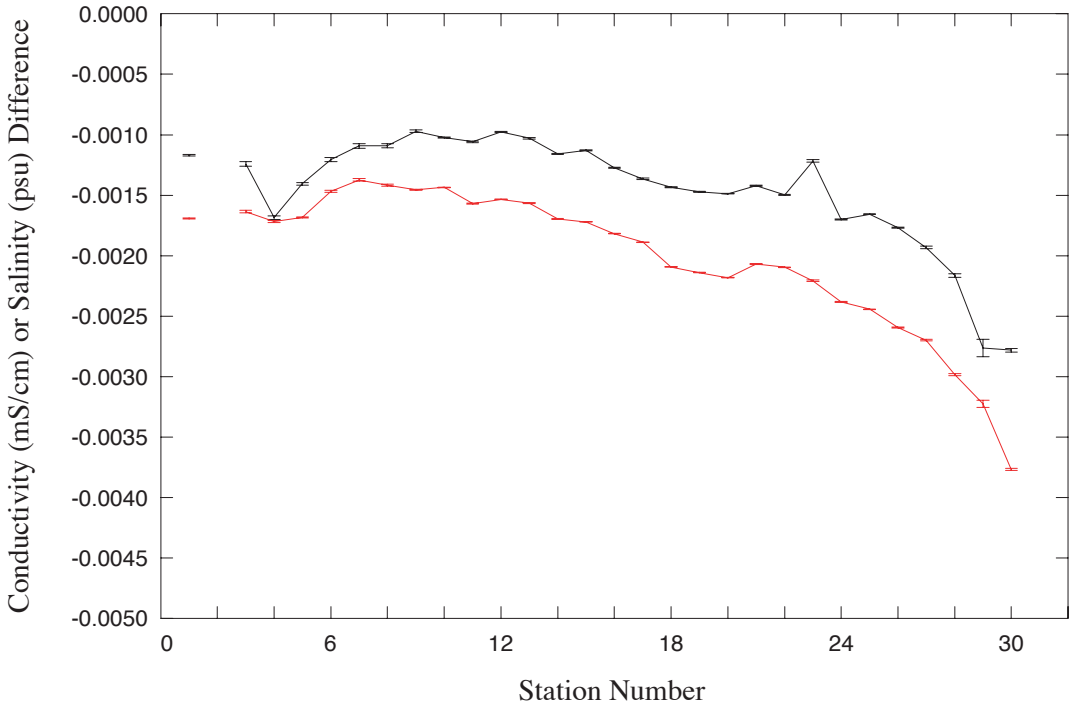

Figure 1.9: The mean difference (primary – secondary) between conductivities (mS/cm, black line) and salinities (psu, red line) as a function of station number.

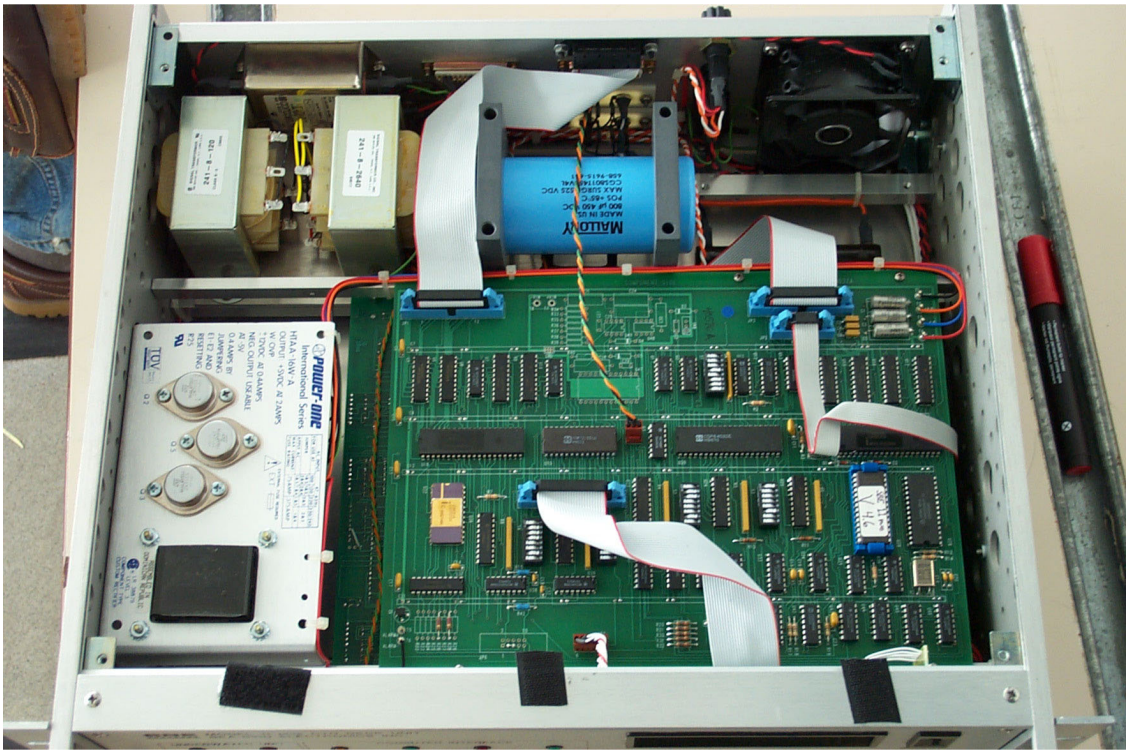

Figure 1.10a: Photograph of the inside of the Deck Unit. The five dip switches are visible on the microprocessor board: S1 centre right; by the lower ribbon lead, S4 and (partly obscured) S5; S2 and S3 to their right.

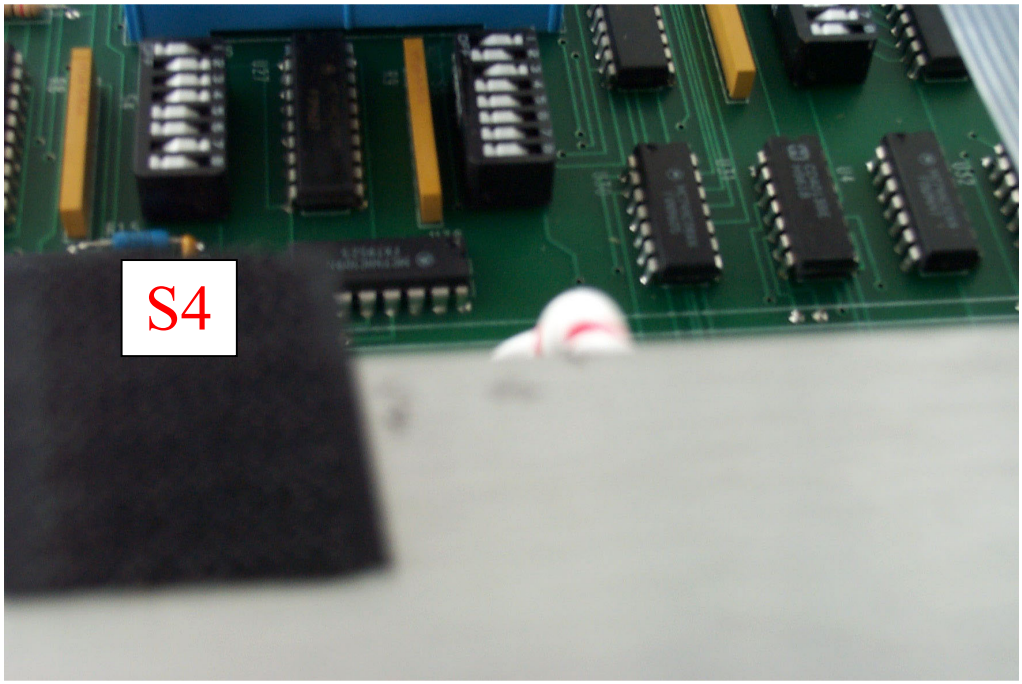

Figure 1.10b: Close up of switch S4 inside the Deck Unit showing the positions of the switches giving the conductivity advance applied to the primary conductivity channel.

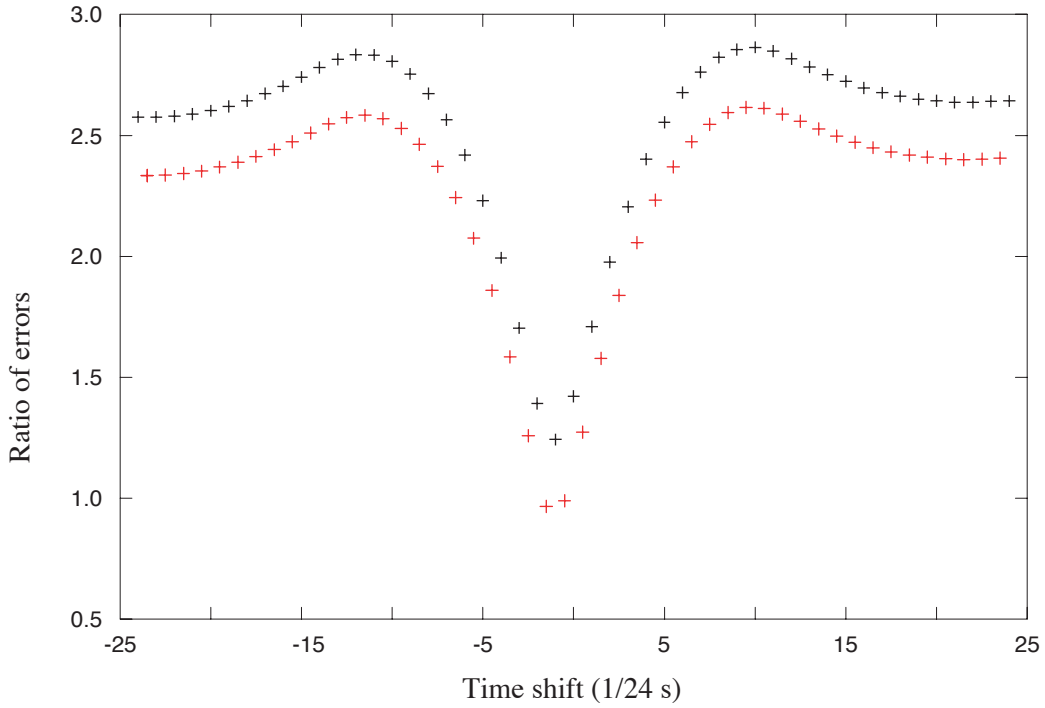

Figure 1.11: Ratio of noise in the secondary salinity to that in the primary salinity as a function of time shift applied to the secondary conductivity in units of cycles (1/24 seconds). The black crosses are for unit time shifts and the red crosses for half-unit time shifts. The difference between the two lines can be explained by the averaging effect of applying a non-unit time shift to the data.

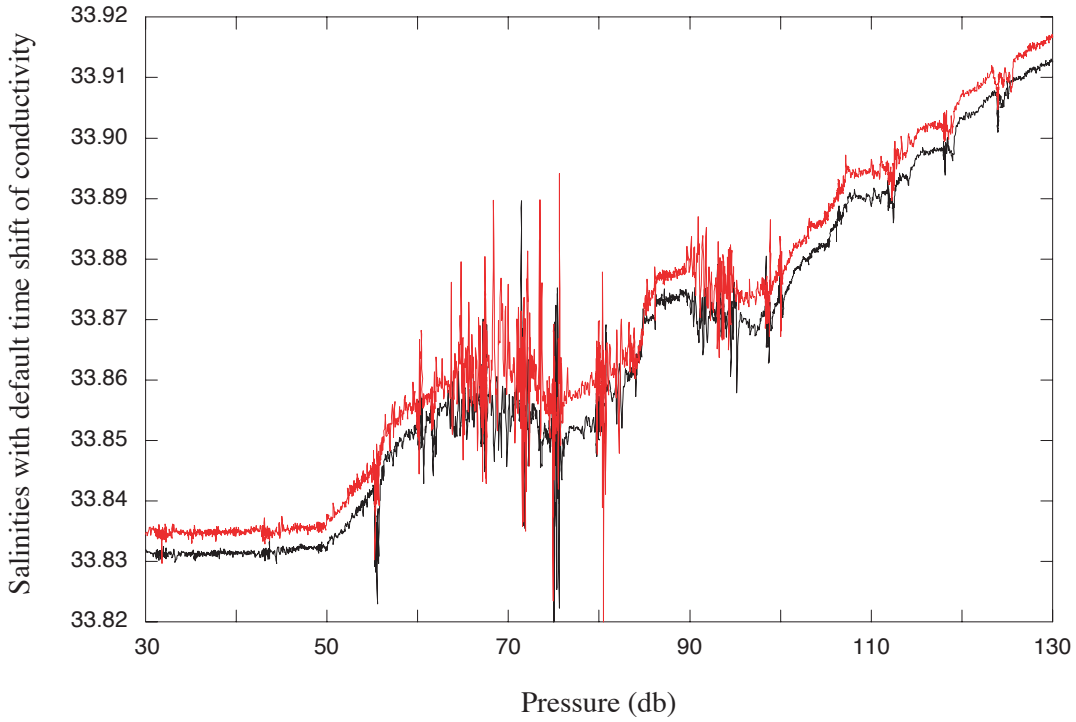

Figure 1.12a: Primary (black) and secondary (red) salinities (psu) for a near-surface 100 db section of Station 016.

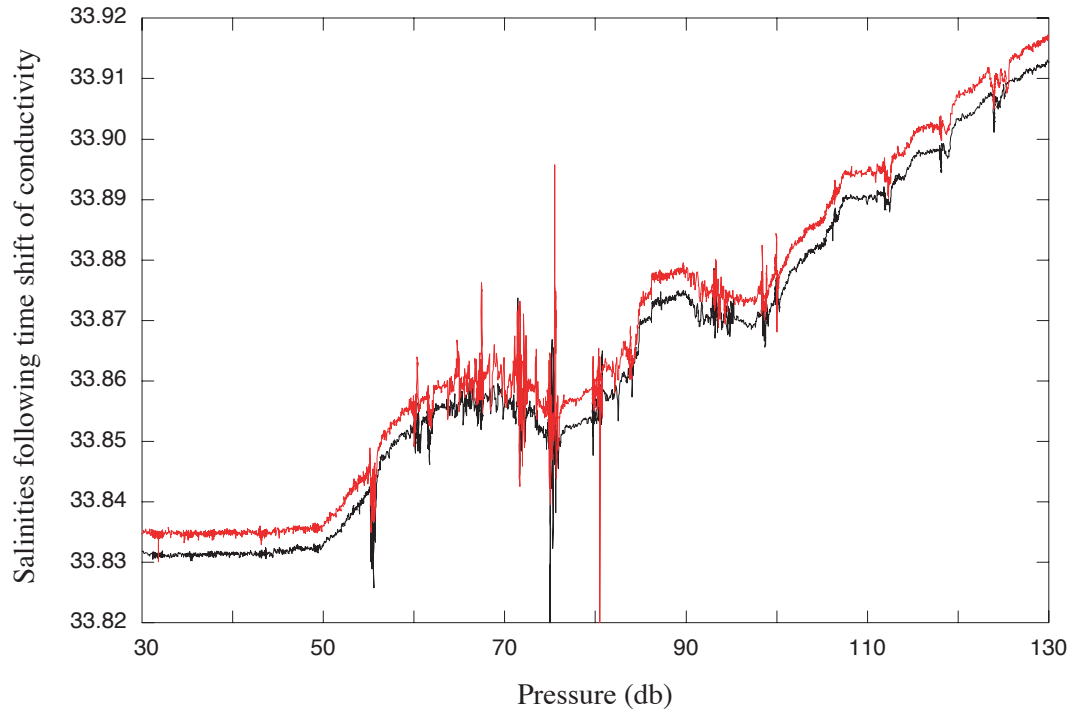

Figure 1.12b: As Figure 1.12a but after applying the optimal values of the time shift to both conductivity channels. Note that the true value of noise in the primary sensor (black line) is greater than suggested by this plot as a shift of 0.5 cycles has introduced an effective 2-point average into the primary salinity.

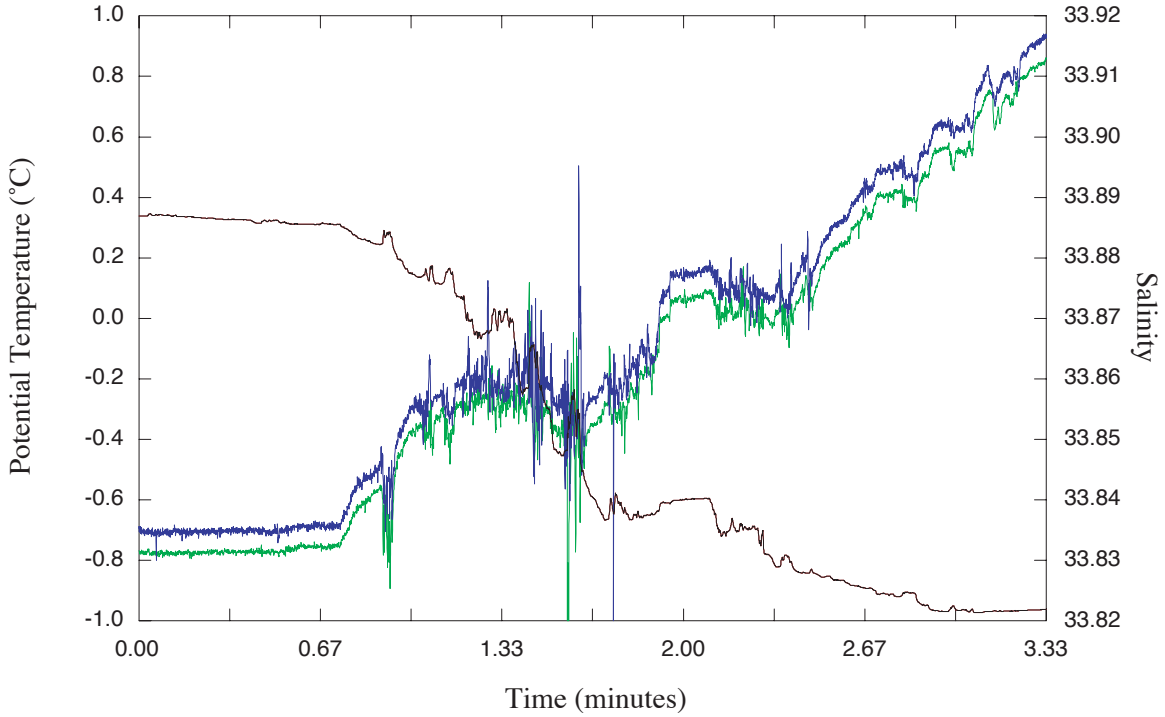

Figure 1.13: Potential temperature (ºC, black primary and red secondary) and salinity (psu, green primary and blue secondary) as a function of time for the same section of Station 016 plotted in Figure 1.12. The effects of the variable descent rate of the CTD package can been seen as peaks in the temperature traces in this high vertical gradient region. The peaks in temperature are associated with noise and peaks in the salinity signals.

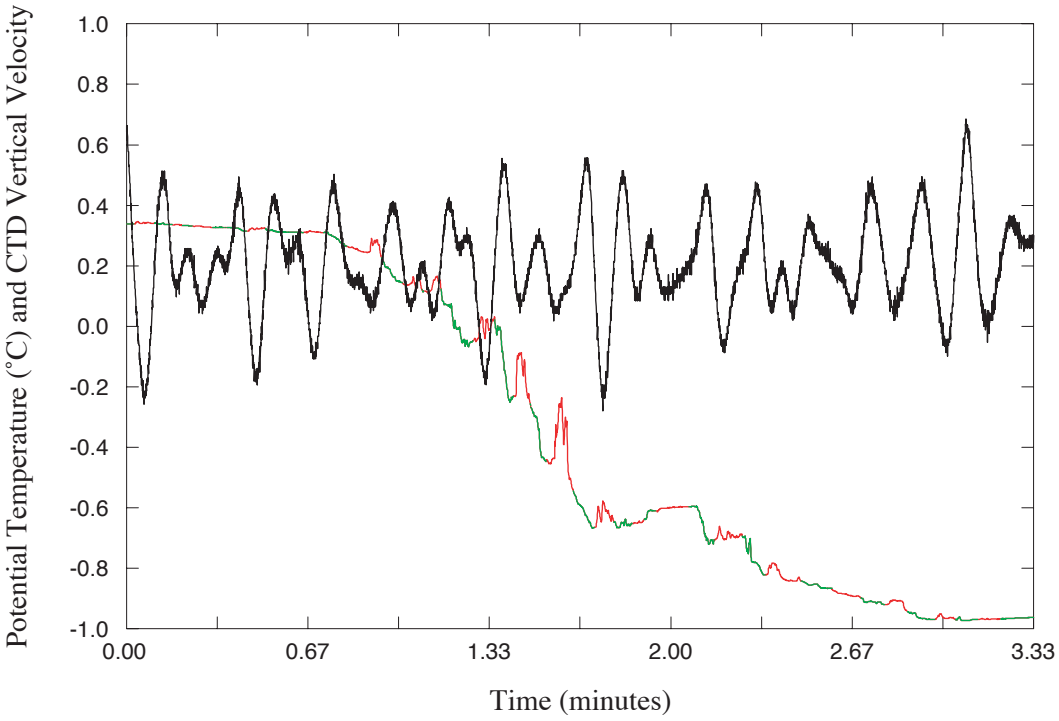

Figure 1.14: Primary potential temperature as in Figure 1.13 in green for large descent rates of the package (black line, arbitrary units) and red for small or negative descent rates. Peaks in the temperature trace are associated with slow descent or upwards movement of the package due to ship motion.

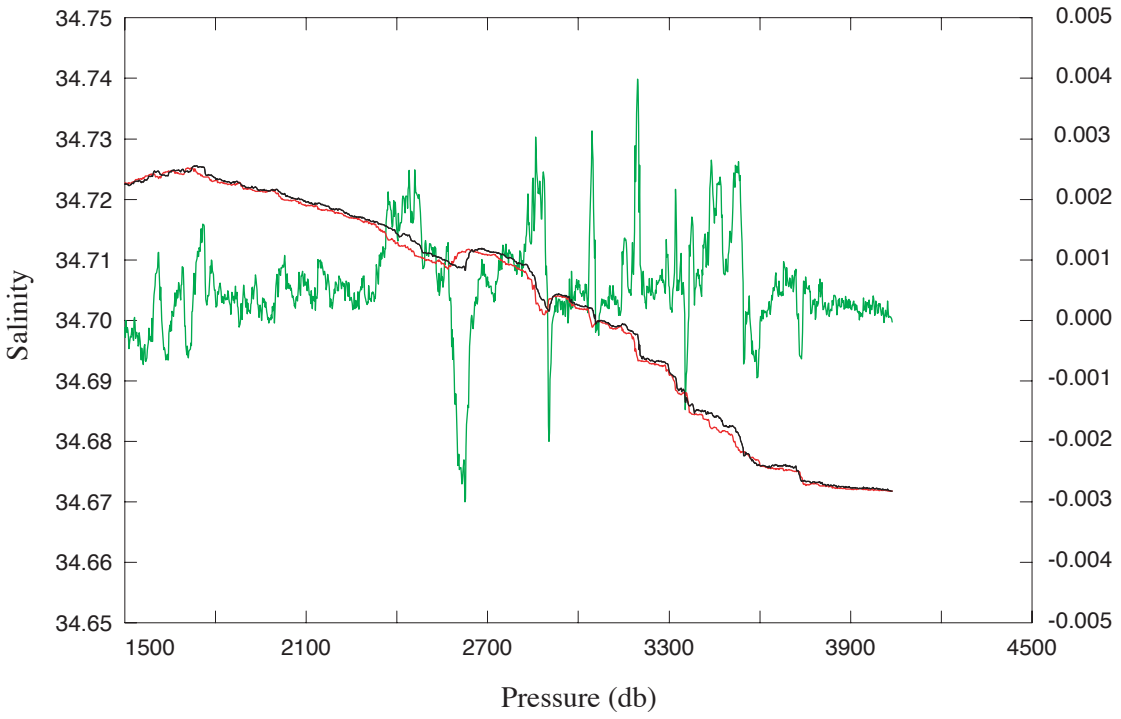

Figure 1.15: Primary salinity (psu, 1 Hz average) on downcast of Station 016 (black line) and upcast (red line). The green line shows the down-upcast salinity difference.

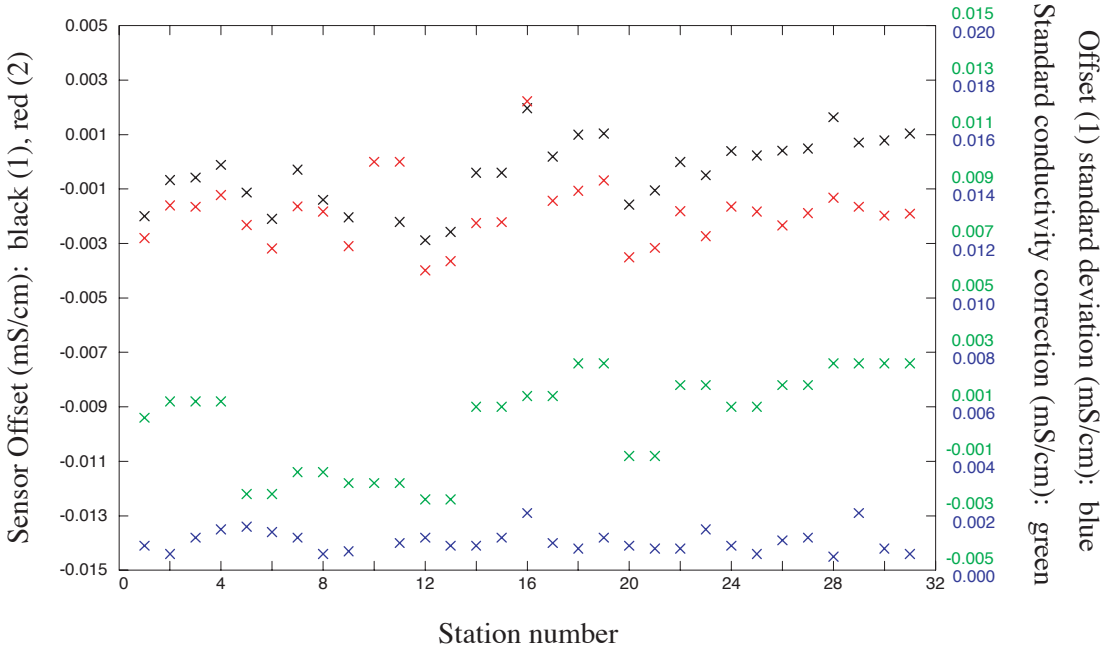

Figure 1.16: Mean conductivity offset (bottle minus CTD) for both CTD conductivity sensors (sensor 1, black; sensor 2, red) for each station, and (for sensor 1) the standard deviation, by station, of the conductivity offset about the mean (blue); salinometer standardisation history (green) expressed as equivalent conductivity correction (arbitrary zero).

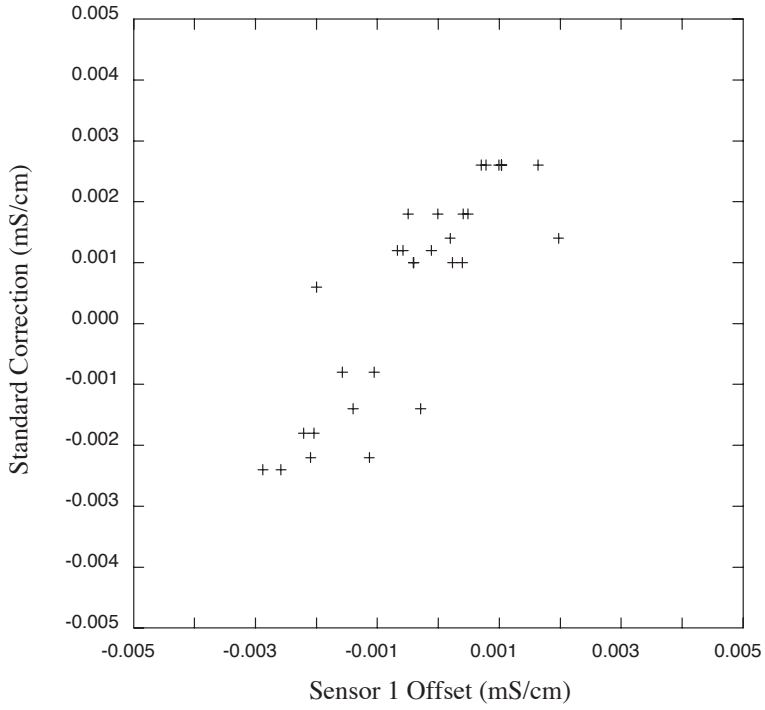

Figure 1.17a: Correlation between salinometer standard correction and CTD conductivity sensor 1 offset for each station.

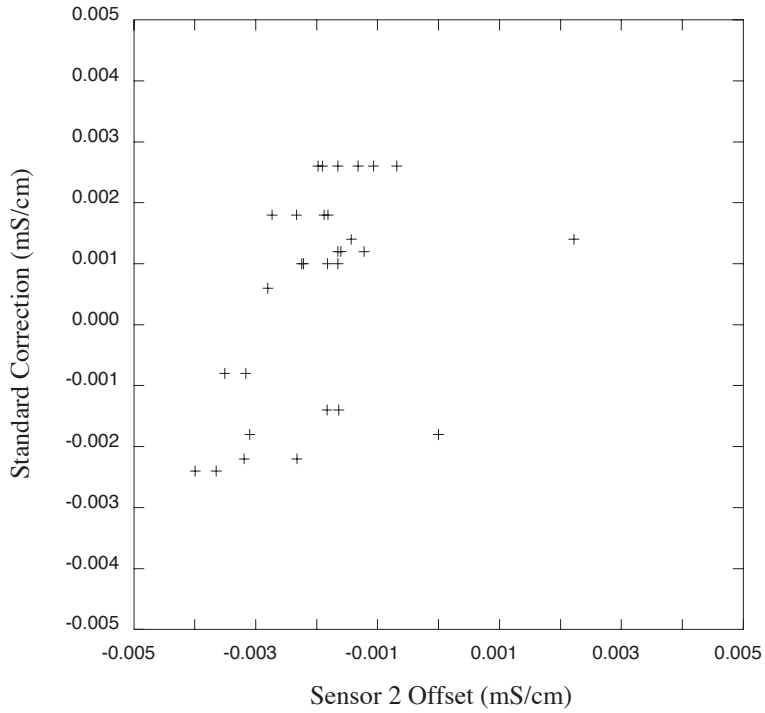

Figure 1.17b: Correlation between salinometer standard correction and CTD conductivity sensor 2 offset for each station.

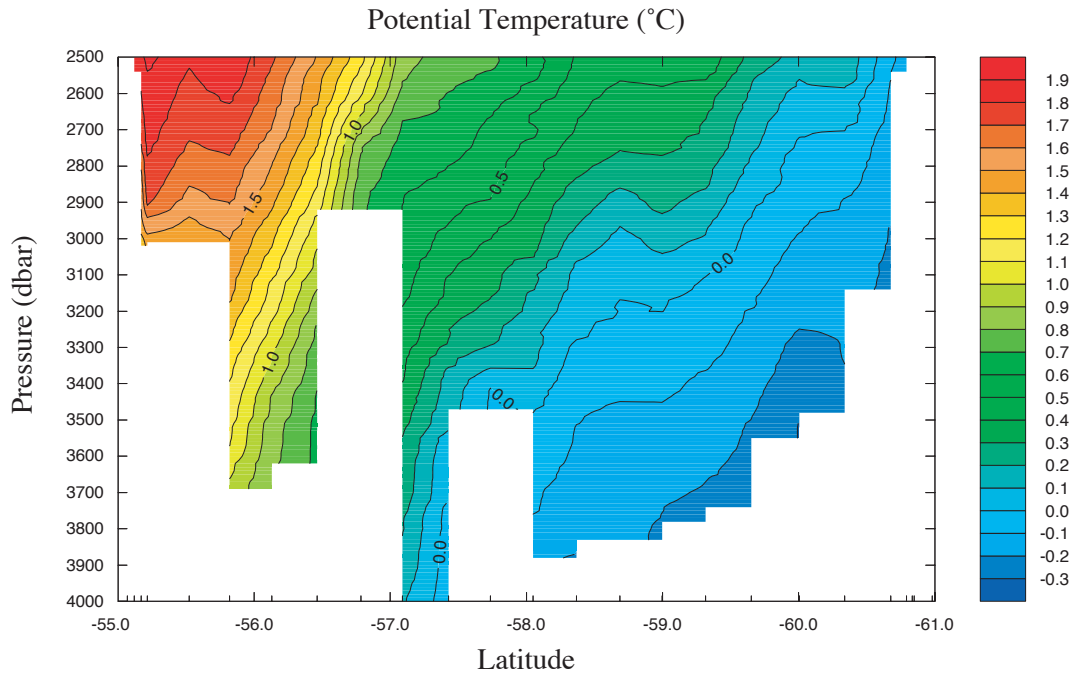

Figure 1.18a: Potential temperature (˚C) across the section below 2500 db.

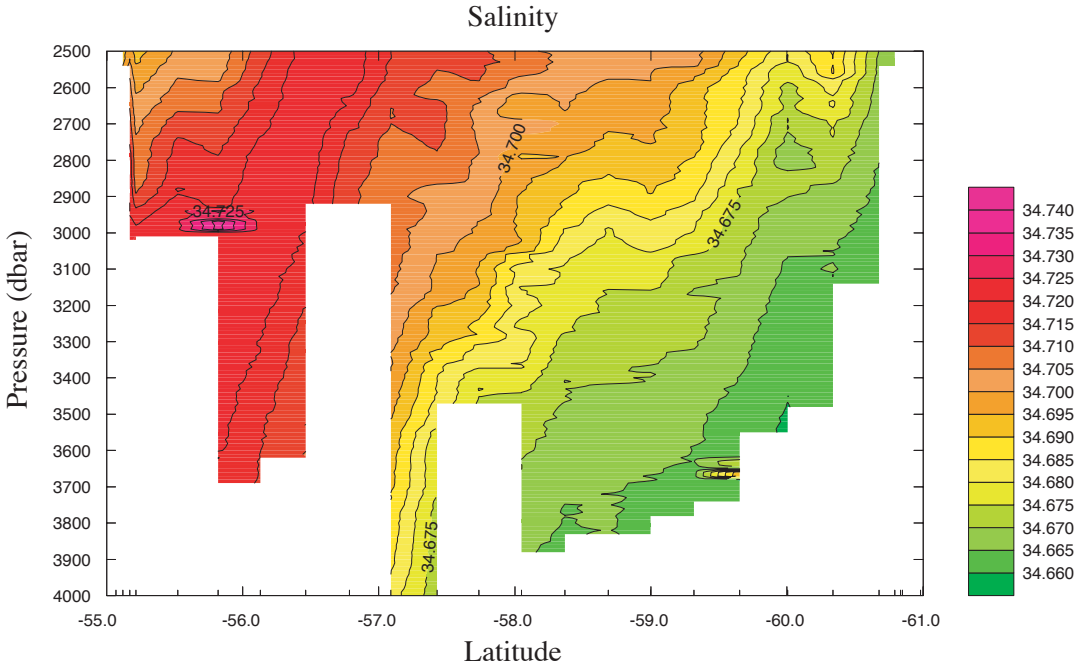

Figure 1.18b: Salinity (CTD sensor pair 1 uncalibrated) across the section below 2500 db.

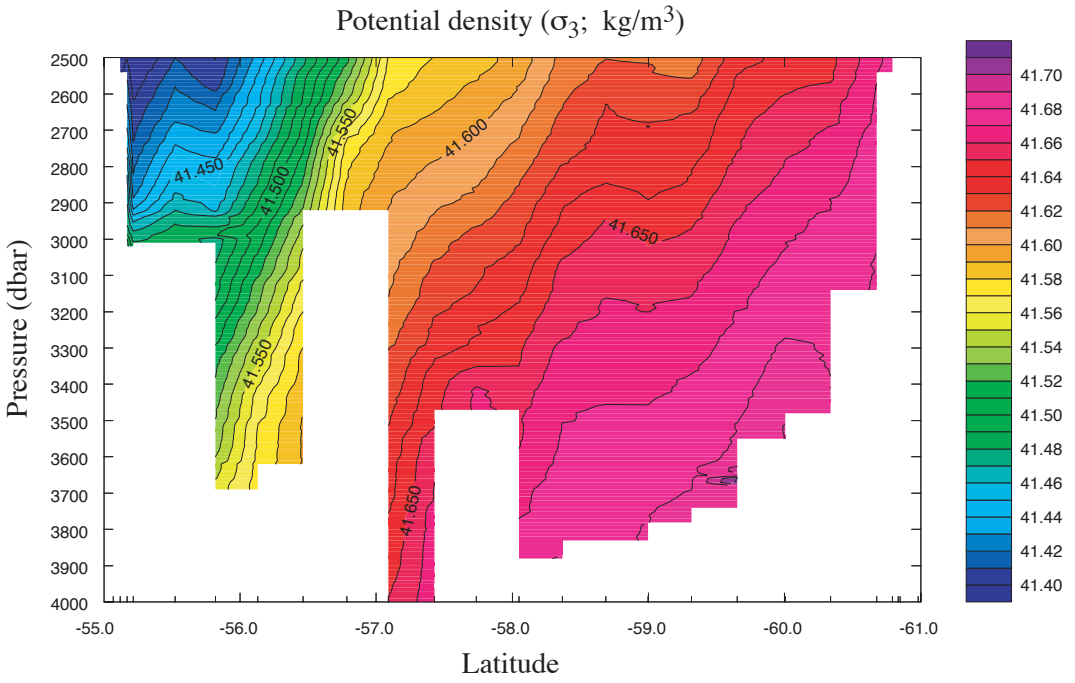

Figure 1.18c: Potential density referenced to 3000 m (σ_3, kg/m^3) across the section below 2500 db.

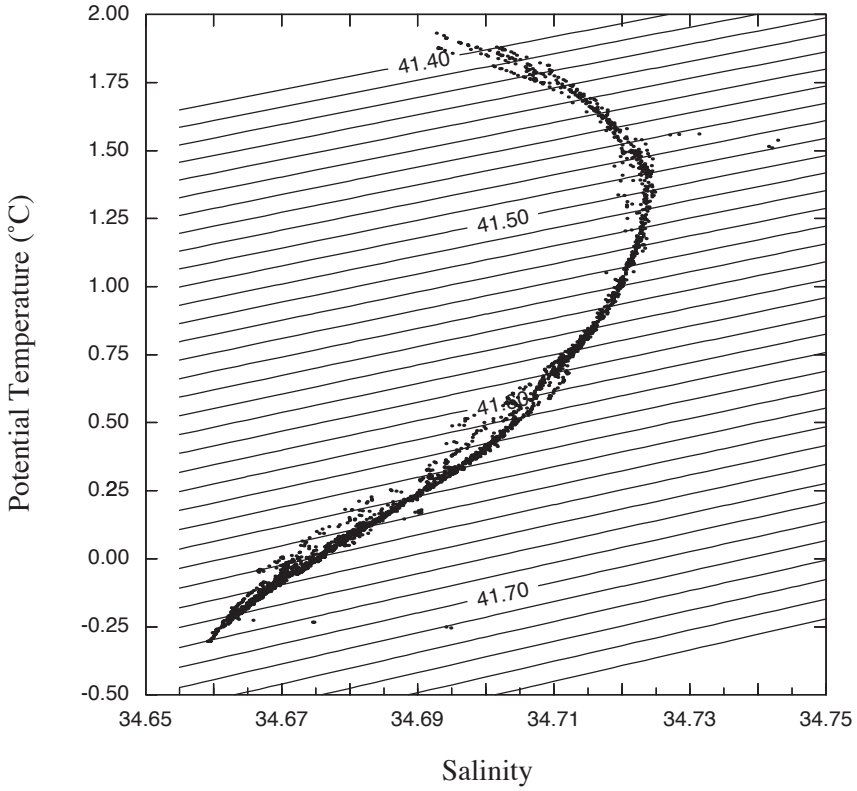

Figure 1.19: CTD potential temperature and salinity data below 2500 db with σ_3 overlay.

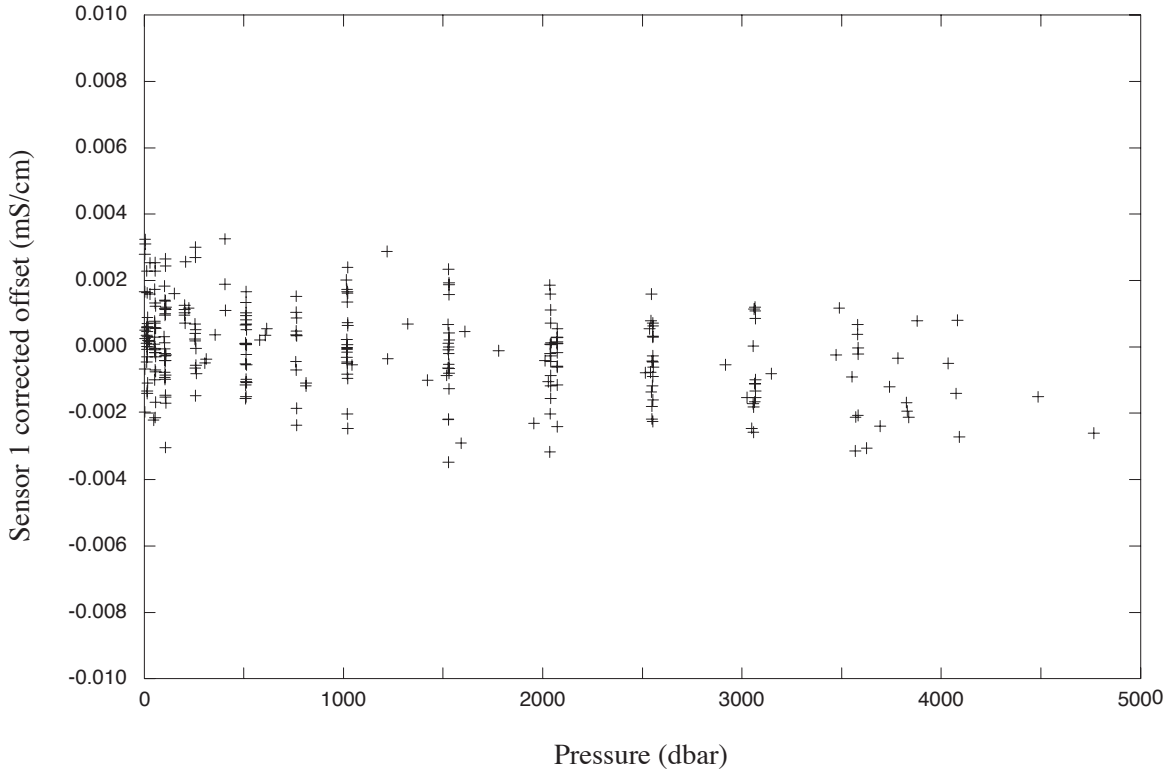

Figure 1.20a: Residual offset (sample minus conductivity) after calibration for sensor 1 vs. pressure.

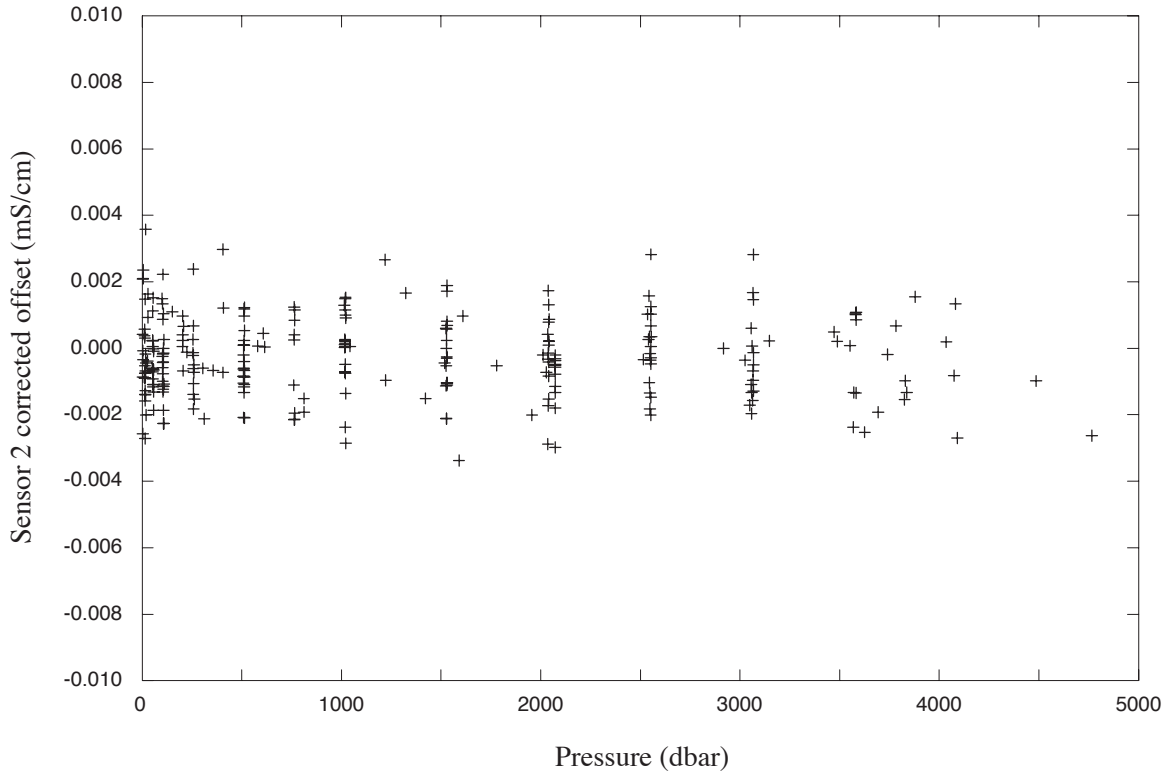

Figure 1.20b: Residual offset (sample minus conductivity) after calibration for sensor 2 vs. pressure.

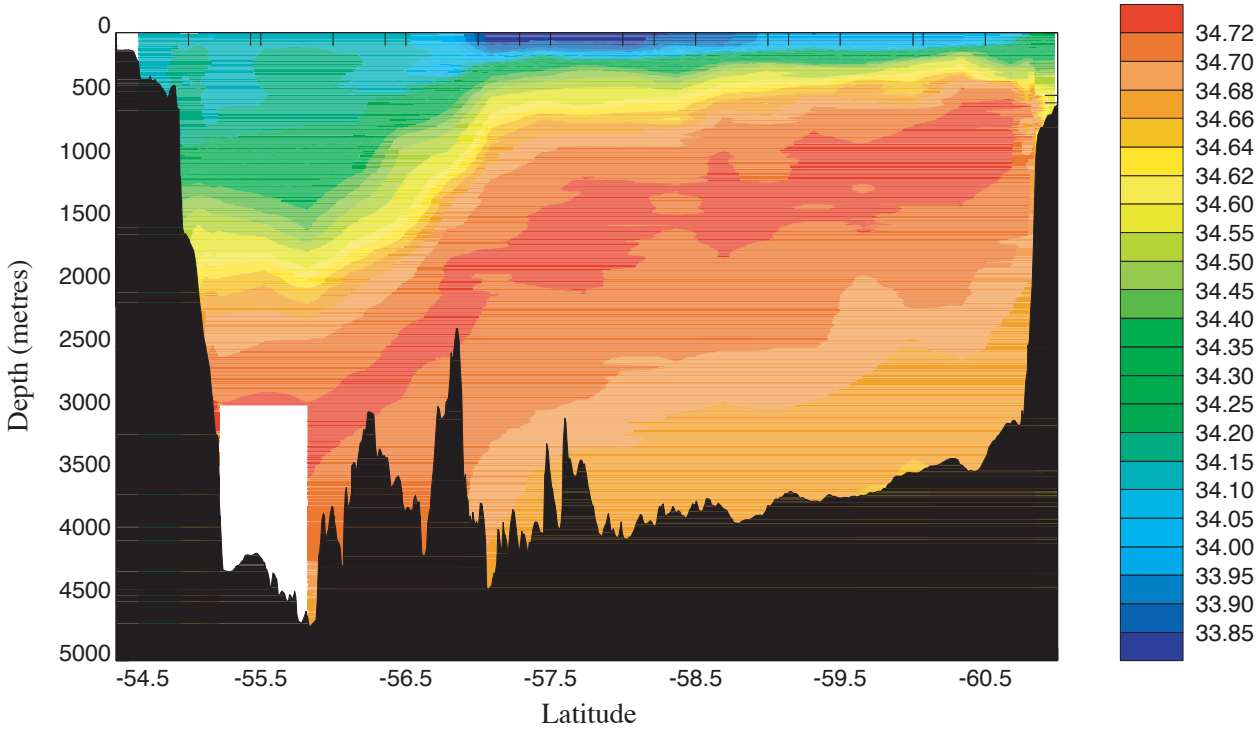

Figure 1.21a: Calibrated secondary salinity (psu) averaged to 5db for Drake Passage section.

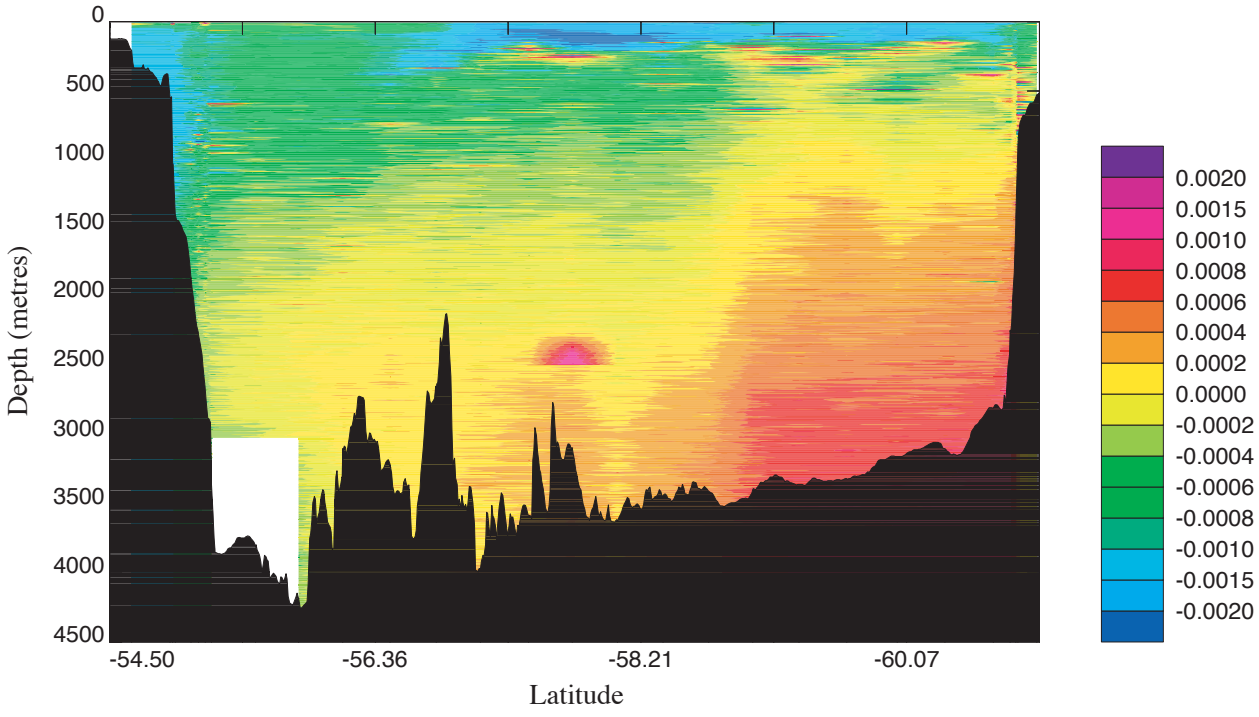

Figure 1.21b: Salinity difference (psu, primary – secondary) for data as in Figure 1.21a.

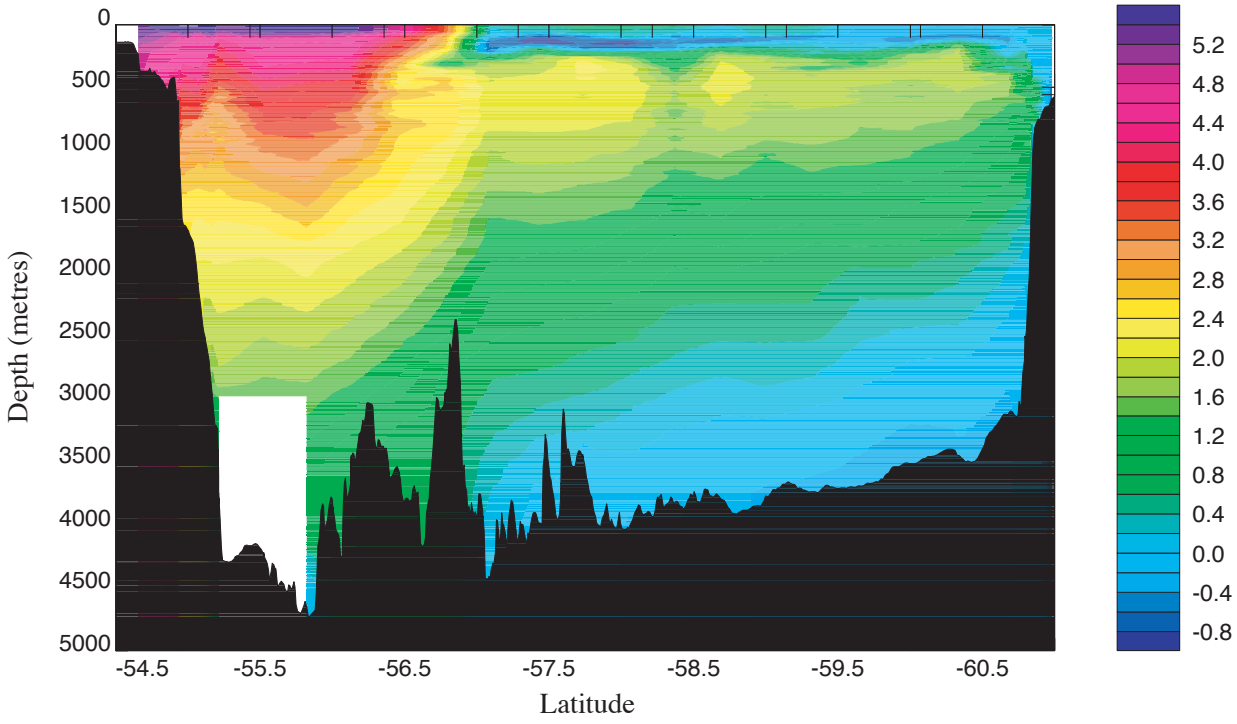

Figure 1.22: Secondary potential temperature (ºC) averaged to 5db for Drake Passage section.

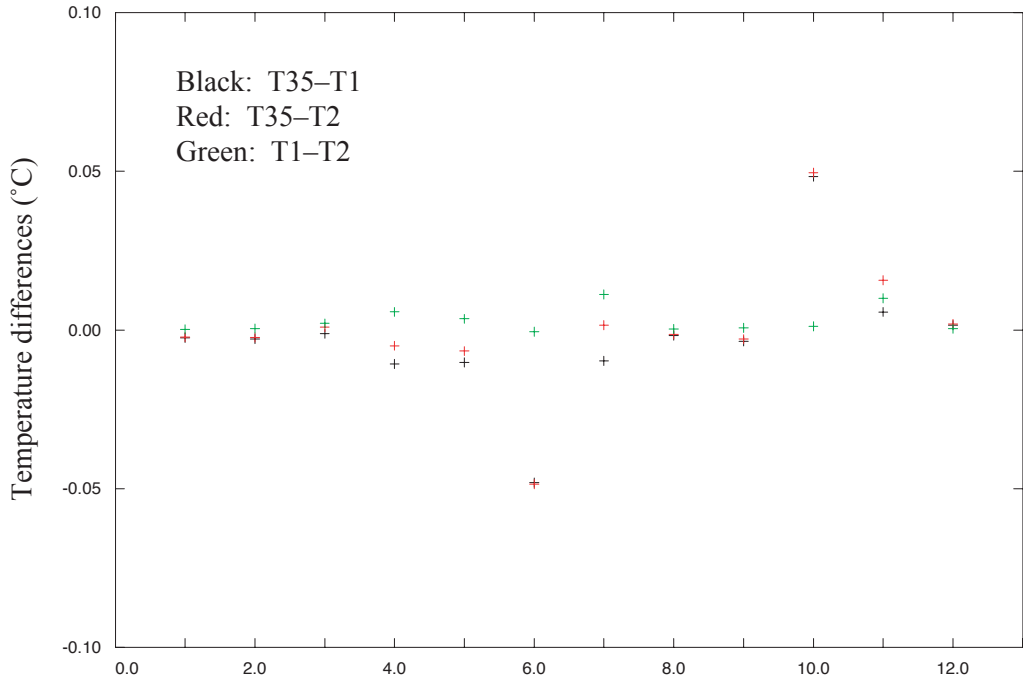

Figure 1.23: The differences between: the SBE35 and primary SBE911 temperature (black); the SBE35 and secondary SBE911 temperature (red); and the primary and secondary SBE911 temperatures (green), vs. rosette position (bottle) number.

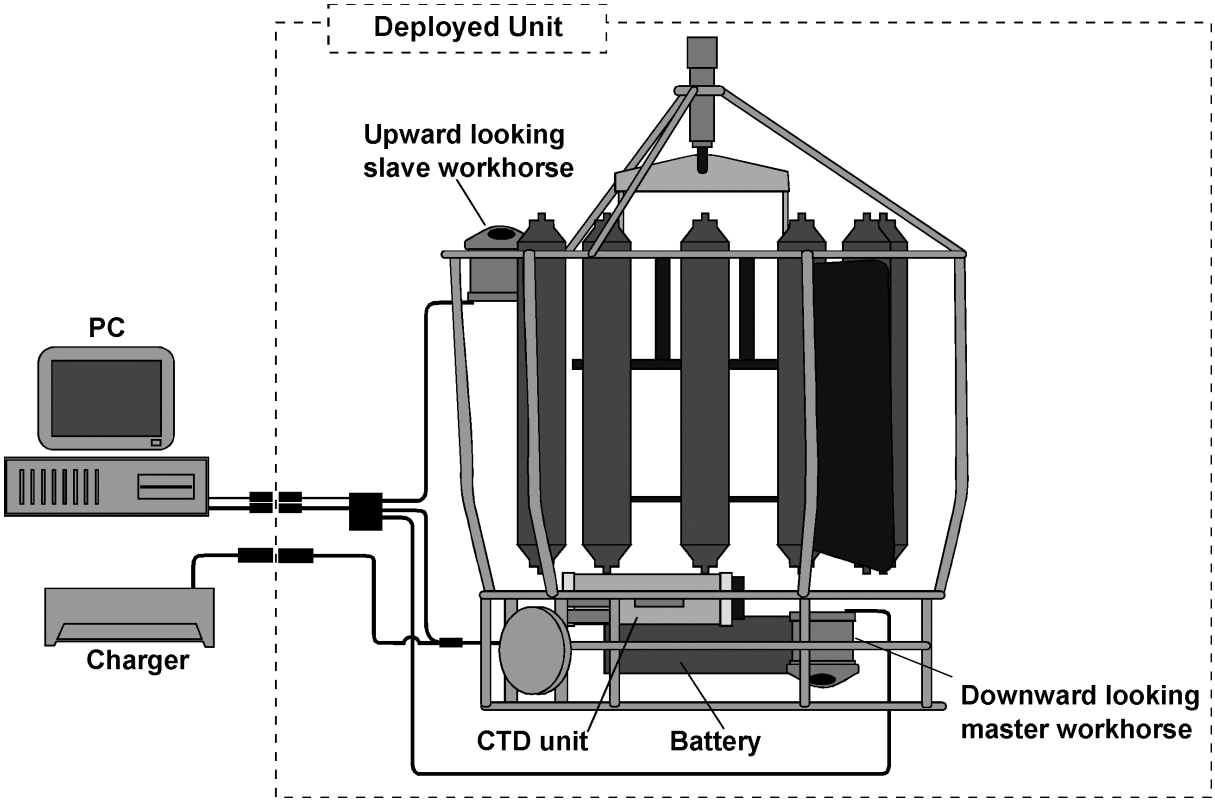

Figure 2.1: Cabling between the two LADCP Workhorse units, the battery, the charger and the PC.

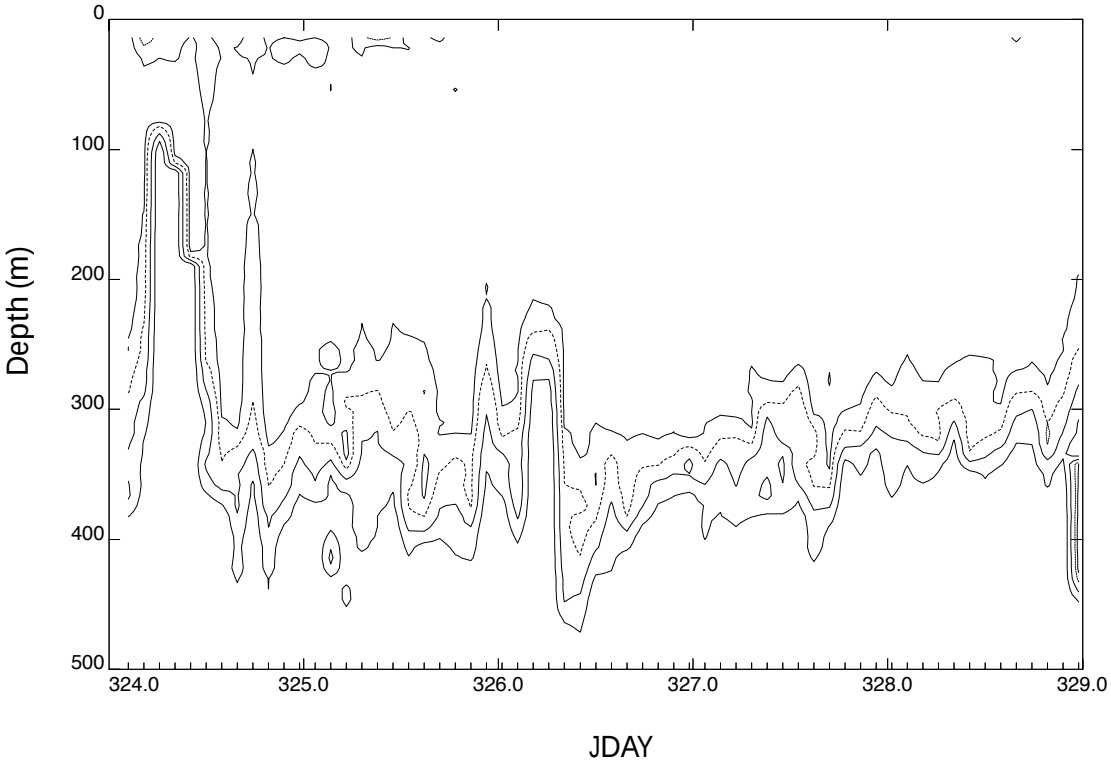

Figure 4.1: Contour plot of depths from which good VM-ADCP data were collected in water track mode during JR67. Contours at 25% (deepest), 50% (bold), 75% (dashed) and 90%.

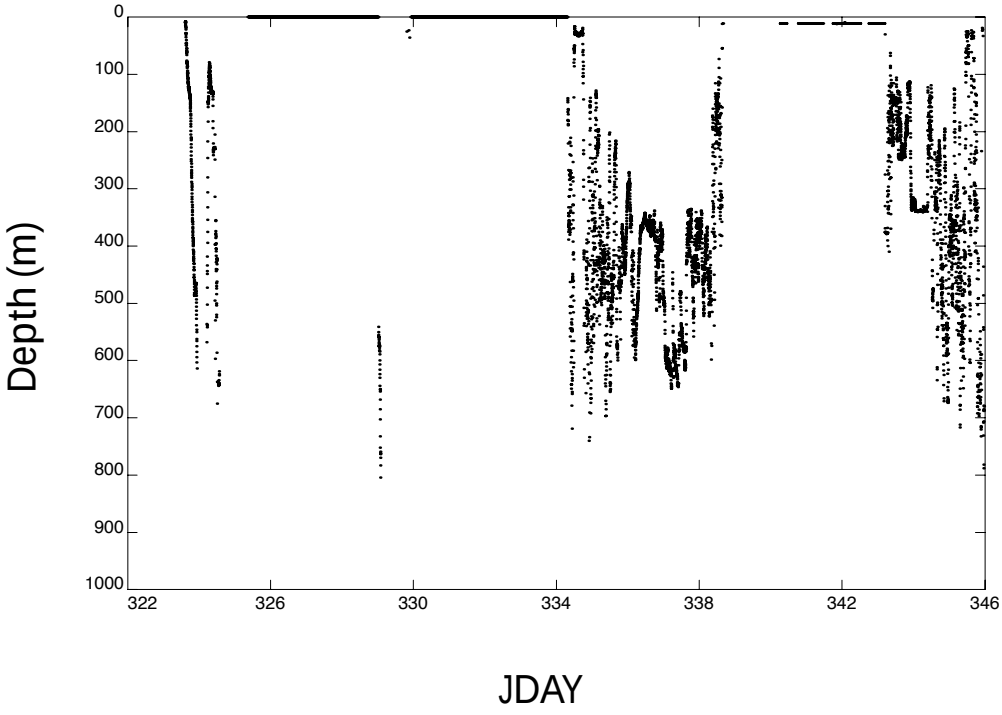

Figure 4.2: Depths from which good VM-ADCP bottom-track data were obtained during JR67.

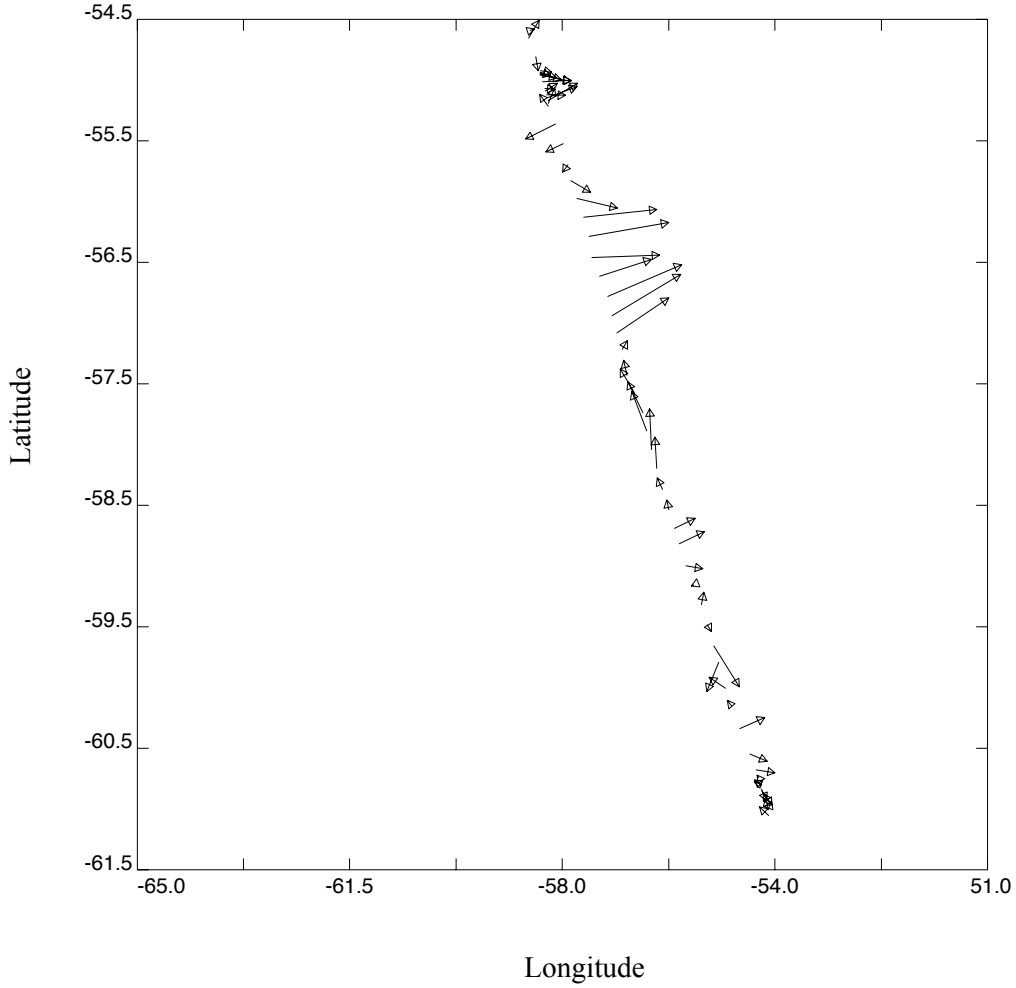

Figure 4.3: Vector plot of water track VM-ADCP data across Drake Passage SR1 section at a depth of 100 m, collected during JR67. Maximum vector magnitude 70.2 cm/s.

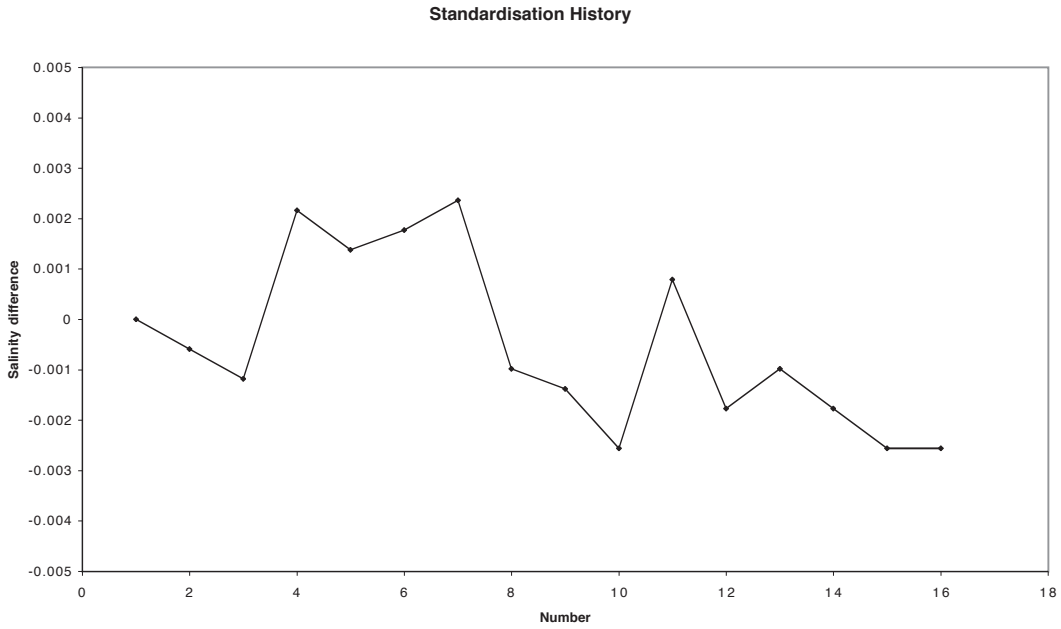

Figure 5.1: BAS 8400B salinometer standardisation history over the cruise.

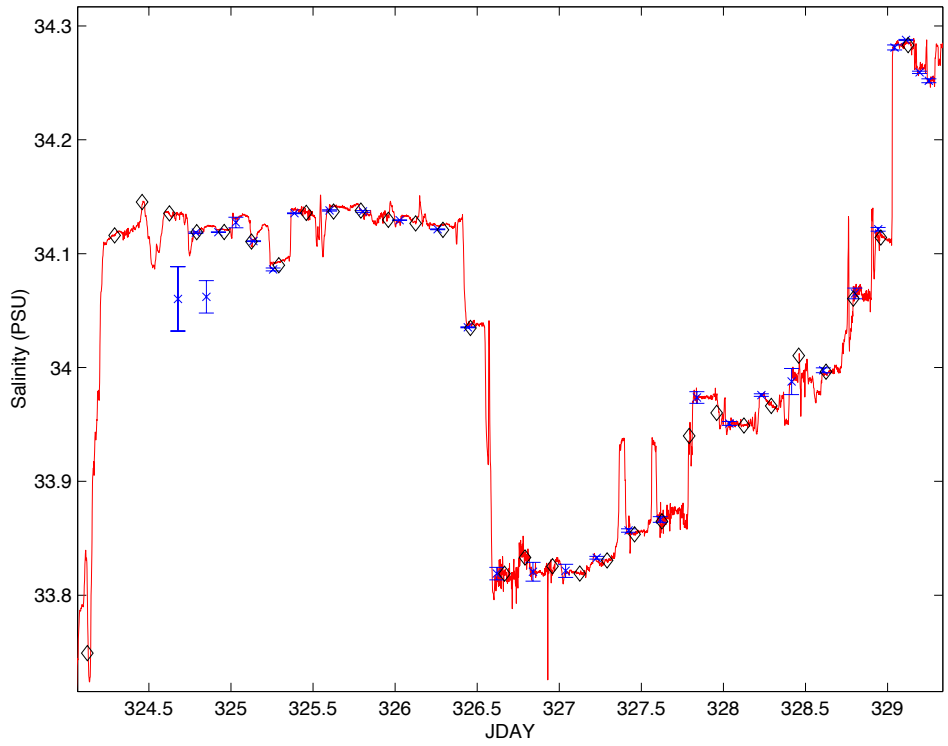

Figure 6.1: Salinity measurements from calibrated TSG (red), underway bottle samples (blue) and surface CTDs (black).

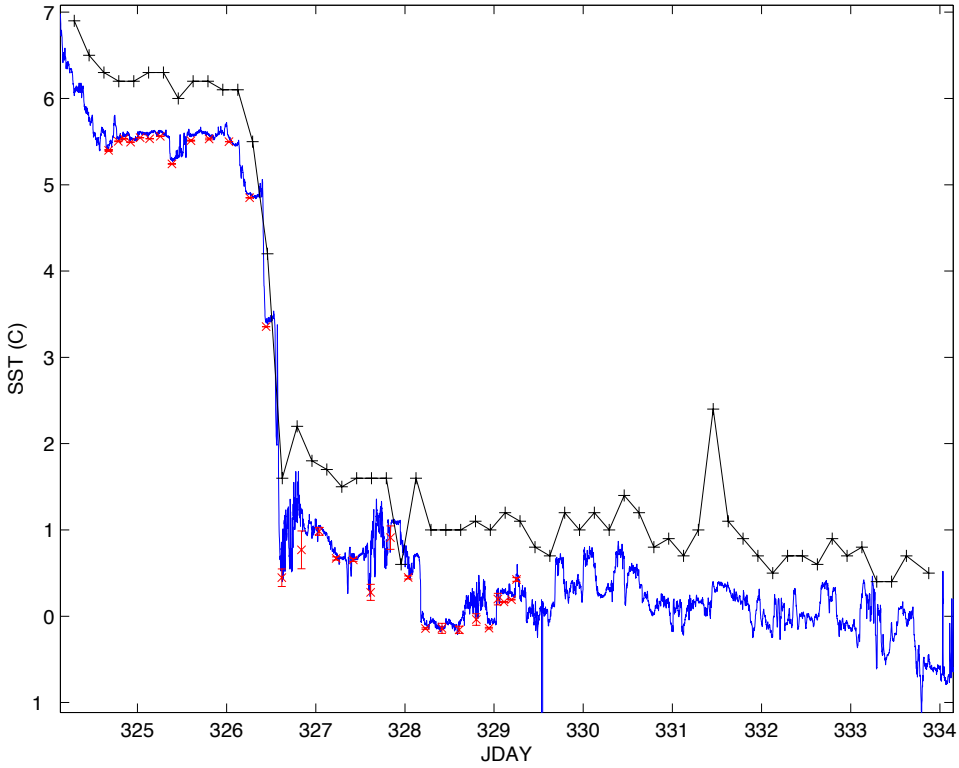

Figure 6.2: SST measurements from oceanlogger (blue), surfaces CTDs (red) and deck log (black).

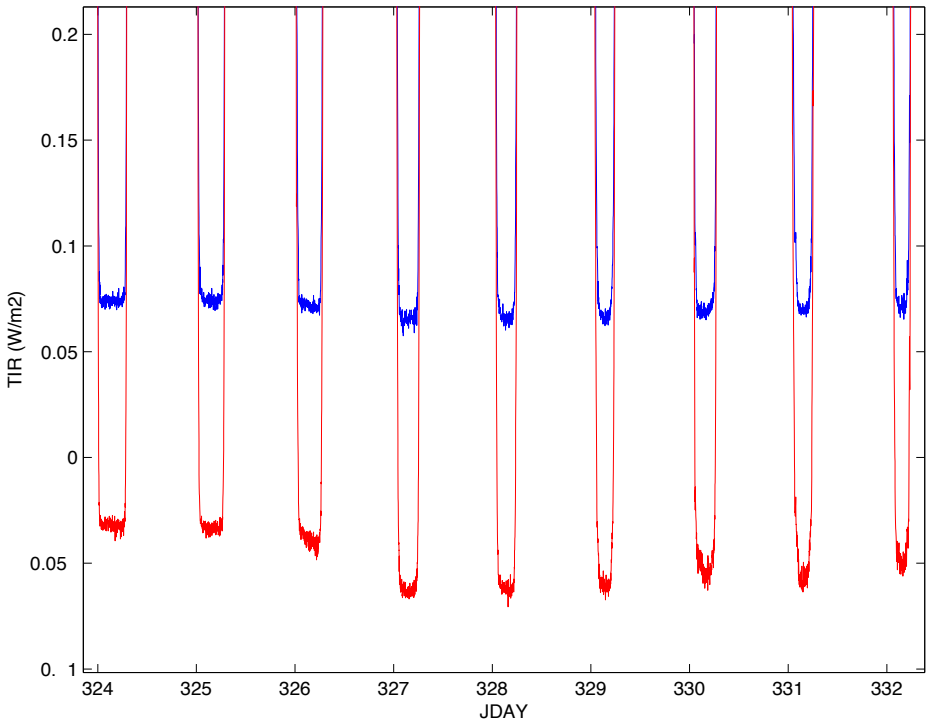

Figure 6.3a: Zero error for TIR sensors.

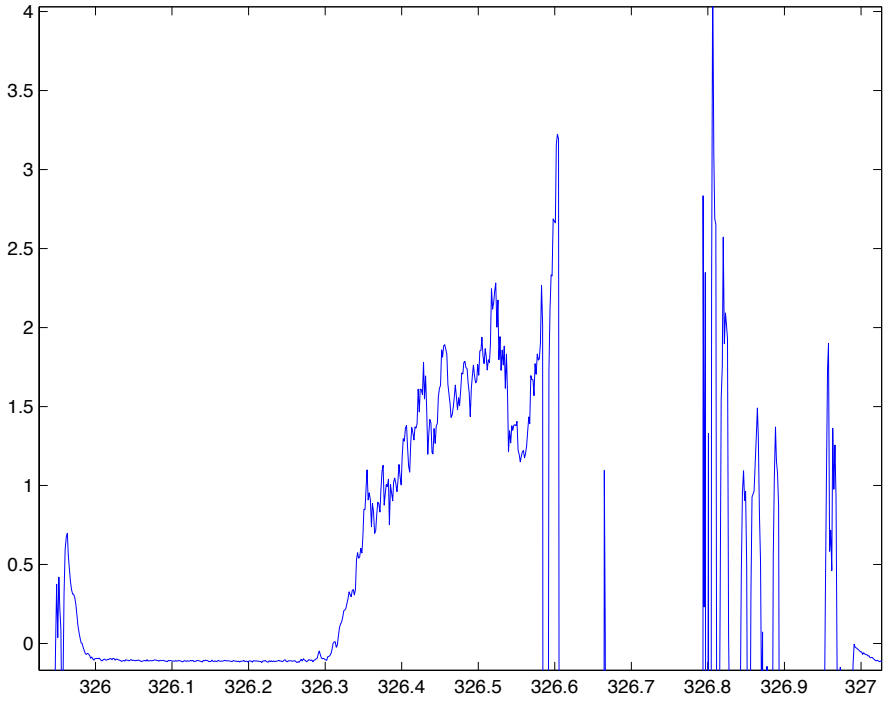

Figure 6.3b: tir2-tir1 for a typical day.

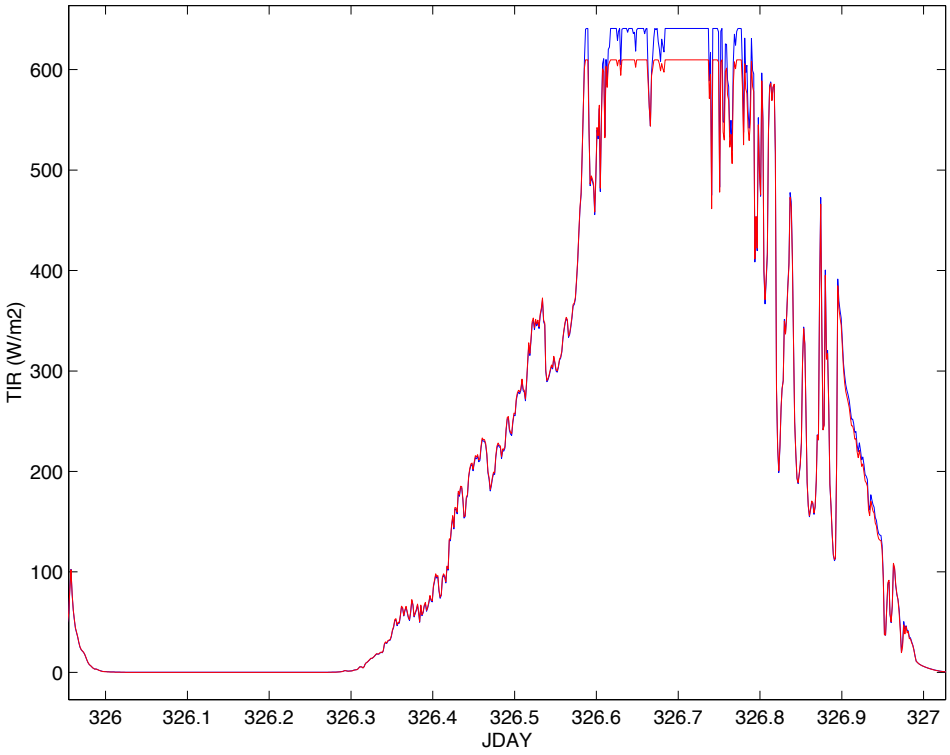

Figure 6.4: Typical daily TIR output.

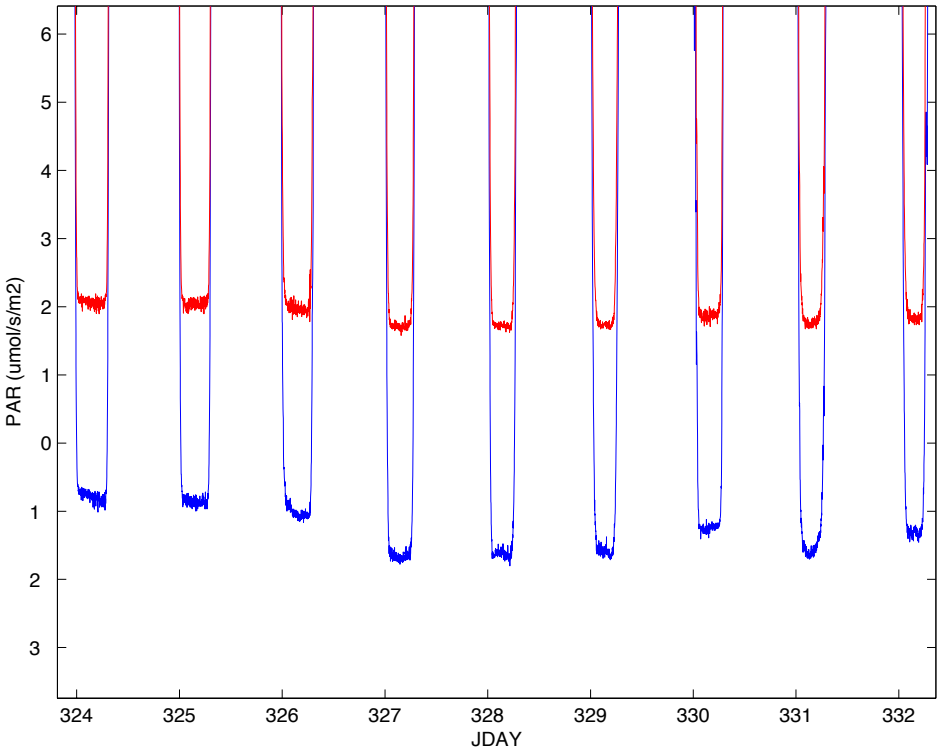

Figure 6.5a: Zero error for PAR sensors.

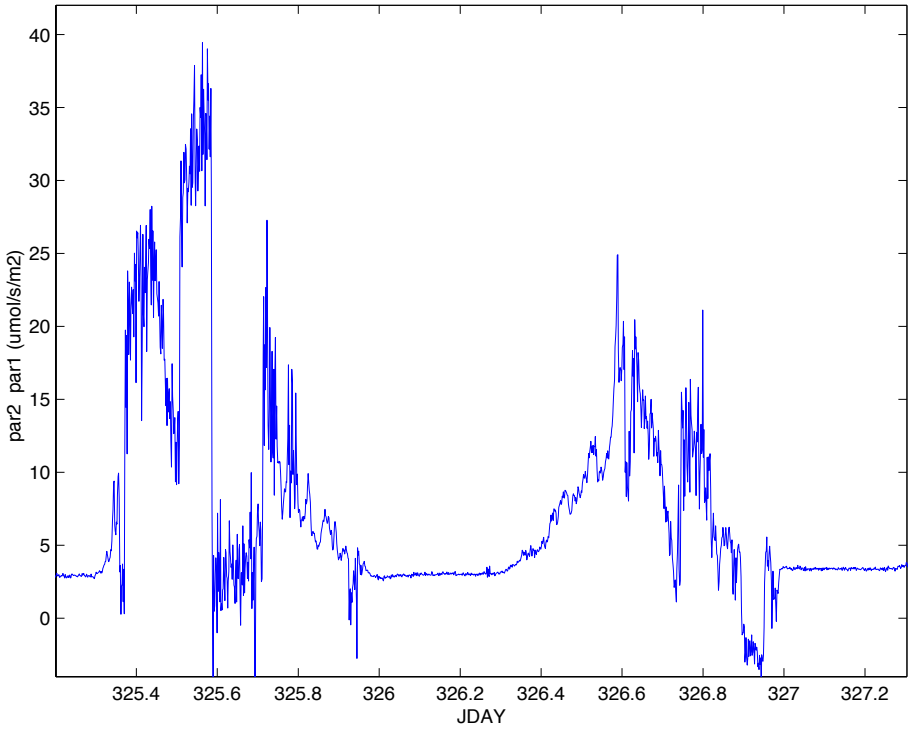

Figure 6.5b: par2-par1 for a typical day.

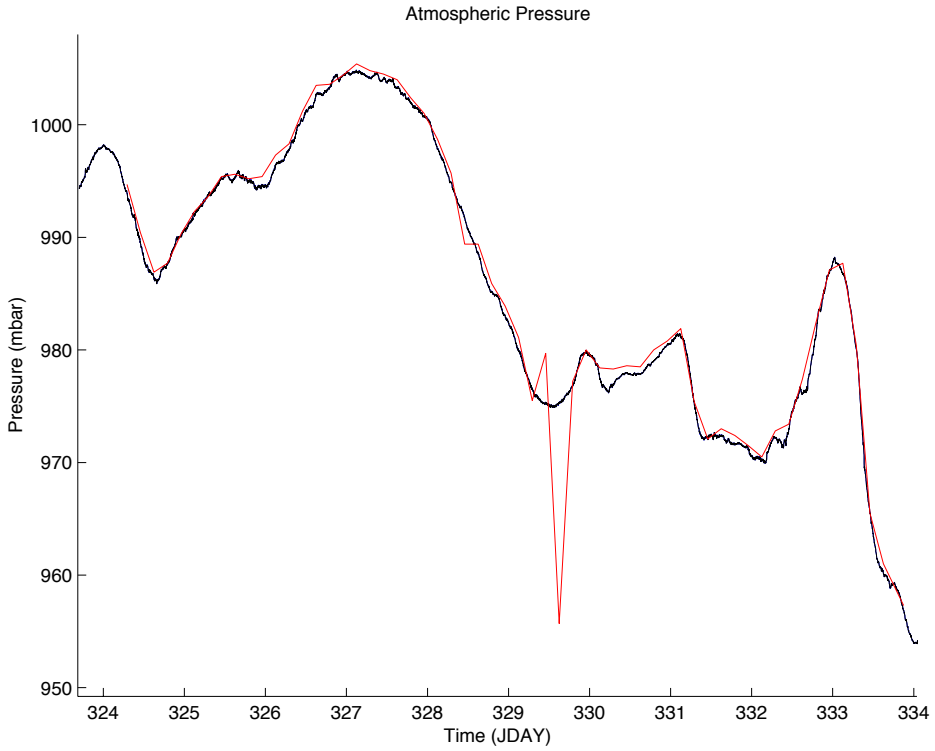

Figure 6.6: Air pressure measurement apress1 (blue), apress2 (blue), deck log barometer (red).

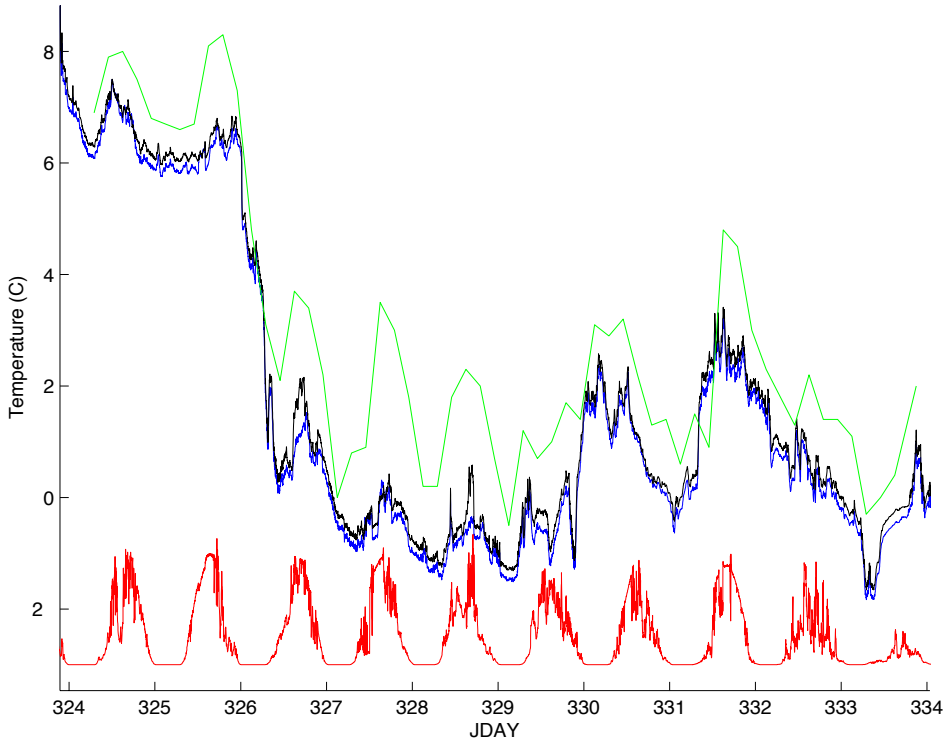

Figure 6.7: Air temperature, atemp2 (blue), atemp1 (black), deck log thermometer (green), reference PAR (red).

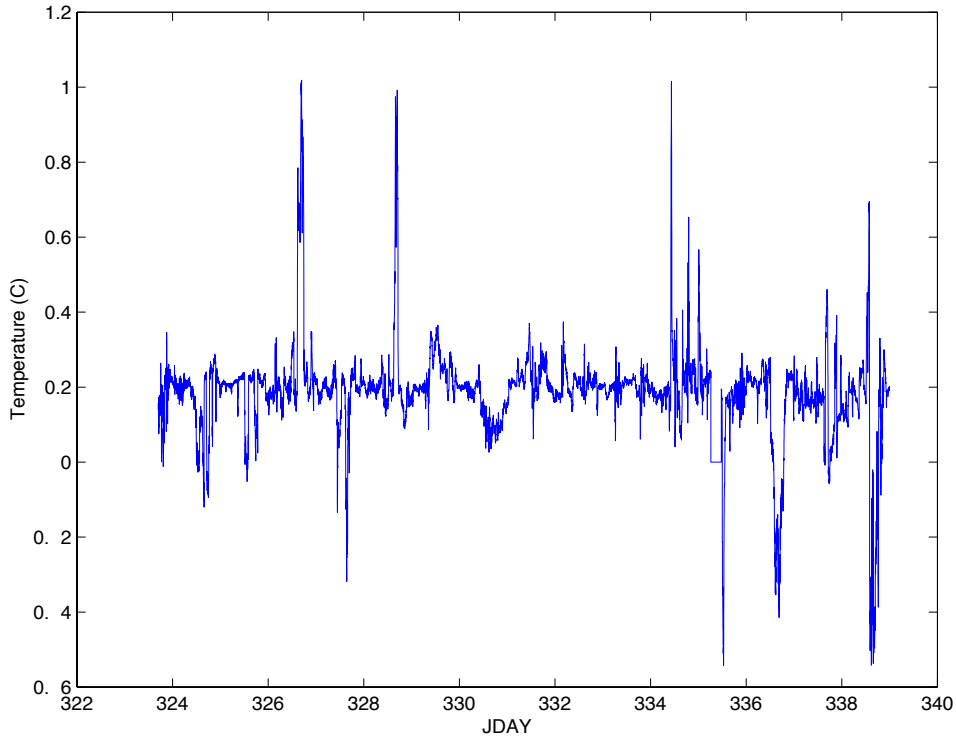

Figure 6.8: Offset between oceanlogger temperature sensors (atemp2 – atemp1).

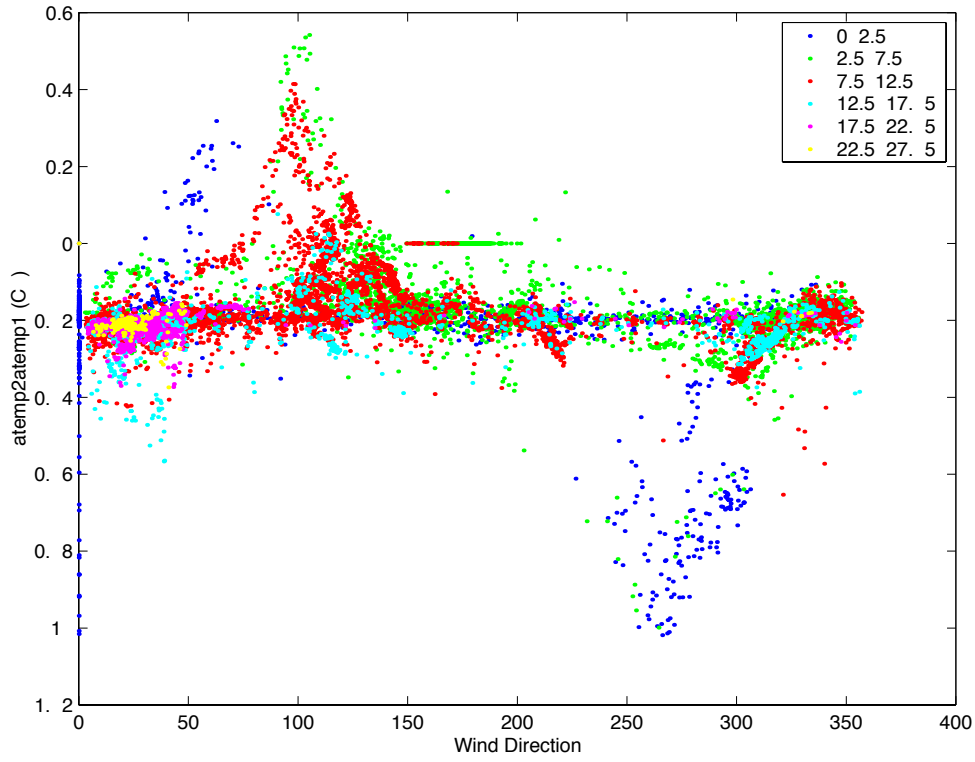

Figure 6.9: Oceanlogger air temperature offset as a function of relative wind direction for various relative wind speeds (m/s, colour scale for wind speed ranges in inset box).

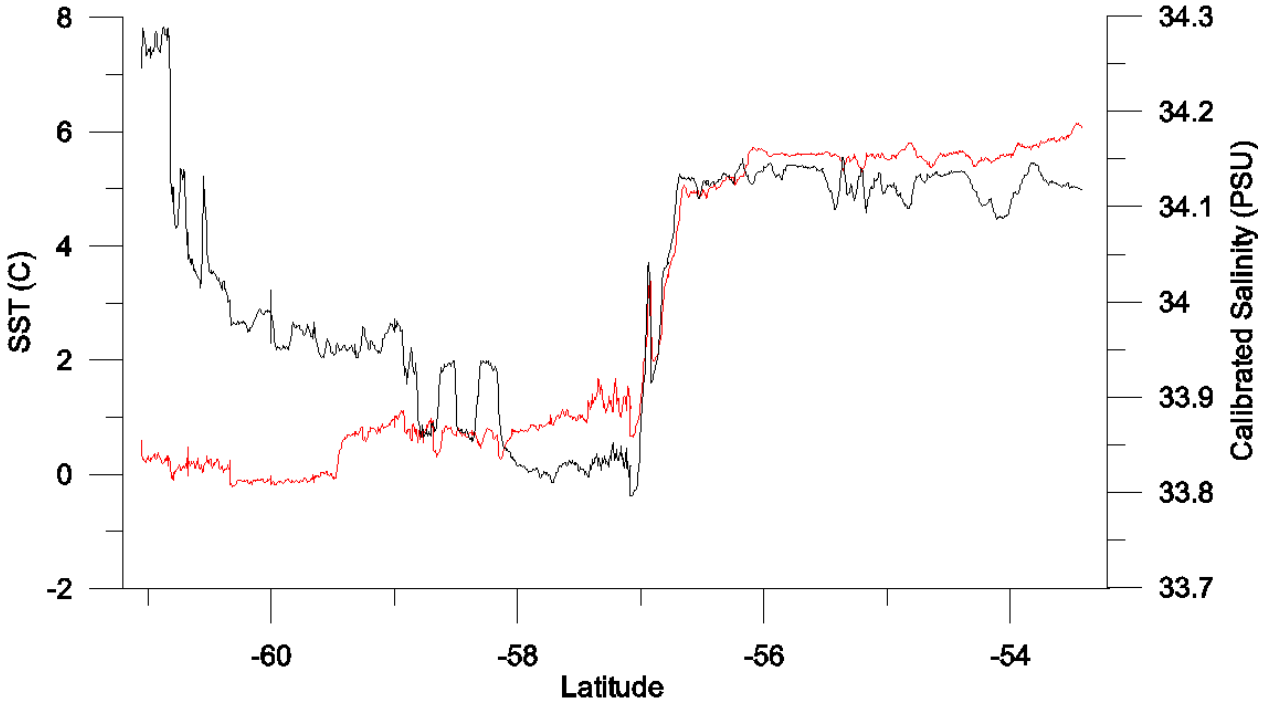

Figure 6.10a: SST (red) and calibrated salinity (black).

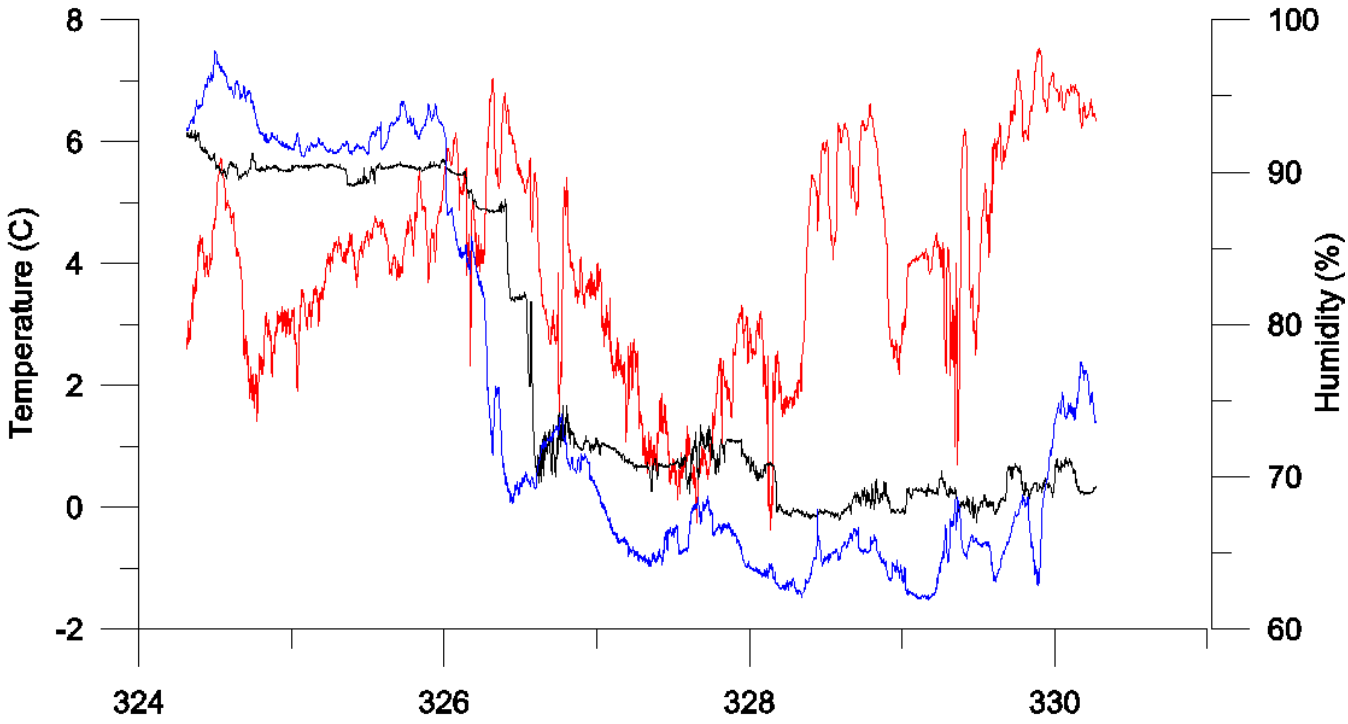

Figure 6.10b: SST (black), humidity (red) and air temperature (blue). Air temperature is calculated by taking the minimum sensor value after the offset: atemp2-0.1843/2 and atemp1+0.1843/2 has been applied (the most exposed sensor would be expected to give the truest value).

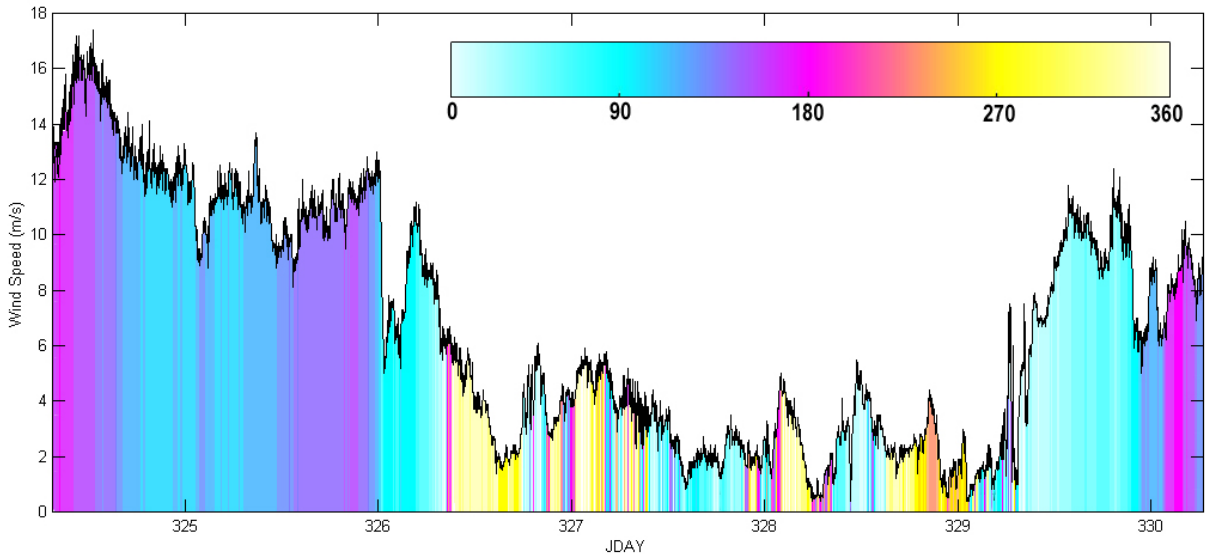

Figure 6.10c: True wind speed, colour coded to show true wind direction (oceanographic convention).

Plate 1: The *James Clark Ross* taken from the Humber in Drake Passage during station 20. *Photo by Dave Rees.*

Plate 2: An evening view of the south of Adelaide Island, looking south-westwards from the east side of North Point, Rothera.

Plate 3: A calm day in the Neumayer Channel.

Plate 4: North Cove, Rothera.

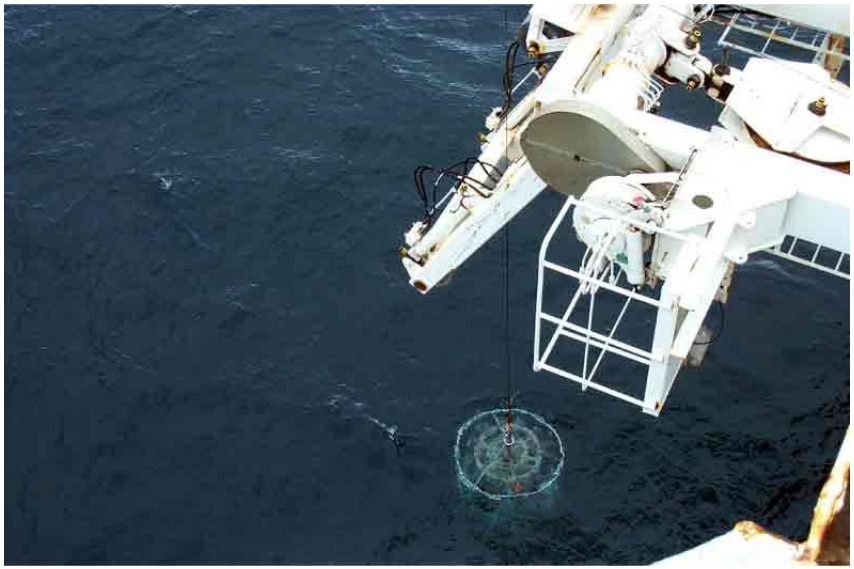

Plate 5: A CTD at the RaTS site, Rothera.

All images on this page by Sheldon Bacon